

INFORMATION TO USERS

This manuscript has been reproduced from the microfilm master. UMI films the text directly from the original or copy submitted. Thus, some thesis and dissertation copies are in typewriter face, while others may be from any type of computer printer.

The quality of this reproduction is dependent upon the quality of the copy submitted. Broken or indistinct print, colored or poor quality illustrations and photographs, print bleedthrough, substandard margins, and improper alignment can adversely affect reproduction.

In the unlikely event that the author did not send UMI a complete manuscript and there are missing pages, these will be noted. Also, if unauthorized copyright material had to be removed, a note will indicate the deletion.

Oversize materials (e.g., maps, drawings, charts) are reproduced by sectioning the original, beginning at the upper left-hand corner and continuing from left to right in equal sections with small overlaps.

Photographs included in the original manuscript have been reproduced xerographically in this copy. Higher quality 6" x 9" black and white photographic prints are available for any photographs or illustrations appearing in this copy for an additional charge. Contact UMI directly to order.

**Bell & Howell Information and Learning
300 North Zeeb Road, Ann Arbor, MI 48106-1346 USA
800-521-0600**

UMI[®]

**CRITICAL SPEEDS AND UNBALANCE RESPONSE OF CANTILEVER-
SLEEVE ROTORS USING FINITE ELEMENTS WITH EFFICIENT
HIGHER ORDER BASIS FUNCTIONS**

Jeyaruban Selliah Amirtharajah

**A Thesis
in
The Departement
of
Mechanical Engineering**

**Presented in Partial Fulfillment of the Requirements
for the Degree of Master of Applied Science at
Concordia University
Montreal, Quebec, Canada**

May 1999

© Jeyaruban Selliah Amirtharajah, 1999



National Library
of Canada

Acquisitions and
Bibliographic Services

395 Wellington Street
Ottawa ON K1A 0N4
Canada

Bibliothèque nationale
du Canada

Acquisitions et
services bibliographiques

395, rue Wellington
Ottawa ON K1A 0N4
Canada

Your file *Votre référence*

Our file *Notre référence*

The author has granted a non-exclusive licence allowing the National Library of Canada to reproduce, loan, distribute or sell copies of this thesis in microform, paper or electronic formats.

The author retains ownership of the copyright in this thesis. Neither the thesis nor substantial extracts from it may be printed or otherwise reproduced without the author's permission.

L'auteur a accordé une licence non exclusive permettant à la Bibliothèque nationale du Canada de reproduire, prêter, distribuer ou vendre des copies de cette thèse sous la forme de microfiche/film, de reproduction sur papier ou sur format électronique.

L'auteur conserve la propriété du droit d'auteur qui protège cette thèse. Ni la thèse ni des extraits substantiels de celle-ci ne doivent être imprimés ou autrement reproduits sans son autorisation.

0-612-43661-6

Canada

ABSTRACT

Critical Speeds and Unbalance Response of Cantilever-Sleeve Rotors Using Finite Elements with Efficient Higher Order Basis Functions

Jeyaruban Selliah Amirtharajah
Concordia University, 1999

Design of industrial rotor-bearing systems requires an understanding of their dynamic behavior, which involves the determination of their critical speeds and unbalance response. Dynamic behavior of simple rotor systems can be studied using analytical techniques. However, for complex rotor systems it is necessary to use approximate techniques. The finite element method is one such approximate technique and has been in use as a computational method for solving these problems. In most cases finite element method requires a fine discretization of the rotor model and this leads to setting up and solving a large number of simultaneous and coupled linear differential equations for the unknown displacements. With such large systems the calculation becomes very time consuming, which may not be economically feasible. The prime objective of the present investigation is to develop an efficient and economical technique for the determination of the critical speeds and the unbalance response of complex rotor-bearing systems such as cantilever-sleeve rotor. The technique is based on higher order finite elements. By using this technique the size of system equations can be significantly reduced without affecting the dynamic characteristics of the system. The technique also incorporates all the natural and essential boundary conditions right in the basis functions at element formulation. Thus, this element adequately represents all the physical situations involved in any combination of displacement, rotation, bending moment and shearing force boundary conditions. The dynamic behavior of a cantilever-sleeve rotor with a disk at the end is studied using such higher order finite elements. More accurate results are obtained using a coarse mesh that has increased number of degrees of freedom. Further no errors are introduced during post processing for stresses, strains, etc.

ACKNOWLEDGEMENT

The author wishes to express his indebtedness to his thesis supervisor Dr. R.B. Bhat for his encouragement and guidance throughout the development of this thesis. The author also expresses his warmest gratitude to the thesis co-supervisor Dr. Rajamohan Ganesan who exposed the author to various technical aspects of the finite element method. The discussions and the support provided by both supervisors are deeply appreciated.

Sincerest thanks are due to members of the faculty, staff and my friends at CONCAVE Research Center for their valuable help and emotional support.

Gratitude is expressed to Scott Linstead for drawing some figures in AutoCAD.

The financial support provided by the NSERC and the Department of Mechanical Engineering at Concordia University is gratefully acknowledged.

The author would like to express his special thanks to the members of his family for their understanding and support.

CONTENTS

ABSTRACT	iii
ACKNOWLEDGEMENT	iv
LIST OF FIGURES	x
LIST OF TABLES	xiii
NOMENCLATURE	xviii
CHAPTER 1 INTRODUCTION, LITERATURE REVIEW, OBJECTIVES AND SCOPE	1
1.1 Introduction	1
1.2 Literature Review	3
1.2.1 The Dynamics of Rotor-Bearing Systems	3
1.2.2 Higher-Derivatives as Nodal Degrees of Freedom	7
1.3 Objectives of the Thesis	14
1.4 Scope of the Present Investigation	17
CHAPTER 2 DYNAMIC ANALYSIS OF ROTORS USING CONVENTIONAL FINITE ELEMENTS	19
2.1 Conventional Finite Element Formulation	19
2.1.1 Introduction	19
2.1.2 Gyroscopic Whirling of a Simple Rotor	19
2.1.3 System Configuration and Coordinates	20
2.1.4 Component Equations	25

2.1.4.1	The Rigid Disk	25
2.1.4.2	Finite Shaft Element	28
2.1.4.3	Bearings	39
2.1.5	System Equations of Motion	40
2.1.6	Solution of System Equations	41
2.1.6.1	Whirl Speed Analysis	42
2.1.6.2	Unbalance Response	44
2.2	Application to Cantilever-Sleeve Rotor-Bearing System	46
2.2.1	Approximate Solutions to Whirl Speeds	50
2.2.2	Synchronous Whirl	56
2.2.3	Finite Element Modeling	60
2.2.4	Numerical Results	66
2.2.5	Comparison of Results and Discussion	68
 CHAPTER 3 EFFICIENT HIGHER ORDER BASIS FUNCTIONS FOR FINITE ELEMENT DYNAMIC ANALYSIS OF BEAMS		 78
3.1	Bending of Beams	78
3.1.1	Euler-Bernoulli Beam Theory	78
3.1.2	Integral Formulation and Interpolation	80
3.2	Finite Element Model with Efficient Higher Order Basis Functions	80
3.2.1	Governing Equation	80

3.2.2	Domain Discretization	81
3.2.3	Derivation of Element Equation	82
3.2.3.1	Weak Form	82
3.2.3.2	Illustration Using a Beam Example	86
3.2.3.3	Interpolation Functions	89
3.3	Formulation of the Eigenvalue Problem	94
3.3.1	Free Lateral Vibration of Beam	94
3.3.2	Finite Element Model	97
3.3.3	Assembly of Element Equations	103
3.3.4	Imposition of Boundary Conditions	108
3.3.5	Natural Frequencies of Uniform Beams with Various End Conditions	110
3.3.5.1	Applications	111
3.4	Discussion of Results	119

**CHAPTER 4 DYNAMIC ANALYSIS OF ROTOR-BEARING SYSTEMS
USING FINITE ELEMENTS WITH EFFICIENT HIGHER
ORDER BASIS FUNCTIONS**

4.1	Introduction	129
4.2	System Configuration and Coordinates	129
4.3	Component Equations	132
4.3.1	The Rigid Disk	132

4.3.2	Finite Shaft Element with Efficient Higher Order Basis	
	Functions	134
4.4	Bearings	149
4.5	System Equations of Motion	149
	4.5.1 Whirl Speed Analysis	150
4.6	Industrial Application	151
	4.6.1 Simple Rotor Model	151
	4.6.1.1 Determination of the Model	151
	4.6.1.2 Critical Speeds of a Uniform Shaft	154
	4.6.2 Finite Element Model	159
	4.6.2.1 Conventional Finite Element Model	159
	4.6.2.2 Finite Element Model With Efficient Higher	
	Order Basis Functions	159
4.7	Numerical Results and Discussion	169
CHAPTER 5 SUMMARY AND CONCLUSIONS		172
5.1	The Conclusions of the present investigation	174
5.2	Recommendations for Future Work	175
REFERENCES		176
APPENDIX I SIGN CONVENTIONS FOR THE DEFLECTIONS OF		

BEAM AND SHAFT

185

APPENDIX-II

**DERIVATIONS INVOLVED IN THE FORMULATION
OF FINITE ELEMENT WITH EFFICIENT HIGHER
ORDER BASIS FUNCTIONS**

191

LIST OF FIGURES

Figure 2.1	Typical system configuration	22
Figure 2.2	Euler's angles of rotation of the disk	22
Figure 2.3	Typical finite rotor element and coordinates	29
Figure 2.4	Cantilever-sleeve rotor	45
Figure 2.5a	Overhung rotor mounted on a light flexible shaft	46
Figure 2.5b	General angular motion of a rotor	48
Figure 2.5c	Angular momentum vectors for the system shown in figure (2.5b)	48
Figure 2.6	Approximate model of an overhung rotor	51
Figure 2.7	Effects of disk inertia on critical speed of a simple overhung rotor	59
Figure 2.8a	System configuration of cantilever-sleeve rotor-bearing system	63
Figure 2.8b	Cantilever-sleeve rotor-bearing finite element model and schematic	63
Figure 2.9	Forms of system arrays for the dual shaft support structure	65
Figure 2.10	Unbalance response of cantilever-sleeve rotor-bearing system	69
Figure 2.11a	Steady state unbalance response in fixed frame coordinates, plot of deflection	70

Figure 2.11b	Steady state unbalance response in fixed frame coordinates, plot of slope	70
Figure 3.1	Bending of a beam	79
Figure 3.2	Discretization of the beam using Euler-Bernoulli beam elements	79
Figure 3.3	The generalized displacement and generalized forces on a typical element	79
Figure 3.4	Interpolation functions N_i , $i = 1 \dots 8$	93
Figure 3.5	First derivatives of interpolation functions N_1 to N_8	93
Figure 3.6	Second derivatives of interpolation functions, N_5 , N_6 , N_7 and N_8	94
Figure 3.7	Third derivatives of interpolation functions N_5 and N_7	94
Figure 3.8	Sign convention for the beam	95
Figure 3.9a	Two-element model of a Cantilever beam in global coordinates	102
Figure 3.9b	Assembly of two beam finite elements in local coordinates	102
Figure 3.10	The inter-element continuity of nodal degrees of freedom	105
Figure 3.11	One-element model of a beam	112
Figure 3.12	Two-element model of a beam	114
Figure 3.13	Convergence of a finite element solution based on the efficient basis functions for a cantilever beam	120
Figure 4.1a	Typical finite element with eight degrees of freedom	136
Figure 4.1b	Coordinates of typical finite rotor element	136

Figure 4.2	Model of the rotor	152
Figure 4.3	Uniform beam represented as a three station lumped mass model	152
Figure 4.4	Equal lumped mass model	152
Figure 4.5	Six-element finite element model	160
Figure 4.6	Three-element finite element model	160
Figure 4.7	Cantilever-sleeve rotor-bearing system using finite element with efficient basis functions	160

LIST OF TABLES

Table 2.1	Critical speeds of a non-rotating uniform cantilever shaft with a non-rotating disk at the end	71
Table 2.2	Critical speeds of a stationary uniform cantilever shaft with a rotating disk at the end	71
Table 2.3	Critical speeds of a rotating uniform cantilever shaft with a rotating disk at the end	72
Table 2.4	Critical speeds of a cantilever-sleeve rotor-bearing system	72
Table 2.5	Comparison of critical speeds obtained using finite elements	73
Table 2.6	Critical speeds of a stationary uniform cantilever shaft with a rotating disk at the end	74
Table 2.7	Critical speeds of a rotating uniform cantilever shaft with a rotating disk at the end	74
Table 3.1	Various boundary conditions of a beam	109
Table 3.2	Natural frequencies of a cantilever beam, obtained using meshes of one and two finite elements with efficient basis functions	117
Table 3.3	Natural frequencies of a cantilever beam, obtained using conventional finite elements	118
Table 3.4	Comparison of the results using the present method with those using conventional finite elements	119
Table 3.5	Natural frequencies of a cantilever beam using finite elements	121

	with efficient basis functions	
Table 3.6	Natural frequencies of a simply-supported beam using finite elements with efficient basis functions and conventional finite elements	122
Table 3.7a	Natural frequencies of a beam with both ends free, using conventional finite elements	123
Table 3.7b	Natural frequencies of a beam with both ends free, using finite element with efficient basis functions	124
Table 3.8	Natural frequencies of a beam with one end pinned and the other free, using finite elements with efficient basis functions and conventional finite elements	125
Table 3.9	Natural frequencies of a beam with one end fixed and the other pinned, using finite elements with efficient basis functions	126
Table 3.10	Natural frequencies of a beam with one end fixed and the other pinned using conventional finite elements	127
Table 3.11	Natural frequencies of a beam with both ends fixed, using finite elements with efficient basis functions and conventional finite elements	128
Table 4.1	Critical speed of a simply supported uniform steel shaft	158
Table 4.2	Critical speeds of a simply supported rotor system with no disk, zero compressive load or bearing pressure and zero bearing spring constant, using conventional finite elements	162
Table 4.3	Critical speeds of a simply supported rotor-disk system	162

	including the mass of the disk using conventional finite elements; $M_d = 16.47$ kg	
Table 4.4	Critical speeds of a simply supported rotor-disk system including the mass moment of inertia of the disk using conventional finite elements; $M_d = 16.47$ kg, $I_d = 9.427 \times 10^{-2}$ kg m ² and $I_p = 0.1861$ kg m ²	163
Table 4.5	Critical speeds of a simply supported rotor-shaft system including the mass moments of inertia of the disk using conventional finite elements; $M_d = 16.47$ kg, $I_d = 0.09427$, $I_p = 0.1861$ kg m ² , $k = 10^7$ N/m and $P = 9689.48$ N	163
Table 4.6	Critical speeds of a simply supported rotor-shaft system including the mass moments of inertia of the disk, bearing spring constant and Compressive load using conventional finite elements with gyroscopic effect; $M_d = 16.47$ kg, $I_d = 0.09427$ kg m ² and $I_p = 0.1861$ kg m ² , $k = 10^7$ N/m and $P = 9689.48$ N	164
Table 4.7	Critical speeds of a simply supported rotor system with no disk, zero compressive load or bearing pressure and zero bearing spring constant using finite elements with efficient basis functions	164
Table 4.8	Critical speeds of a simply supported rotor-disk system including the mass of the disk using finite elements with efficient basis functions; $M_d = 16.47$ kg	165

Table 4.9	Critical speeds of a simply supported rotor-disk system including the mass moment of inertia of the disk using finite elements with efficient basis functions; $M_d=16.47$ kg and $I_d = 0.09427$ kg m ²	165
Table 4.10	Critical speeds of a simply supported rotor-shaft system including the mass moments of inertia of the disk using finite elements with efficient basis functions; $M_d=16.47$ kg, $I_d= 0.09427$ kg m ² , $I_p=0.1861$ kg m ² , $k=10^7$ N/m and $P=9689.48$ N	166
Table 4.11	Critical speeds of a simply supported rotor system with no disk, zero compressive load or bearing pressure and zero bearing spring constant using beam theory, conventional finite element method and finite element with efficient basis functions, respectively	166
Table 4.12	Critical speeds of a simply supported rotor-shaft system including the mass moments of inertia of the disk using a mesh of six conventional finite elements and a mesh of three finite elements with efficient basis functions; $M_d=16.47$ kg, $I_d= 0.09427$ kg m ² , $I_p=0.1861$ kg m ² , $k=10^7$ N/m and $P=9689.48$ N	167
Table 4.13	Critical speeds of a non-rotating cantilever-sleeve rotor-bearing system using mesh of two elements using finite elements with efficient basis functions	167
Table 4.14	Critical speeds of a non-rotating cantilever-sleeve rotor-	168

bearing system using a mesh of twelve conventional finite elements and a mesh of two finite elements with efficient basis functions

NOMENCLATURE

A		cross-section area
$B(u, w), B(w, w)$		bilinear form of the weak form
a, b, c		coordinates of the rotor system
b		$= EI =$ bending stiffness
$[C^b], [K^b]$		bearing damping and stiffness matrices
$C_{xx}^b, C_{xy}^b, C_{yx}^b, C_{yy}^b$		elements of $[C^b]$
E		Young's modulus
$(F, G), (f, g)$		forces in $(Y, Z), (y, z)$ directions
F		shear force
h		thickness
$[I]$		identity matrix
I		area moment of inertia of the beam cross-section about neutral axis
I_p^e		polar moment of inertia of element as a rigid body
$I(u), I(w)$		linear form of the weak form
$I_e(w)$		potential energy
J, T		kinetic energy
$k_{xx}^b, k_{xy}^b, k_{yx}^b, k_{yy}^b$		elements of $[K^b]$
$k_{rr}, k_{r\psi}, k_{\psi\psi}$		stiffness influence coefficients
L		length of the beam
$[M], [G], [K]$		assembled mass, gyroscopic, and stiffness matrices
$[\hat{M}] [\hat{G}] [\hat{K}]$		transformed mass, gyroscopic and stiffness matrices

$(M, N), (m, n)$	moments in $(Y, Z), (y, z)$ directions
M_d, I_d, I_p	disk mass, diametral inertia, polar inertia
M	bending moment
N_i	interpolation function ($i= 1$ to 8)
P	axial load
$p(x)$	distributed load
$\{Q\}, \{P\}$	external force vector relative to \mathcal{J} and \mathcal{R} frame
$\{q_c\}, \{q_s\}$	unbalance response associated with $\cos\Omega t, \sin\Omega t$
$\{Q_c\}, \{Q_s\}$	unbalance force associated with $\cos\Omega t, \sin\Omega t$
Q_i	generalized force (i 1 to 4)
$\{q\}, \{p\}$	displacement vector relative to \mathcal{J} and \mathcal{R} frame
$[R]$	orthogonal rotation matrix
r	element length
t	time
U	strain energy
$u(x)$	weight function
V	primary variables at global node
$(V, W), (v, w)$	translation in $(Y, Z), (y, z)$ directions
$\{v\}$	primary variables at local node $\{w \ \theta \ F \ M\}^T$
w	displacement
X, Y, Z	Coordinates of the rotor system
x	axial position along an element
$(B, \Gamma), (\beta, \gamma)$	small angle rotation about $(Y, Z), (y, z)$ axes

$[\Phi]$	matrix of rotation displacement function; $\psi_i'(s) \ i = 1 \dots 8$
$\Omega, d\phi/dt$	spin speed
$[\Psi]$	matrix of translation displacement functions; $\psi_i(s) \ i = 1 \dots 8$
α	eigenvalue
δW	virtual work of external forces
ϕ	spin angle
η_d, ζ_d	location of disk mass center in b, c directions
$\eta(x), \zeta(x)$	location of shaft mass center eccentricity
η_L, ζ_L	$= \eta(0), \zeta(0)$ = location of shaft mass center eccentricity at the left end
η_R, ζ_R	$= \eta(r), \zeta(r)$ = location of shaft mass center eccentricity at the right end
$\lambda = \Omega/\omega$	whirl ratio
$\mu = \rho A$	element mass per unit length
θ	slope of the beam
ρ	mass density
σ_d	shaft element diametral inertia per unit length
σ_p	shaft element polar inertia per unit length
ω	whirl speed
ω_n	natural frequency
ω_s	natural frequency (zero spin)
$\omega_a, \omega_b, \omega_c$	angular rate components of \mathcal{N} relative to \mathcal{F}
\mathcal{N}	cross-section reference frame (abc)
\mathcal{F}	fixed reference frame (XYZ)

\mathcal{R}	rotating reference frame (xyz)
ϕ	potential energy
(\prime)	differentiation with respect to position
(\bullet)	differentiation with respect to time

Superscripts

b	bearing
c	condensed
d	disk
e	element
n	mode number
s	system
T	transpose

Subscripts

A	axial load
B	bending
c	cosine
d	disk
L, R	left and right
R	rotational
s	sine
T	translational

CHAPTER 1

INTRODUCTION, LITERATURE REVIEW, OBJECTIVE AND SCOPE

1.1 Introduction

Rotor Dynamics is the study of the dynamic behavior of the machines and components resulting from excitations originating from its rotating parts, and has a very important role to play throughout the modern industrial world. Rotating machinery is used in many applications such as in turbo-machines, power stations, machine tools, automobiles and aerospace applications. The interaction of these machines with their surroundings is of great importance due to the fact that if these machines are not operating at the correct speeds, vibration can occur and may ultimately cause failure of the machines. Many investigations in linear rotor dynamics deal with the problems of natural, unbalance and transient vibrations.

Simple rotor systems may be analyzed using exact analytical methods. However, complex rotor systems normally used in industries are not amenable to exact analysis. It is necessary to follow some approximate methods to study the dynamic behavior of complex rotor systems.

Powerful approximation methods, such as the *finite element method*, are available for analyzing complex structures. In most cases, a fine discretization of the rotor model is necessary which leads to a large set of simultaneous and coupled linear differential equations for the unknown displacements. With such large systems the calculation is

very time consuming, which may not be economically feasible. Therefore methods are needed which would allow a reduction and possibly a de-coupling of the equations. One of the classical techniques used for calculating the response of non-rotating elastic systems with symmetric and proportional damping is known as modal analysis. The idea is to reduce a system of simultaneous and coupled ordinary differential equations into a set of independent ordinary differential equations. The successful application of the method requires the solution of an eigenvalue problem associated with the given system.

In rotor dynamics, the governing equations are non-self-adjoint as a result of the gyroscopic effects, and the classical modal analysis fails to uncouple them. The system matrices, when constructed in stationary (inertial) coordinates, are characterized by the presence of skew symmetric parts due to gyroscopic effects and internal damping, and non-symmetric terms due to journal bearing properties; this leads to non-self-adjoint eigenvalue problems. On the other hand, when the system matrices are formed in rotating (body fixed) coordinates, skew symmetric parts are introduced due to Coriolis terms and external damping as well as gyroscopic effects, and there are periodic parameters due to bearing properties; this makes the modal analysis even more difficult. Another difficulty in modal analysis arises from the fact that the elements of system matrices generally depend on the rotational speed. Reduction methods such as Guyan reduction and component mode synthesis can also be used to reduce the number of equations or to reduce the coupling between equations.

1.2 Literature Review

1.2.1 The Dynamics of Rotor-Bearing Systems

Typical analysis of rotor-dynamic systems includes the determination of the free vibration natural frequencies, modes of whirl and the stability characteristics of these modes. The critical speeds of a rotor system are defined as rotating assembly spin speeds, which provide excitations that coincide with one of the system's natural frequencies, thereby producing a resonant condition.

Earlier work on the prediction of critical speeds of rotors was introduced by Jeffcott [1], where the rotor system was modeled as a single mass mounted on a shaft supported on identical bearings and the equations of motion were solved by the direct method. The model was improved by Green [2] by introducing the gyroscopic effects on the critical speeds of simple rotor systems. There has been an impressive progress in the study of rotor dynamics in the past years. Current state-of-the-art methods for calculating the natural frequencies and critical speeds are based on either a Holzer-Myklestad-Prohl shaft model or a finite element model, both of which may be applied to quite general shaft-disk systems.

The use of finite elements for the simulation of rotor systems makes it possible to formulate increasingly complex problems, and the recent advances in digital computers make the numerical solutions of large-order problems feasible. Flexible rotor-bearing systems have been analyzed by various mathematical methods. Ruhl's [3] contribution to utilize a finite element model to a turbo-rotor system to study stability and unbalance

response was the precursor to many studies using finite element approach on rotor dynamics problems. His model includes only elastic bending energy and translational kinetic energy. In these early investigations the effects of rotary inertia, gyroscopic moments, shear deformations, axial load, and internal damping were neglected. Thorkildsen [4] included rotary inertia and gyroscopic moment, for the first time.

Polk [5] used a Rayleigh beam finite element in his work. Thomas and Dokumaci [6] analyzed pre-twisted blade vibration using simple finite elements. Krishna Murty [7] analyzed the rotating structure elements using finite element technique. Chivens and Nelson [8] carried out studies to determine the influence of disk flexibility on the transverse bending natural frequencies and critical speeds of a rotating shaft-disk system.

The use of finite elements for analyzing rotor-bearing systems and the basic concepts and development of the equation of motion for a rotating finite shaft element were presented by Nelson and McVaugh [9]. It includes the effects of rotatory inertia, gyroscopic moments, and axial load using consistent mass matrix approach. In addition, the element and system equations are presented in both fixed and rotating reference frames. Zorzi and Nelson [10] used finite element modeling of rotor-bearing system to establish the Lagrangian equations of motion in a fixed frame.

One factor that might need to be considered in the design/development stages of a rotor system is the effect of axial torque. Krishna Murty and Sridhara Murty [11] presented the finite element method for the natural vibration analysis of rotors with taper and pretwist. Zorzi and Nelson [12] investigated the effect of constant axial torque on the dynamics of rotor-bearing systems using the finite element model. The inclusion of the axial torque gave rise to an incremental torsional stiffness matrix. The model was used to

determine the static buckling torque and the critical speeds of a uniform shaft for short and long bearing. This paper presented a finite element model, which included axial torque and thereby allowed for a more reliable prediction of lateral shaft dynamics. A finite rotating shaft element using Timoshenko beam theory, which was developed by Nelson [13] was used to find out the critical speeds and the system's natural frequencies. Ozguven [14] generalized the combined effects of rotary inertia, gyroscopic moment, axial load, shear deformations and internal hysteretic and viscous damping in the same model. Ozguven [15] developed an approximate method to find out the critical speed of the shaft-disk system from a single degree-of-freedom model.

Most analyses utilize linear equations of motion based on amplitude motions in the neighborhood of an equilibrium configuration. In some cases, however, the strength of the nonlinearities is so large that linearization does not provide sufficiently accurate simulations. In these cases, the most common approach is to integrate the nonlinear equations of motion numerically either directly in physical coordinates or in modal coordinates. Nelson, Meacham et al [16] analyzed this kind of problem in terms of modal coordinates associated with some form of component mode synthesis. When the set of differential equations is nonlinear, analytical solutions are generally not possible. Those special cases with known closed-form solutions are usually weakly nonlinear and of a small order. For large-order nonlinear problems, such as multi-shaft flexible rotor systems, only a few options are available to the analyst for obtaining solution. Exact solutions are not possible, except in very special cases, and approximate solutions can only be obtained numerically. There are several procedures, other than numerical integration, that have been utilized for searching for the possible response of large order

systems, and these are also briefly discussed by Padovan and Adams [17]. Although several authors using the finite element method over the last 25 years have investigated the effects of various factors on the dynamics of rotor-bearing systems, there is no published work that could incorporate all the boundary conditions.

The other common approach for analyzing the dynamics of rotor-bearing systems is called the state vector transfer matrix method or simply the transfer matrix method. This method is particularly well suited for “chainlike” structures such as large-order multi-shaft rotor systems. The first use of this method is usually attributed to Holzer in the area of torsional vibrations. Subsequent contributors to such formulation are Myklestad, [18] and Prohl [19] who adapted the procedure to lateral vibrations of beams and rotor systems. Prohl extended the direct method and presented the first calculation of synchronous whirling of complex shafts consisting of variable shaft sections with multiple disks. Prohl’s method is still considered as one of the best in the general class of transfer matrix method and also one of the most practical and widely used solution schemes for today’s complex rotor-bearing systems. Lund [20] has presented procedures for the use of this method for almost all aspects of rotor dynamic analysis. Kikuchi [21] solved a multi disk rotor system using the transfer matrix method. Most recently Rao [22] analyzed the rotor systems using time marching transfer matrix technique. Other refinements have made this a reliable and widely used analytical procedure for engine manufacturers and rotor dynamics experts throughout the world. Murphy and Vance [23] have shown that by rearranging the calculations performed in the transfer matrix method that it is possible to calculate the coefficients of the characteristic polynomial directly.

Another most widely used method by several investigators to study the behavior

of rotor-bearing systems is the experimental modal analysis. In experimental modal analysis the modal properties of the system such as mass, stiffness and damping are determined experimentally, which are used to obtain the dynamic characteristics of the rotor. Gunter, Choy and Allaire [24] used the planar modes of the rotor system without the effects of disk gyroscopics, damping of rotor and cross-coupled bearing properties. Berthier, Ferraris and Lalanne [25] have studied the behavior of rotor systems using finite element model employing modes of the rotor at rest. Glasgow and Nelson [26] presented the so-called modal component mode method in conjunction with complex model analysis. Bhat [27] developed the complex modal analysis technique for simple rotor systems supported on fluid film bearings with the absence of physical damping. All modal reduction techniques reduce the size of system matrices. Round-off errors associated with extensive system mass and stiffness matrix reductions are very high in these operations.

1.2.2 Higher Derivatives as Nodal Degrees of Freedom

In 1744 Euler obtained a differential equation for the lateral vibration of bars and determined the functions known now as *normal functions* and the equation we now call the *frequency equation* for beams with free, clamped, or simply supported ends.

The first systematic treatise on vibration was written by Lord Rayleigh [28]. He formalized the idea of normal functions, as introduced by Daniel Bernoulli and Clebsch, and introduced the ideas of generalized forces and generalized coordinates. He further introduced systematically the concepts of energy and approximate methods in vibration

analysis, without solving differential equations. Rayleigh improved the classical theory by allowing for the effects of rotary inertia of the cross-sections of the beam. Timoshenko [29] extended the theory to include the effects of shear deformation. The resulting equations are known as the Timoshenko beam equations.

Prescott [30] and Volterra [31] suggested, by independent reasoning, various Timoshenko-type beam models. Solutions of Timoshenko equations for a cantilever beam of rectangular cross section have been given by Sutherland and Goodman [32] and also by Huang [33]. Anderson [34] and Dolph [35] gave a general solution and complete analysis of a simply supported uniform beam. Huang [33] gave frequency equations and normal modes of vibration for various cases of a beam using homogeneous boundary conditions. Ritz and Galerkin methods were used by Huang [36] to obtain frequencies of simply supported beams. The finite difference method was used by Thomas [37] to obtain frequencies of vibration of uniform, tapered and pretwisted Timoshenko beams with fixed-free end conditions.

A number of finite element models have been presented for the analysis of Euler-Bernoulli and Timoshenko beams by various investigators. Many of them experienced difficulties in incorporating all the boundary conditions. Although some authors claimed that their finite element model was designed to incorporate all the boundary conditions, none of them so far have been able to apply them in practice. The various possible true boundary conditions are as follows: (a) free end—zero bending moment and zero shear force; (b) hinged end—zero total deflection and zero bending moment; (c) fixed end—zero total deflection and zero bending slope. The conditions of deflection and slope are caused by restraints or external forces applied and can be referred to as forced boundary

(or displacement or geometric) conditions while the others can be referred to as the natural boundary (or force) conditions.

McCalley [38] derived consistent mass and stiffness matrices by selecting total deflection, w , and total slope $\partial w/\partial x$, as nodal co-ordinates. Archer [39] used these matrices to obtain frequencies of a cantilevered Timoshenko beam, using the boundary conditions at the fixed end to be $w = \partial w/\partial x = 0$. The condition $\partial w/\partial x = 0$ at this end is not valid as only bending slope is zero and not that due to shear deflection. Boundary conditions at the free end were not and could not be applied in this model.

Kapur [40] improved on this model by taking bending deflection, shear deflection, bending slope and shear slope as the nodal co-ordinates, and derived the stiffness and mass matrices. Frequency parameters also were obtained for cantilevered and simply supported beams. The true boundary conditions were applied only at the fixed end. At the free end the shear force is assumed to be zero but the condition of zero bending moment could not be imposed. For the hinged end the bending deflection and shear deflection were assumed zero but again the zero bending moment condition could not be applied. Although it is an improvement over Archer's [39] model it still lacked the facility of applying the true boundary condition in all the cases.

Carnegie, Thomas and Dokumaci [41] presented an internal node element considering the total deflection and bending slope as the co-ordinates at the two terminal nodes and two internal nodes, thus giving eight degrees of freedom element. This, however, lacked the facility to impose the natural boundary conditions at the free end. Egle [42] presented an approximate Timoshenko beam theory designed to eliminate the coupling between shear deformation and rotary inertia. He postulated a constraint,

consistent with Euler—Bernoulli theory, that the shear force be given by the first derivative of bending moment. This constraint implies that this theory is valid only when shear deformation is negligible in comparison to the bending deformation.

Nickel and Secor [43] derived stiffness and mass matrices for what they called TIM7 element, using total deflection, total slope and bending slope as the nodal coordinates and the bending slope at mid point, giving rise to matrices of order seven. The boundary conditions used for a cantilever beam were the same as Kapur's [40], and thus again the zero bending moment condition at the free end was missing. Nickel and Secor [43] further reduced the order of the matrix from seven to four by using the constraint postulated by Egle [42]. This element was referred to as TIM 4. The natural boundary conditions at the free end could not be applied to this element.

Davis, Henshell and Warburton [44] used an element model similar to TIM 4 with the same approximation and constraint postulated by Egle [42]. The stiffness matrix was obtained from the static equilibrium condition based on a cubic polynomial for total deflection. This has the same limitations as TIM 4 model in that the natural boundary conditions at the free end or hinged end could not be applied. Thomas and Abbas [45] developed an element model with total deflection, slope, bending slope and the first derivative of bending slope as nodal co-ordinates. This model is capable of incorporating all the forced and natural boundary conditions associated with various end conditions. Then again this model is proven for dynamic analysis of Timoshenko beam element only.

The development of higher order tapered beam element was carried out to study the axial vibration of a bar by Yang and Sun [46], transverse impact problems by Sun and Huang [47] and vibration analysis of uniform beams by Fried [48]. They all claim that

improved accuracy can be obtained more efficiently with an increase in the number of degrees of freedom in the element.

To [49] had developed expressions for mass and stiffness matrices of two higher order tapered beam elements for vibration analysis. In his paper, the element properties (namely, the mass and stiffness matrices) of a beam finite element are presented in which a seventh degree polynomial displacement function is used. Representing four degrees of freedom per node (the transverse displacement w , the slope $\partial w/\partial x$, the curvature $\partial^2 w/\partial x^2$, and the gradient of curvature $\partial^3 w/\partial x^3$) are derived and the explicit expressions for the mass and stiffness matrices are given. These element properties are subsequently used for the vibration analysis of mast antenna structures individually treated as a tapered cantilever beam with a mass, incorporating rotary inertia, attached to its free end. Hou, Tseng and Ling [50] developed a new finite element model of a Timoshenko beam to analyze the free vibration of uniform beams. An important characteristic of the model is that the natural boundary conditions are included in the element formulation. Houmat [51] presented a 2-node Timoshenko beam finite element with variable degrees of freedom. Comparisons are made with exact Timoshenko beam finite element solution. Comparison shows that using one or two variable order Timoshenko beam element with a few trigonometric terms yields better accuracy with fewer system degrees of freedom than using many polynomials.

A number of Timoshenko beam finite elements in which only polynomial terms are used to describe the element degree of freedom are available in the literature. Dawe [52] presented a new Timoshenko beam finite element and reviewed the other existing elements. Dawe [52] suggested that an increase in efficiency would result if finite

element of order higher than those used in previous Timoshenko beam models were utilized. Many authors have shown the desirability of using higher order finite element for vibration problems. Quintic displacement function was first considered by Handa [53]. Thomas and Dokumaci [54] have shown that the higher order finite element yield improved results for the vibration of tapered beams. In their work two improved tapered elements for vibration analysis were derived using quintic polynomial displacement function. Results are compared with those given by the basic cubic polynomial approximation and analytical solutions for various end conditions. Pestel [55] on the other hand, studied the effect of imposing nodal continuity of successively higher derivatives of deflection and noted that such family of elements can be formulated simply by the use of Hermitian polynomials of orders higher than the fourth. The fourth order Hermitian leads to the basic elements.

Cook, Malkus and Plesha [56] have mentioned that for achieving the minimally acceptable degree of inter-element compatibility, it is necessary to define “essential” degrees of freedom (d.o.f) as the particular nodal d.o.f. More details about essential nodal d.o.f are discussed in chapter 3: for example, u_i and v_i for bars and plane elements, w_i and θ_i for beam elements. We define a “higher derivative” as one that is not needed to define inter-element compatibility. Thus, in the axial deformation of a bar or in plane stress, all derivatives of u and v would be considered “higher.” In bending of a beam or a thin plate, higher derivatives are second and higher order derivatives of lateral displacement, which are the force and moment. The author further says that those elements with higher-derivative d.o.f. have certain advantages. They are based on fields having many generalized coordinates, and hence they provide good accuracy in a coarse

mesh. However, elements having higher-derivative d.o.f are sometimes awkward to use. At an elastic-plastic boundary, or where there is an abrupt change in stiffness or material properties, continuity of higher derivatives d.o.f. must not be enforced. For example, if two beam elements of different stiffnesses are joined, they have the same moment but different curvatures at the node they share. A maneuver appropriate to such a situation is to release the curvature d.o.f in one of the elements before assembly. But by doing so, we reduce the benefit of these d.o.f where it is most needed-near a high-stress gradient.

To seek for a more accurate solution Akin [57] and Reddy [58] have developed a fifth order Hermite polynomial. The Hermite family includes members with additional derivatives at the two ends. This has three variables per node: deflection, rotation and moment. For a two node finite element, the equation of deflection, the shape function (C^2) and the element stiffness matrices are given. A comparison of result is presented. Also the author had developed the Hermitian interpolation in unit coordinates for a 7-th order polynomial (C^3). In the work by Reddy [58] it is said that, if higher order (higher than cubic) approximation of w is desired, one must identify additional dependent (primary) unknowns at each of the two nodes. In addition to that we must note that the cubic polynomial that interpolates w at four nodal points (two internal and two end nodes) of the element is not admissible, although the continuity conditions are met, because the polynomial does not satisfy the second set of end conditions.

Shames and Dym [59] have gone one step further and given a common form to develop C^l or higher connectivity between elements for a one-dimensional element. They suggest further that one may use the Hermite polynomial element, where $w(x)$ as well as derivatives $dw/dx, d^2w/d^2x, \dots, d^p w/d^p x$ at the nodes can be considered as degrees of

freedom, and not just the field variable as was the case of Lagrange interpolation functions. First consider a linear element with ends 1 and 2 of length r . The field variable w and its derivations up to $(m-1)$ are to be degrees of freedom at the ends of the element. Then

$$\begin{aligned}
 w = & N_1 w_1 + N_2 \left(\frac{dw}{dx} \right)_1 + \dots + N_m \left(\frac{d^{m-1}w}{dx^{m-1}} \right)_1 \\
 & + N_{m+1} w_2 + N_{m+2} \left(\frac{dw}{dx} \right)_2 + \dots + N_{2m} \left(\frac{d^{m-1}w}{dx^{m-1}} \right)_2
 \end{aligned} \tag{1.1}$$

where the N 's are the Hermite polynomials. To construct the proper interpolation function, they use a polynomial representation for each N_i of order $2m-1$ and having $2m$ constants. That is, using normalized coordinates $s = x/r$, we have

$$N_i = (C_1)_i + (C_2)_i s + (C_3)_i s^2 + \dots + (C_{2m})_i s^{(2m-1)} \tag{1.2}$$

1.3 Objectives of the Thesis

The objectives of the present investigation is primarily to develop an efficient and economical method to obtain the critical speeds and the unbalance response of a cantilever-sleeve rotors using higher order finite elements. By using this technique the size of the system equations of such complex rotor can be reduced without affecting the dynamic characteristics of the system and allow the use of all the natural and essential boundary conditions right in the basis functions at the time of element formulation.

This thesis presents a finite element model with nodal degrees of freedom that can

incorporate the entire essential (such as deflection and slope) and natural (such as moment and shear force) boundary conditions of a rotor shaft. The mass and stiffness matrices of the element are derived from kinetic and strain energies by assigning polynomial expressions for total deflection and bending slope. The superiority of this element is illustrated by comparing the results with conventional finite element model.

The material properties, geometric properties and boundary conditions dictate the behavior of a mechanical component or structure. For a given material and configuration, the boundary conditions significantly influence the static as well as its dynamic response. The displacement-based finite element method provides an adequate representation of material and structural configuration. When complex aircraft structures are analyzed using finite element method, any deviations from the actual conditions at the boundaries will give erroneous results, particularly, at higher frequencies. Moreover, such errors are magnified in obtaining the stress values in the structure.

A beam of length L has two boundary conditions at each end. The state of every section of a beam is completely specified if we specify position (w), slope ($\partial w/\partial x$), moment ($EI \partial^2 w/\partial x^2$) and shear ($EI \partial^3 w/\partial x^3$). Two conditions relating the four are usually known at every boundary section. In the displacement-based finite element method, it is possible to represent only the geometrical boundary conditions such as displacements and slopes at the element formulation level. The natural boundary conditions, which are the moments and shear forces at the boundaries, should be represented through imposition of boundary conditions after assembly. If the basic functions are derived considering all the boundary conditions at the nodes, the resulting elements will lead to achieving more accurate results even with a coarser mesh, which in turn will result in computational

advantages.

The present study aims at developing finite elements, which would accept natural boundary conditions such as moments and shear forces right in the element formulation. Thus, this element adequately represents all the physical situations involved in any combination of displacement, rotation, bending moment and shearing force. The explicit element mass and stiffness matrices eliminate the loss of computer time and round-off errors associated with extensive matrix operations, which are necessary in the numerical evaluation of these expressions. Further, the deflection pattern within each element is represented using an appropriate polynomial. This will be done in a way to increase the accuracy of the result, particularly the stress values in the structure. The approach and methodology are demonstrated through a one-dimensional problem, i.e., beam flexure and a two-dimensional problem, i.e., rotor dynamics. Furthermore, in general the eigenvalues obtained by employing the higher order elements converge more rapidly to the exact solution than those obtained by using the lower order elements.

The development of this higher order beam-shaft element is motivated by two main factors. First, the vibration analysis of uniform beams with improved accuracy can be obtained more efficiently with an increase of the number of degrees of freedom in the element rather than with an increase of the number of elements having fewer degrees of freedom. Furthermore, in general, finite elements based on lower degree polynomial displacement functions incorporate only crude curvature distributions and usually yield discontinuous bending moments between elements. Moreover, the increased effort devoted to the initial finite element formulation will yield higher benefits in the analysis stage for complex systems such as a cantilever-sleeve rotor.

1.4 Scope of the Present Investigation

Chapter 1 provided a brief introduction and then made a survey of the literature where rotor dynamics studies were carried out using finite element methods. Further some discussion on attempts to use higher order finite elements was given. Chapter 1 also provides the objectives of the thesis and the scope.

Chapter 2 develops basic finite element mathematical formulations including the effects of rotatory inertia, gyroscopic moments, and axial load for a rotating shaft element. The finite-element method consists in the determination of the equation of motion and its solution. The equation of motion is a matrix equation. The formulation of the matrices of the model from the element matrices is shown in this chapter. The element equation of motion is presented in both fixed and rotating frames. The vibration behavior of shafts with disk is dealt with in Chapter 2, using cantilever-sleeve rotor system. The solution of the eigenvalue problem is reduced to a standard form, similar to that corresponding to the non-gyroscopic system by a method developed by Meirovitch [60].

Chapter 3 gives a basic and reasonably complete development of higher order beam finite elements and interpolation functions and the application of the higher order beam elements to the transverse vibration of simply supported beam structure. The treatment of higher order finite elements was expanded to reflect the importance of rotor-bearing system. The mathematical formulation of finite element solutions to free vibrations and transient response is developed.

Chapter 4, which is devoted to applications of new higher order finite element,

presents a finite element application to free vibration of an overhung sleeve rotor system. The thesis ends with Chapter 5, which provides some of the conclusions and some recommendations for future work.

CHAPTER 2

DYNAMIC ANALYSIS OF ROTORS USING CONVENTIONAL FINITE ELEMENTS

2.1 Conventional Finite Element Formulation

2.1.1 Introduction

A finite element analysis of a cantilever-sleeve rotor-bearing system is presented in this chapter, taking into account the rotary inertia, gyroscopic moment and axial force. The equation of motion for the finite-element model and its solution are obtained. Initially the geometric configuration illustrated in figure 2.1 was modeled as a Bernoulli-Euler beam carrying disks at discrete locations and discrete bearings. The special case of a non-rotating shaft carrying a rotating disk at its tip is analyzed using both Rayleigh and Dunkerley methods for a quick estimation of its critical speed. Finally the cantilever-sleeve rotor is modeled and analyzed.

2.1.2 Gyroscopic Whirling of a Simple Rotor

In a Jeffcott rotor, the disk is assumed to be placed between the bearings at the center of the shaft for simplicity. Since the slope is always zero at the disk location when the rotor undergoes dynamic flexural displacements, the disk has no rotational motion

about its diametral axes and hence only the translational motion of the disk is considered. In general, however, the disks may not be mounted at the middle, and hence besides the displacement of the disk, its rotation about diametral axes must also be considered. As a result its moment of inertia and gyroscopic effect are called into play.

This gyroscopic couple effect changes the bending moment equations across the mass. If the disks are located at nodal points, their gyroscopic effects are predominant, because there is a precession of the disk corresponding to the changes in slope, which is maximum at this location. At anti-nodal points, there is a pure translation of the disk and there is no gyroscopic effect, because of zero slope. Hence for overhung rotors, with disk at the free end, the gyroscopic couple has considerable influence on their dynamic behavior. The gyroscopic moment has the effect of making the natural frequencies dependent on rotor rotational speed, while at the same time increasing their value. The co-rotating (forward) modes tend to increase in frequency as the spin speed magnitude increases due to a gyroscopic stiffening effect, while the counter-rotating (backward) modes tend to decrease in frequency. The effect of gyroscopic couple on the bending critical speeds of a cantilever-sleeve rotor supported on radially rigid bearings is considered in this chapter. In this configuration the axial torque and shear deformation are neglected. In addition, the element and system equations are presented in both fixed and rotating reference frames.

2.1.3 System Configuration and Coordinates

The basic elements of a rotor are the disk, the shaft, the bearings and the seals. Kinetic

energy expressions are necessary to characterize the disk, shaft and unbalances, if any. Strain energy is necessary to characterize the shaft. The forces due to bearings or seals are used to calculate their virtual work, and then corresponding forces acting on the shaft are obtained. The general rotor equations are provided by means of the following:

- The kinetic energy T , the strain energy U and the virtual work δW of external forces for the elements of the system.
- Lagrange's equations are applied in the following form:

$$\frac{d}{dt} \left(\frac{\partial T}{\partial \dot{q}_i} \right) - \frac{\partial T}{\partial q_i} + \frac{\partial U}{\partial q_i} = F_i$$

where i (1 to N) is the number of degrees of freedom, q_i are generalized independent coordinates, F_i are generalized forces, and the over-dot denotes differentiation with respect to time t .

- Two reference frames are utilized to describe the system equations of (see figure 2.1). The $XYZ: \mathfrak{S}$ ($xyz: \mathfrak{R}$) triad is a fixed (rotating) reference with the X and x -axis being co-linear and coincident with the undeformed rotor centerline. \mathfrak{R} is defined relative to \mathfrak{S} by single rotation ωt about X with ω denoting the whirl speed.

A typical cross section of the rotor in a deformed state is defined relative to the fixed frame \mathfrak{S} by the translation $V(s, t)$ and $W(s, t)$ in the Y and Z directions, respectively. In order to locate the elastic centerline further, the small angle rotations $B(s, t)$ and $\Gamma(s, t)$ about Y and Z -axes, respectively, are used which to orient the plane of the cross-section. The cross section also spins normal to its face relative to frame \mathfrak{S} .

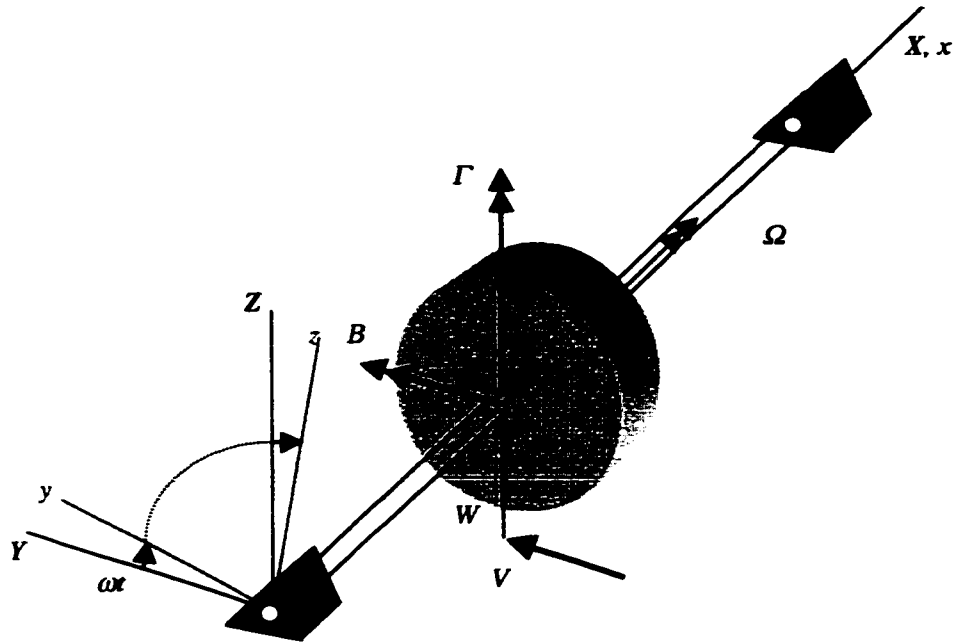


Figure 2.1 Typical system configuration

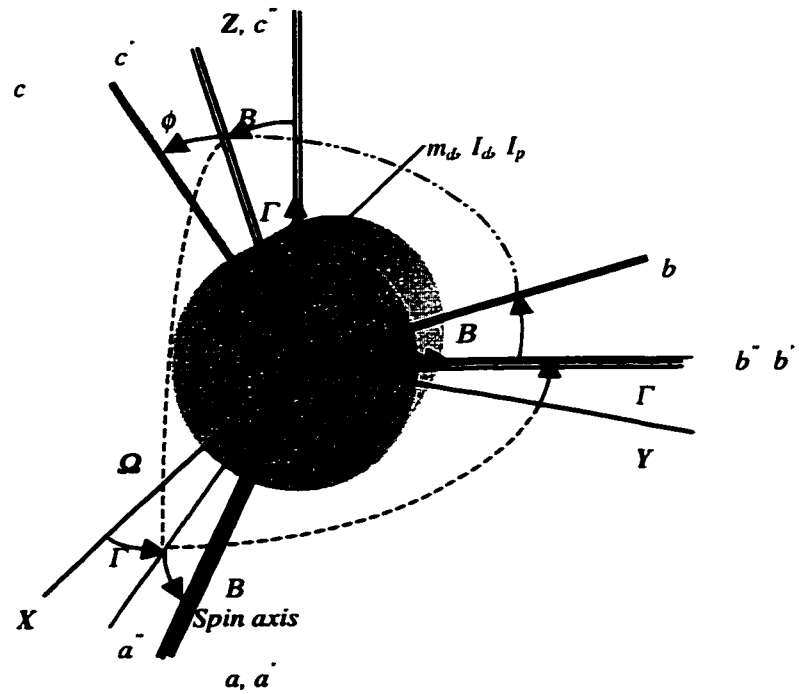


Figure 2.2 Euler's angles of rotation of the disk

The $abc:\mathfrak{R}$ triad is attached to the cross-section with the “ a ” axis normal to the cross-section. \mathfrak{R} is defined by the three successive rotations. (figure 2.2)

1. Γ about Z defines $a'' b'' c''$
2. B about b'' defines $a' b' c'$
3. ϕ about a' defines abc ,

and the angular rate of rotation relative to frame \mathfrak{S} is

$$\begin{Bmatrix} \omega_a \\ \omega_b \\ \omega_c \end{Bmatrix} = \begin{bmatrix} -\sin B & 1 & 0 \\ \cos B \sin \phi & 0 & \cos \phi \\ \cos B \cos \phi & 0 & -\sin \phi \end{bmatrix} \begin{Bmatrix} \dot{\Gamma} \\ \dot{\phi} \\ \dot{B} \end{Bmatrix} \quad (2.1)$$

For small deformation the (B, Γ) rotations are approximately co-linear with the (Y, Z) axes, respectively. The spin angle ϕ , for a constant speed system and negligible torsional deformation, is Ωt where Ω denotes the rotor spin speed.

At a given point the rotor has four degrees of freedom: two displacements v and w , two slopes about the Y and Z -axes which are, respectively, β and γ . The displacements (v, w, β, γ) relative to \mathfrak{R} of a typical cross section are transformed to corresponding displacements (V, W, B, Γ) relative to \mathfrak{S} by the orthogonal transformation

$$\{q\} = [R] \{p\} \quad (2.2)$$

with

$$\{q\} = \begin{Bmatrix} V \\ W \\ B \\ \Gamma \end{Bmatrix}, \quad \{p\} = \begin{Bmatrix} v \\ w \\ \beta \\ \gamma \end{Bmatrix} \quad (2.3a)$$

$$[R] = \begin{bmatrix} \cos \omega t & -\sin \omega t & 0 & 0 \\ \sin \omega t & \cos \omega t & 0 & 0 \\ 0 & 0 & \cos \omega t & -\sin \omega t \\ 0 & 0 & \sin \omega t & \cos \omega t \end{bmatrix} \quad (2.3b)$$

and for later use the first two time derivatives of equation (2.2) are given below:

$$\{\dot{q}\} = \omega[S]\{p\} + [R]\{\dot{p}\} \quad (2.4a)$$

$$\{\ddot{q}\} = [R]\left(\{\ddot{p}\} - \omega^2\{p\}\right) + 2\omega[S]\{\dot{p}\} \quad (2.4b)$$

where

$$[S] = (1/\omega) [dR/dt] \quad (2.4c)$$

$$[S] = \begin{bmatrix} -\sin \omega t & -\cos \omega t & 0 & 0 \\ \cos \omega t & -\sin \omega t & 0 & 0 \\ 0 & 0 & -\sin \omega t & -\cos \omega t \\ 0 & 0 & \cos \omega t & -\sin \omega t \end{bmatrix} \quad (2.4d)$$

$$\frac{d[S]}{dt} = -[R]\omega \quad (2.4e)$$

2.1.4 Component Equations

Nelson and McVaugh [9] and Zorzi and Nelson [10] presented the basic concept and development of the equations of motion for a rotating finite shaft element. In these studies, a fixed frame (XYZ) triad, as shown in figure 2.1, was used to establish the Lagrangian equations of motion. The typical rotor-bearing system is considered to comprise a set of interconnecting components consisting of rigid disk, rotor segments with distributed mass and elasticity, and linear bearings. For finite element analysis of the rotor bearing system, the rotor shaft segments are often modeled by beam elements, which include shaft rotation effects. Generally the axi-symmetric geometry of rotor elements gives the same mass and stiffness matrices in both the X - Y and the X - Z planes. The kinetic and potential energy expressions for an element are established. The finite rotor element equation of motion is developed in an analogous manner by specifying spatial shape functions and then treating the rotor element as an integration of an infinite set of differential disks.

2.1.4.1 The Rigid Disk

The disk is assumed to be rigid and is then characterized solely by its kinetic energy. The mass of the disk is m_d and its tensor of inertia, defined about its center O with xyz being the principal directions of inertia, is denoted by $[I]$. It is given by

$$I = \begin{bmatrix} I_p & 0 & 0 \\ 0 & I_d & 0 \\ 0 & 0 & I_d \end{bmatrix} \quad (2.5)$$

The kinetic energy of a typical rigid disk with mass center coincident with the elastic rotor centerline is given by the expression

$$J_d = \frac{1}{2} \begin{Bmatrix} \dot{V} \\ \dot{W} \end{Bmatrix}^T \begin{bmatrix} m_d & 0 \\ 0 & m_d \end{bmatrix} \begin{Bmatrix} \dot{V} \\ \dot{W} \end{Bmatrix} + \frac{1}{2} \begin{Bmatrix} \omega_a \\ \omega_b \\ \omega_c \end{Bmatrix}^T \begin{bmatrix} I_d & 0 & 0 \\ 0 & I_d & 0 \\ 0 & 0 & I_p \end{bmatrix} \begin{Bmatrix} \omega_a \\ \omega_b \\ \omega_c \end{Bmatrix} \quad (2.6a)$$

which can be simplified here since the disk is symmetric, the angles Γ and B are small, and the angular velocity is constant; that is, $d\phi/dt = \Omega$. The use of equation (2.6a), with the retention of only second order terms, becomes

$$J_d = \frac{1}{2} \begin{Bmatrix} \dot{V} \\ \dot{W} \end{Bmatrix}^T \begin{bmatrix} m_d & 0 \\ 0 & m_d \end{bmatrix} \begin{Bmatrix} \dot{V} \\ \dot{W} \end{Bmatrix} + \frac{1}{2} \begin{Bmatrix} \dot{B} \\ \dot{\Gamma} \end{Bmatrix}^T \begin{bmatrix} I_d & 0 \\ 0 & I_d \end{bmatrix} \begin{Bmatrix} \dot{B} \\ \dot{\Gamma} \end{Bmatrix} - \dot{\phi} \dot{\Gamma} B I_p \quad (2.6b)$$

where the term $\frac{1}{2} I_d \Omega^2$, which is a constant, has no influence in the equations and represents the energy of the disk rotating at Ω , all the other displacements being zero. The last term, represents the gyroscopic (Coriolis) effect.

The Lagrangian equation of motion of the rigid disk using equation (2.6b) and the constant spin speed restriction, $d\phi/dt = \Omega$, is

$$([M_T^d] + [M_R^d])\{\ddot{q}^d\} - \Omega[G^d]\{\dot{q}^d\} = \{Q^d\} \quad (2.7a)$$

where

$$[M_T^d] = \begin{bmatrix} m_d & 0 & 0 & 0 \\ 0 & m_d & 0 & 0 \\ 0 & 0 & 0 & 0 \\ 0 & 0 & 0 & 0 \end{bmatrix}, \quad [M_R^d] = \begin{bmatrix} 0 & 0 & 0 & 0 \\ 0 & 0 & 0 & 0 \\ 0 & 0 & I_d & 0 \\ 0 & 0 & 0 & I_d \end{bmatrix} \quad (2.7b)$$

$$[G_d] = \begin{bmatrix} 0 & 0 & 0 & 0 \\ 0 & 0 & 0 & 0 \\ 0 & 0 & 0 & I_p \\ 0 & 0 & -I_p & 0 \end{bmatrix} \quad (2.7c)$$

Equation (2.7a) is the equation of motion of the rigid disk referred to frame \mathfrak{S} with the forcing term including mass unbalance, interconnection forces, and other external effects on the disk. For the disk mass center located at (η_d, ζ_d) relative to \mathfrak{N} , the unbalance force in frame \mathfrak{S} is

$$\begin{aligned} \{Q^d\} &= \begin{Bmatrix} \eta_d \\ \zeta_d \\ 0 \\ 0 \end{Bmatrix} \cos \Omega t + \begin{Bmatrix} -\zeta_d \\ \eta_d \\ 0 \\ 0 \end{Bmatrix} \sin \Omega t \\ &= \{Q_c^d\} \cos \Omega t + \{Q_s^d\} \sin \Omega t \end{aligned} \quad (2.8)$$

By using equations (2.2), (2.3) and (2.4) and premultiplying by $[\mathbf{R}]^T$, equation (2.7a) yields

$$\begin{aligned}
& \left([M_T^d] + [M_R^d] \right) \left\{ \ddot{p}^d \right\} + \omega \left(2 \left([\hat{M}_T^d] + [\hat{M}_R^d] \right) - \lambda [G^d] \right) \left\{ \dot{p}^d \right\} \\
& - \omega^2 \left(\left([M_T^d] + [M_R^d] \right) + \lambda [\hat{G}^d] \right) \left\{ p^d \right\} = \left\{ P^d \right\}
\end{aligned} \tag{2.9a}$$

For the case of a thin disk ($I_p = 2I_d$) equation (2.9a) transforms to

$$\begin{aligned}
& \left([M_T^d] + [M_R^d] \right) \left\{ \ddot{p}^d \right\} + \omega \left(2 \left([\hat{M}_T^d] + [\hat{M}_R^d] \right) + (1 - \lambda) [G^d] \right) \left\{ \dot{p}^d \right\} \\
& - \omega^2 \left([M_T^d] + (1 - 2\lambda) [M_R^d] \right) \left\{ p^d \right\} = \left\{ P^d \right\}
\end{aligned} \tag{2.9b}$$

Equation (2.9) is the equation of motion of a rigid disk referred to \mathfrak{R} with whirl ratio $\lambda = \Omega/\omega$. The term $-\omega^2 \left([M_R^d] + [M_T^d] + \lambda [G^d] \right) \{p^d\}$ contains the so-called Green's [2] gyroscopic stiffening effect.

2.1.4.2 Finite Shaft Element

A typical cross section of finite rotor element is illustrated in figure 2.3. The shaft is modeled as a beam with a uniform circular cross-section. It should be noted here that the time-dependent element cross-section displacements (V, W, B, Γ) are also functions of position x along the axis of the element. The finite element used has two nodes, and hence the matrices are of eighth order, including four displacements and four rotations. The rotations (B, Γ) are related to the translations (V, W) by the equations

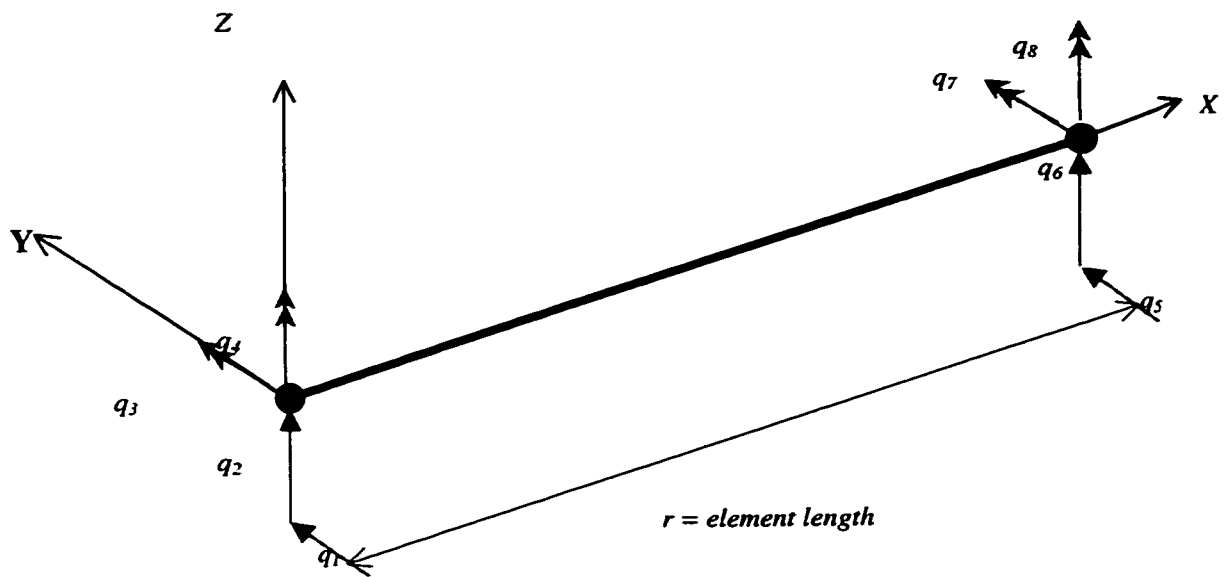
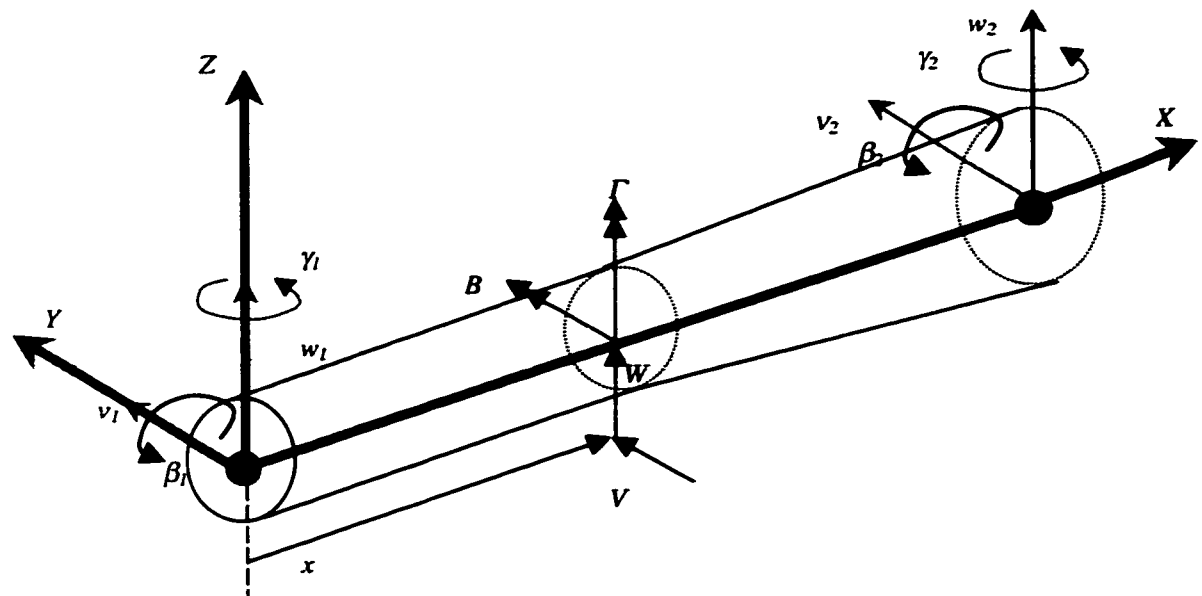


Figure. 2.3 Typical finite rotor element and coordinates

$$B = -\frac{\partial W}{\partial x} \quad (a) \quad (2.10)$$

$$\Gamma = \frac{\partial V}{\partial x} \quad (b)$$

and the nodal displacement vector is

$$\{p_1^e\} = \begin{Bmatrix} v_1 \\ w_1 \\ \beta_1 \\ \gamma_1 \end{Bmatrix}, \quad \{p_2^e\} = \begin{Bmatrix} v_2 \\ w_2 \\ \beta_2 \\ \gamma_2 \end{Bmatrix} \quad (2.11)$$

which includes the displacements $\{p_y\}$ and $\{p_z\}$ corresponding, respectively, to the motions in the Y and Z directions: that is

$$\{p_y^e\} = \{v_1, \gamma_1, v_2, \gamma_2\}^T \quad (2.12a)$$

$$\{p_z^e\} = \{w_1, \beta_1, w_2, \beta_2\}^T \quad (2.12b)$$

The coordinates $(q_1^e, q_2^e, \dots, q_8^e)$ are the time-dependent end point displacements (translations and rotations) of the finite element and are indicated in figure 2.3.

The translation of a typical point internal to the element is approximated by the relation

$$\begin{Bmatrix} V(x,t) \\ W(x,t) \end{Bmatrix} = [P(x)]\{q^e(t)\} \quad (2.13)$$

where the spatial constraint matrix $[\Psi(x)]$ is given by

$$[\Psi] = \begin{bmatrix} \psi_1 & 0 & 0 & \psi_2 & \psi_3 & 0 & 0 & \psi_4 \\ 0 & \psi_1 & -\psi_2 & 0 & 0 & \psi_3 & -\psi_4 & 0 \end{bmatrix} \quad (2.14)$$

and is a matrix of displacement functions. In this case the individual functions represent the static displacement modes associated with a unit displacement of one of the end point coordinates with all others being constrained to zero. These functions are

$$\begin{aligned} \psi_1 &= 1 - 3\left(\frac{x}{r}\right)^2 + 2\left(\frac{x}{r}\right)^3 & (a) \\ \psi_2 &= x \left[1 - 2\left(\frac{x}{r}\right) + \left(\frac{x}{r}\right)^2 \right] & (b) \\ \psi_3 &= 3\left(\frac{x}{r}\right)^2 - 2\left(\frac{x}{r}\right)^3 & (c) \\ \psi_4 &= r \left[-\left(\frac{x}{r}\right)^2 + \left(\frac{x}{r}\right)^3 \right] & (d) \end{aligned} \quad (2.15)$$

From the equations (2.10) and (2.13) the rotations of a typical cross section of the element can be expressed in the form

$$\begin{Bmatrix} B \\ \Gamma \end{Bmatrix} = [\Phi] \{q^e\} \quad (2.16)$$

with

$$[\Phi] = \begin{bmatrix} [\Phi_B] \\ [\Phi_r] \end{bmatrix} \quad (2.17a)$$

or

$$[\Phi] = \begin{bmatrix} 0 & -\psi'_1 & \psi'_2 & 0 & 0 & -\psi'_3 & \psi'_4 & 0 \\ \psi'_1 & 0 & 0 & \psi'_2 & \psi'_3 & 0 & 0 & \psi'_4 \end{bmatrix} \quad (2.17b)$$

representing a matrix of rotation shape functions.

For a differential disk located at distance x , the elastic bending, axial deformation and kinetic energy expressions are, respectively,

$$\begin{aligned} d\mathcal{E}_B^e &= \frac{1}{2} \begin{Bmatrix} V'' \\ W'' \end{Bmatrix}^T \begin{bmatrix} EI & 0 \\ 0 & EI \end{bmatrix} \begin{Bmatrix} V'' \\ W'' \end{Bmatrix} dx \\ d\mathcal{E}_A^e &= -\frac{1}{2} \begin{Bmatrix} V' \\ W' \end{Bmatrix}^T \begin{bmatrix} P & 0 \\ 0 & P \end{bmatrix} \begin{Bmatrix} V' \\ W' \end{Bmatrix} dx \\ dJ^e &= \frac{1}{2} \begin{Bmatrix} \dot{V} \\ \dot{W} \end{Bmatrix}^T \begin{bmatrix} \mu & 0 \\ 0 & \mu \end{bmatrix} \begin{Bmatrix} \dot{V} \\ \dot{W} \end{Bmatrix} dx + \frac{1}{2} \dot{\phi}^2 \sigma_p dx + \frac{1}{2} \begin{Bmatrix} \dot{B} \\ \dot{I} \end{Bmatrix}^T \begin{bmatrix} \sigma_d & 0 \\ 0 & \sigma_d \end{bmatrix} \begin{Bmatrix} \dot{B} \\ \dot{I} \end{Bmatrix} dx - \dot{\phi} \dot{I} B \sigma_p dx \end{aligned} \quad (2.18)$$

where μ is the mass per unit length of shaft and σ_d and σ_p are diametral and polar mass moments of inertia per unit length of shaft. By using the equations (2.13) and (2.16), equation (2.18) can be written in the matrix form as

$$\begin{aligned} d\mathcal{E}_B^e &= \frac{1}{2} EI \{q^e\}^T [\Psi''] [\Psi''] \{q^e\} dx \\ d\mathcal{E}_A^e &= -\frac{1}{2} P \{q^e\}^T [\Psi'] [\Psi'] \{q^e\} dx \\ dJ^e &= \frac{1}{2} \mu \{\dot{q}^e\}^T [\Psi] [\Psi] \{\dot{q}^e\} dx + \frac{1}{2} \dot{\phi}^2 \sigma_p dx + \frac{1}{2} \sigma_d \{\dot{q}^e\}^T [\Phi] [\Phi] \{\dot{q}^e\} dx \\ &\quad - \dot{\phi} \sigma_p \{\dot{q}^e\}^T [\Phi_r] [\Phi_B] \{\dot{q}^e\} dx \end{aligned} \quad (2.19)$$

The energy of the complete element is obtained by integrating equations (2.19) over the length of the element to obtain

$$\begin{aligned} \phi_B^e + \phi_A^e + J^e = & \frac{1}{2} \{q^e\}^T ([K_B^e] - [K_A^e]) \{q^e\} + \frac{1}{2} \{\dot{q}^e\}^T ([M_r^e] + [M_k^e]) \{\dot{q}^e\} \\ & + \frac{1}{2} I_p \dot{\phi}^2 + \dot{\phi} \{q^e\}^T [N^e] \{\dot{q}^e\} \end{aligned} \quad (2.20)$$

where

$$\begin{aligned} [M_r^e] &= \int_0^l \mu [\Psi]^T [\Psi] dx \\ [M_k^e] &= \int_0^l \sigma_d [\Phi]^T [\Phi] dx \\ [N^e] &= \int_0^l \sigma_p [\Phi_r]^T [\Phi_B] dx \\ [K_B^e] &= \int_0^l EI [\Psi''^T] [\Psi''] dx \\ [K_A^e] &= \int_0^l P [\Psi'^T] [\Psi'] dx \end{aligned} \quad (2.21)$$

For the case of a uniform cross-section element under constant axial load P with the identity $\sigma_p = 2\sigma_d = 2I$, the elements of the matrices of equations (2.21) are obtained as

$$M_T = \frac{\mu \cdot r}{420} \begin{bmatrix} 156 & 0 & 0 & 22 \cdot r & 54 & 0 & 0 & -13 \cdot r \\ 0 & 156 & -22 \cdot r & 0 & 0 & 54 & 13 \cdot r & 0 \\ 0 & -22 \cdot r & 4 \cdot r^2 & 0 & 0 & -13 \cdot r & -3 \cdot r^2 & 0 \\ 22 \cdot r & 0 & 0 & 4 \cdot r^2 & 13 \cdot r & 0 & 0 & -3 \cdot r^2 \\ 54 & 0 & 0 & 13 \cdot r & 156 & 0 & 0 & -22 \cdot r \\ 0 & 54 & -13 \cdot r & 0 & 0 & 156 & 22 \cdot r & 0 \\ 0 & 13 \cdot r & -3 \cdot r^2 & 0 & 0 & 22 \cdot r & 4 \cdot r^2 & 0 \\ -13 \cdot r & 0 & 0 & -3 \cdot r^2 & -22 \cdot r & 0 & 0 & 4 \cdot r^2 \end{bmatrix} \quad (2.21a)$$

$$M_R = \frac{\rho \cdot I}{30 \cdot r} \begin{bmatrix} 36 & 0 & 0 & 3 \cdot r & -36 & 0 & 0 & 3 \cdot r \\ 0 & 36 & -3 \cdot r & 0 & 0 & -36 & -3 \cdot r & 0 \\ 0 & -3 \cdot r & 4 \cdot r^2 & 0 & 0 & 3 \cdot r & -r^2 & 0 \\ 3 \cdot r & 0 & 0 & 4 \cdot r^2 & -3 \cdot r & 0 & 0 & -r^2 \\ -36 & 0 & 0 & -3 \cdot r & 36 & 0 & 0 & -3 \cdot r \\ 0 & -36 & 3 \cdot r & 0 & 0 & 36 & 3 \cdot r & 0 \\ 0 & -3 \cdot r & -r^2 & 0 & 0 & 3 \cdot r & 4 \cdot r^2 & 0 \\ 3 \cdot r & 0 & 0 & -r^2 & -3 \cdot r & 0 & 0 & 4 \cdot r^2 \end{bmatrix} \quad (2.21b)$$

$$N = \frac{\rho \cdot I}{15 \cdot r} \begin{bmatrix} 0 & -36 & 3 \cdot r & 0 & 0 & 36 & 3 \cdot r & 0 \\ 0 & 0 & 0 & 0 & 0 & 0 & 0 & 0 \\ 0 & 0 & 0 & 0 & 0 & 0 & 0 & 0 \\ 0 & -3 \cdot r & 4 \cdot r^2 & 0 & 0 & 3 \cdot r & -r^2 & 0 \\ 0 & 36 & -3 \cdot r & 0 & 0 & -36 & -3 \cdot r & 0 \\ 0 & 0 & 0 & 0 & 0 & 0 & 0 & 0 \\ 0 & 0 & 0 & 0 & 0 & 0 & 0 & 0 \\ 0 & -3 \cdot r & -r^2 & 0 & 0 & 3 \cdot r & 4 \cdot r^2 & 0 \end{bmatrix} \quad (2.21c)$$

$$K_B = \frac{b}{r^3} \begin{bmatrix} 12 & 0 & 0 & 6 \cdot r & -12 & 0 & 0 & 6 \cdot r \\ 0 & 12 & -6 \cdot r & 0 & 0 & -12 & 6 \cdot r & 0 \\ 0 & -6 \cdot r & 4 \cdot r^2 & 0 & 0 & 6 \cdot r & 2 \cdot r^2 & 0 \\ 6 \cdot r & 0 & 0 & 4 \cdot r^2 & -6 \cdot r & 0 & 0 & 2 \cdot r^2 \\ -12 & 0 & 0 & -6 \cdot r & 12 & 0 & 0 & -6 \cdot r \\ 0 & -12 & 6 \cdot r & 0 & 0 & 12 & 6 \cdot r & 0 \\ 0 & 6 \cdot r & 2 \cdot r^2 & 0 & 0 & 6 \cdot r & 4 \cdot r^2 & 0 \\ 6 \cdot r & 0 & 0 & 2 \cdot r^2 & -6 \cdot r & 0 & 0 & 4 \cdot r^2 \end{bmatrix} \quad (2.21d)$$

$$K_A = \frac{p}{30 \cdot r} \begin{bmatrix} 36 & 0 & 0 & 3 \cdot r & -36 & 0 & 0 & 3 \cdot r \\ 0 & 36 & -3 \cdot r & 0 & 0 & -36 & -3 \cdot r & 0 \\ 0 & -3 \cdot r & 4 \cdot r^2 & 0 & 0 & 3 \cdot r & -r^2 & 0 \\ 3 \cdot r & 0 & 0 & 4 \cdot r^2 & -3 \cdot r & 0 & 0 & -r^2 \\ -36 & 0 & 0 & -3 \cdot r & 36 & 0 & 0 & -3 \cdot r \\ 0 & -36 & 3 \cdot r & 0 & 0 & 36 & 3 \cdot r & 0 \\ 0 & -3 \cdot r & -r^2 & 0 & 0 & 3 \cdot r & 4 \cdot r^2 & 0 \\ 3 \cdot r & 0 & 0 & -r^2 & -3 \cdot r & 0 & 0 & 4 \cdot r^2 \end{bmatrix} \quad (2.21e)$$

The Lagrangian equations of motion for the finite rotor element using equation (2.20) and the constant spin speed restriction, $d\phi/dt = \Omega$, is

$$([M_T^c] + [M_R^c]) \{ \ddot{q}^c \} - \Omega [G^c] \{ \dot{q}^c \} + ([K_B^c] - [K_A^c]) \{ q^c \} = \{ Q^c \} \quad (2.22)$$

with

$$[G^c] = ([N^c] - [N^c]^T) \quad (2.23a)$$

$$G = \frac{\rho \cdot I}{15 \cdot r} \begin{bmatrix} 0 & -36 & 3 \cdot r & 0 & 0 & 36 & 3 \cdot r & 0 \\ 36 & 0 & 0 & 3 \cdot r & -36 & 0 & 0 & 3 \cdot r \\ -3 \cdot r & 0 & 0 & -4 \cdot r^2 & 3 \cdot r & 0 & 0 & r^2 \\ 0 & -3 \cdot r & 4 \cdot r^2 & 0 & 0 & 3 \cdot r & -r^2 & 0 \\ 0 & 36 & -3 \cdot r & 0 & 0 & -36 & -3 \cdot r & 0 \\ -36 & 0 & 0 & -3 \cdot r & 36 & 0 & 0 & -3 \cdot r \\ -3 \cdot r & 0 & 0 & r^2 & 3 \cdot r & 0 & 0 & -4 \cdot r^2 \\ 0 & -3 \cdot r & -r^2 & 0 & 0 & 3 \cdot r & 4 \cdot r^2 & 0 \end{bmatrix} \quad (2.23b)$$

and is referred to fixed frame coordinates. All the matrices of equation (2.22) are symmetric except the gyroscopic matrix $[G]$ in equation (2.23), which is skew symmetric. The force vector $\{Q\}$ includes mass unbalance, interconnection forces, and other element external effects. For the element with distributed mass center eccentricity $(\eta(x), \zeta(x))$, the equivalent unbalance force utilizing the consistent matrix approach introduced by Archer [61] is given by

$$\begin{aligned} \{Q^e\} &= \int \rho A \Omega^2 [\Psi]^T \left(\begin{Bmatrix} \eta(x) \\ \zeta(x) \end{Bmatrix} \cos \Omega t + \begin{Bmatrix} -\zeta(x) \\ \eta(x) \end{Bmatrix} \sin \Omega t \right) \\ &= \{Q_c^e\} \cos \Omega t + \{Q_s^e\} \sin \Omega t \end{aligned} \quad (2.24)$$

By assuming a linear distribution of the mass center locations in the finite rotor segment, the mass eccentricities in Y and Z directions measured at $t = 0$ for a differential disk located at distance x , a linear mass unbalance distribution over the element can be represented by the expressions,

$$\begin{aligned}
\eta(x) &= \eta_L \left(1 - \frac{x}{r}\right) + \eta_R \left(\frac{x}{r}\right) \\
\zeta(x) &= \zeta_L \left(1 - \frac{x}{r}\right) + \zeta_R \left(\frac{x}{r}\right)
\end{aligned}
\tag{2.25}$$

with (η_L, ζ_L) and (η_R, ζ_R) denoting the mass center eccentricity at $x = 0$ (left end) and $x = r$ (right end) in Y and Z directions, respectively. The equivalent unbalance force from equation (2.24) is presented in equation (2.26) as

$$\{Q_c^e\} = \rho A \Omega^2 \left\{ \begin{array}{c} \frac{7}{20} \eta_L r + \frac{3}{20} \eta_R r \\ \frac{7}{20} \zeta_L r + \frac{3}{20} \zeta_R r \\ -\frac{1}{20} \zeta_L r^2 - \frac{1}{30} \zeta_R r^2 \\ \frac{1}{20} \eta_L r^2 + \frac{1}{30} \eta_R r^2 \\ \frac{3}{20} \eta_L r + \frac{7}{20} \eta_R r \\ \frac{3}{20} \zeta_L r + \frac{7}{20} \zeta_R r \\ \frac{1}{30} \zeta_L r^2 + \frac{1}{20} \zeta_R r^2 \\ -\frac{1}{30} \eta_L r^2 - \frac{1}{20} \eta_R r^2 \end{array} \right\}, \quad \{Q_s^e\} = \rho A \Omega^2 \left\{ \begin{array}{c} -\frac{7}{20} \zeta_L r - \frac{3}{20} \zeta_R r \\ \frac{7}{20} \eta_L r + \frac{3}{20} \eta_R r \\ -\frac{1}{20} \eta_L r^2 - \frac{1}{30} \eta_R r^2 \\ -\frac{1}{20} \zeta_L r^2 - \frac{1}{30} \zeta_R r^2 \\ -\frac{3}{20} \zeta_L r - \frac{7}{20} \zeta_R r \\ \frac{3}{20} \eta_L r + \frac{7}{20} \eta_R r \\ \frac{1}{30} \eta_L r^2 + \frac{1}{20} \eta_R r^2 \\ \frac{1}{30} \zeta_L r^2 + \frac{1}{20} \zeta_R r^2 \end{array} \right\}
\tag{2.26}$$

Equation (2.22) is transformed to whirl frame coordinates by using equations (2.2), (2.3) and (2.4) extended to include eight coordinates (four coordinates in each direction) at each end of the element.

$$\begin{aligned}
& \left([M_\tau^c] + [M_R^c] \right) \left([R] \left\{ \ddot{p} \right\} - \omega^2 \left\{ p \right\} \right) + 2\omega [S] \left\{ \dot{p} \right\} - \Omega [G^c] \left(\omega [S] \left\{ p \right\} + [R] \left\{ \dot{p} \right\} \right) \\
& + \left([K_B^c] - [K_A^c] \right) [R] \left\{ p \right\} = \left\{ P^c \right\}
\end{aligned} \tag{2.27}$$

After premultiplying by $[R]^T$ and rearranging, one gets

$$\begin{aligned}
& \left([M_\tau^c] + [M_R^c] \right) \left\{ \ddot{p} \right\} + \left(2\omega [R]^T [M_\tau^c] [S] + 2\omega [R]^T [M_R^c] [S] - \Omega [G] \right) \left\{ \dot{p} \right\} \\
& + \left(\left([K_B^c] - [K_A^c] \right) - \omega^2 \left([M_\tau^c] + [M_R^c] \right) - \omega \Omega [R]^T [G] [S] \right) \left\{ p \right\} = \left\{ P^c \right\}
\end{aligned} \tag{2.28}$$

In addition, since $[R]^T [R] = [I]$, we get

$$[R]^T [M_R^c] [S] = \frac{1}{2} [G^c] \tag{2.29}$$

Finally, for the case of a symmetric shaft (i.e. $\sigma_p = 2\sigma_d = 2I$) the transformed equation

(2.28) becomes

$$\begin{aligned}
& \left([M_\tau^c] + [M_R^c] \right) \left\{ \ddot{p}^c \right\} + \omega \left(2[\hat{M}_\tau^c] + (1 - \lambda)[G^c] \right) \left\{ \dot{p}^c \right\} \\
& + \left(\left([K_B^c] - [K_A^c] \right) - \omega^2 \left([M_\tau^c] + (1 - 2\lambda)[M_R^c] \right) \right) \left\{ p^c \right\} = \left\{ P^c \right\}
\end{aligned} \tag{2.30}$$

where $\Omega/\omega = \lambda$, and

$$[\hat{M}_\tau^c] = [R]^T [M_\tau^c] [S] \tag{2.31}$$

2.1.4.3 Bearings

The coupling between forces and displacements, and between slopes and bending moments are neglected here. The equations are limited to those which obey the governing equations of the form

$$[C^b] \left\{ \dot{q}^b \right\} + [K^b] \left\{ q^b \right\} = \{Q^b\} \quad (2.32)$$

in fixed frame coordinates, where

$$\{q^b\} = \begin{Bmatrix} V \\ W \end{Bmatrix}, [K^b] = \begin{bmatrix} k_{yy} & k_{yz} \\ k_{zy} & k_{zz} \end{bmatrix}, [C^b] = \begin{bmatrix} c_{yy} & c_{yz} \\ c_{zy} & c_{zz} \end{bmatrix}$$

and $\{Q^b\}$ is the bearing external force vector. Using equation (2.2) in equation (2.32) and premultiplication by $[R]^T$ gives the transformed form

$$[R]^T [C^b] [R] \left\{ \dot{p}^b \right\} + [R]^T [K^b] [R] \left\{ p^b \right\} = \{P^b\} \quad (2.33)$$

in whirl frame coordinates. For orthotropic bearings $k_{yz} = k_{zy} = 0$. For isotropic bearings, however, equation (2.33) reduces to an equation with constant coefficients,

$$c[I] \left\{ \dot{p}^b \right\} + k[I] \left\{ p^b \right\} = \{P^b\} \quad (2.34)$$

where c and k are the isotropic bearing damping and stiffness coefficients, respectively.

2.1.5 System Equations of Motion

The assembled undamped system equation of motion, consisting of component equations of the form of equations (2.7), (2.22) and (2.23) is

$$[M^s] \{ \ddot{q}^s \} - \Omega [G^s] \{ \dot{q}^s \} + [K^s] \{ q^s \} = \{ Q^s \} \quad (2.35)$$

in fixed frame coordinates.

For computational purposes equation (2.35) can be written in a matrix form as [62]

$$\begin{bmatrix} [0] & [M^s] \\ [M^s] & -\Omega [G^s] \end{bmatrix} \begin{Bmatrix} \{ \ddot{q} \} \\ \{ \dot{q} \} \end{Bmatrix} + \begin{bmatrix} [-M^s] & [0] \\ [0] & [K^s] \end{bmatrix} \begin{Bmatrix} \{ \dot{q} \} \\ \{ q \} \end{Bmatrix} = \begin{Bmatrix} \{ 0 \} \\ \{ Q^s \} \end{Bmatrix} \quad (2.36)$$

The matrices have band structure with an overlapping of the element matrices. The mass matrix is symmetric as for non-rotating structures, and describes the translatory and rotary inertial behavior of the rotor. However the gyroscopic matrix is skew-symmetric. If we ignore the internal damping (oil film) the stiffness matrix is symmetric.

2.1.6 Solution of System Equations

For a specified set of shaft spin speeds, the system equations are generated. Whirl speeds can be determined from the solution of the eigenvalue problem resulting from the free vibration equation

$$[M^r] \{ \ddot{q}^r \} - \Omega [G^r] \{ \dot{q}^r \} + [K^r] \{ q^r \} = 0 \quad (2.37)$$

The boundary conditions are then imposed at the left and right boundary points of each shaft. Typical boundary conditions at the ends for the xz plane are as follows:

$$\text{fixed} \quad w = \beta = 0$$

$$\text{simply supported} \quad w = 0$$

Analogous conditions exist for the xy plane. After the introduction of the appropriate boundary conditions, the eigenvalue problem associated with equation (2.37) can be reduced to a standard form, similar to that corresponding to the non-gyroscopic system, by a method suggested by Meirovitch [60]. It is possible to rewrite equation (2.37) as

$$[M^*] \{ \dot{h} \} + [G^*] \{ h \} = 0 \quad (2.38)$$

where

$$[M^*] = \begin{bmatrix} [M] & [0] \\ [0] & [K] \end{bmatrix}, \quad [G^*] = \begin{bmatrix} \Omega [G] & [K] \\ -[K] & [0] \end{bmatrix}, \quad \{ h \} = \begin{Bmatrix} \{ \dot{q} \} \\ \{ q \} \end{Bmatrix}$$

are $2n \times 2n$ real non-singular matrices, the first being symmetric and the second skew symmetric. Moreover, $[M]^*$ is positive definite. By introducing

$$[K]^* = [G]^{*T} [M]^{*-1} [G]^* \quad (2.39)$$

the eigenvalue problem can be reduced to one in terms to two real symmetric matrices, similar in form to the standard form as

$$[K]^* \{u\} = \lambda [M]^* \{u\} \quad (2.40)$$

where $\lambda = \omega^2$. Moreover, because $[M]^*$ and $[K]^*$ are positive definite all eigenvalues λ , are positive.

2.1.6.1 Whirl Speed Analysis

Consider the homogeneous case of equation (2.35). For an assumed solution of the form,

$$\begin{Bmatrix} \{\dot{q}\} \\ \{q\} \end{Bmatrix} = \{h\} = \{h_0\} e^{\alpha} \quad (2.41)$$

the associated eigenvalue problem is

$$\begin{bmatrix} [0] & [I] \\ -[K']^{-1} [M'] & \Omega [K']^{-1} [G'] \end{bmatrix} \{h_0\} = \frac{1}{\alpha} \{h_0\} \quad (2.42)$$

The eigenvalues of equation (2.42) appear as pure imaginary conjugate parts with the magnitude equal to natural whirl speed. The superposition of a solution with its conjugate represents an associated elliptical precession mode.

For whirl frame coordinates equation (2.35) transforms to the form

$$[M^s] \left\{ \ddot{p}^s \right\} + \omega (2[\hat{M}^s] - \lambda [G^s]) \left\{ \dot{p}^s \right\} + ([K^s] - \omega^2 ([M^s] + \lambda [\hat{G}^s])) \left\{ p^s \right\} = \left\{ P^s \right\} \quad (2.43)$$

The natural circular whirl speeds and mode shapes can be obtained from the homogeneous form of equation (2.43). For an undamped rotor with isotropic supports, the orbits of the natural modes of whirl are circular relative to the fixed XYZ reference frame. In a rotating xyz reference frame with a rotation rate equal to the whirl speed, the whirl mode appears as a fixed curve in a plane through the x axis. Because of the axial symmetry, the order of the system equations can be cut in half by taking this plane to be one of the coordinate planes, say, the xz plane. In other words, it is possible to consider one of the two planes of motion because the modes are constant relative to \mathfrak{R} and two planes of motion are 90 degrees apart. If we assume a constant solution $\{p^s\} = \{p_0\} =$ constant, the associated eigenvalue problem is

$$[K^s] \{p_0\} = \omega^2 ([M^s] + \lambda [\hat{G}^s]) \{p_0\} \quad (2.44)$$

The 2n eigenvalues are real and the positive values, ω_i , with associated vectors $\{p_0\}^i$ representing natural circular whirl speeds and mode shapes relative to \mathfrak{R} at the specified whirl ratio λ .

2.1.6.2 Unbalance Response

In fixed frame coordinates, the unbalance force in equation (2.35) is of the form

$$\{Q^s\} = \{Q_c^s\} \cos \Omega t + \{Q_s^s\} \sin \Omega t \quad (2.45)$$

Thus a steady state solution of the same form

$$\{q^s\} = \{q_c^s\} \cos \Omega t + \{q_s^s\} \sin \Omega t \quad (2.46)$$

substituted in equation (2.35) yields

$$\begin{aligned} \Omega^2 [M^s] \{q_c^s\} \cos \Omega t - \Omega^2 [G^s] \{q_s^s\} \cos \Omega t + [K^s] \{q_c^s\} \cos \Omega t \\ - \Omega^2 [M^s] \{q_s^s\} \sin \Omega t + \Omega^2 [G^s] \{q_c^s\} \sin \Omega t + [K^s] \{q_s^s\} \sin \Omega t = \{Q^s\} \end{aligned} \quad (2.47)$$

and identification of the terms in $\sin \Omega t$ and $\cos \Omega t$ in equations (2.47) and (2.45) gives the equation

$$\begin{Bmatrix} \{q_c^s\} \\ \{q_s^s\} \end{Bmatrix} = \begin{bmatrix} -\Omega^2 [M^s] + [K^s] & -\Omega^2 [G^s] \\ \Omega^2 [G^s] & -\Omega^2 [M^s] + [K^s] \end{bmatrix}^{-1} \begin{Bmatrix} \{Q_c^s\} \\ \{Q_s^s\} \end{Bmatrix} \quad (2.48)$$

The solution of equation (2.48) and back substitution into equation (2.46) provides the undamped system unbalance response for any value of Ω .

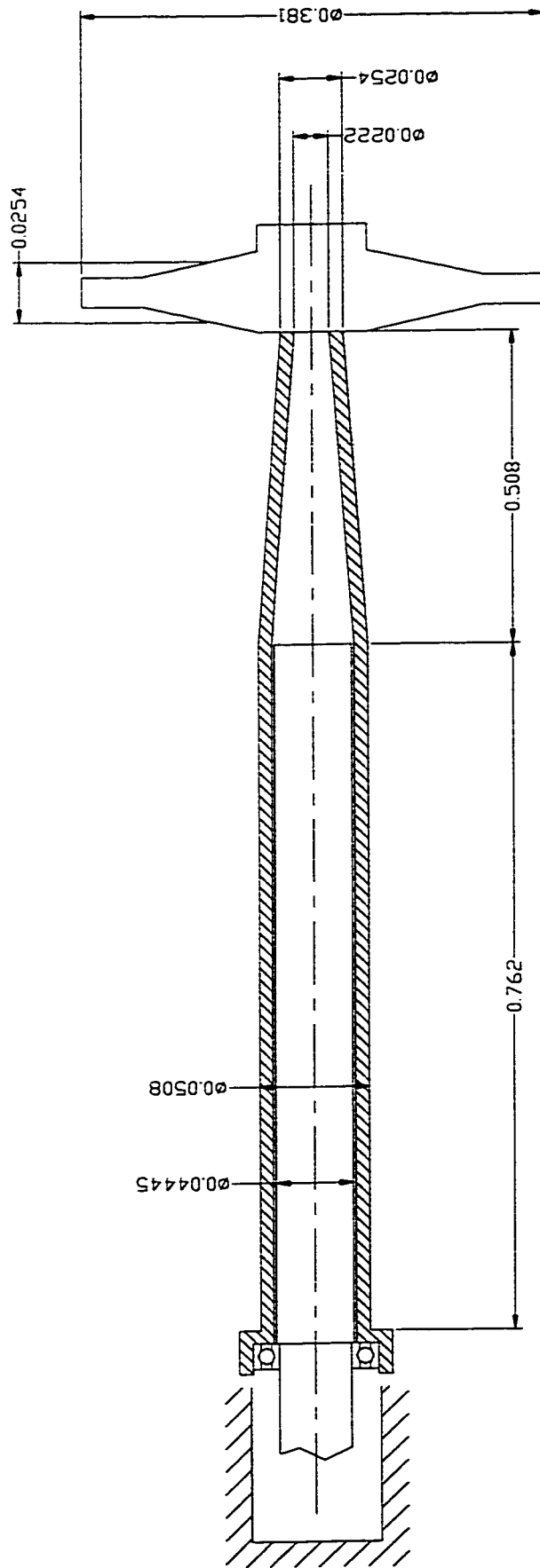


Figure 2.4 Cantilever-sleeve rotor

For whirl frame coordinates with isotropic bearings, the unbalance response is obtained from equation (2.43) with $\omega = \Omega$ (i.e., $\lambda = 1$). In this case the unbalance force in equation (2.43) is a constant relative to \mathfrak{R} and hence, the unbalance response is also a constant relative to \mathfrak{R} . From either of the two planes of motion (2.43) the undamped unbalance response is given by

$$\{p'\} = \left[[K'] - \Omega^2 ([M'] + [\hat{G}']) \right]^{-1} \{P'\} \quad (2.49)$$

2.2 Application to Cantilever-Sleeve Rotor-Bearing System

The method of analysis developed above is applied to an industrial cantilever-sleeve rotor in order to illustrate the concepts. The cantilever-sleeve rotor is shown in figure 2.4 and we study its free vibration. The problem illustrated has unique applications in the industry, for example, in cotton yarn winding, dental drill etc.

Three numerical examples selected from cantilever-sleeve rotor bearing system are given to demonstrate the gyroscopic effects on critical speeds. The solution is obtained for the following cases:

- (i) Natural frequency of a non-rotating uniform cantilever shaft with a non-rotating disk at the end.
- (ii) Whirl speeds of a non-rotating uniform cantilever shaft with a rotating disk at the end.
- (iii) Whirl speeds of a rotating uniform cantilever shaft with a rotating disk at the end (overhung rotor).
- (iv) Whirl speeds and unbalance response of a non-uniform cantilever-sleeve

rotor-bearing system with a non-rotating shaft, a rotating sleeve shaft and a rotating disk.

For problems described in case (ii), (iii) and (iv), the rotor mass is mounted on the shaft such that, at the location of the rotor, deflection of the shaft also tends to result in a change in slope of the shaft. Typically this might be the case when the rotor is overhung. When this is the case the deflected rotor forms a conical surface of revolution and centrifugal forces will act on the rotor mass as shown in figure 2.5a. The effect of these centrifugal forces is to straighten the shaft, constraining it to prevent any change of slope at the rotor location. Because of this the deflection of the shaft will not be significant and its stiffness will effectively increase; as a consequence there will be a corresponding increase in the system natural frequency.

Using the same notations as in this chapter, we consider the spinning disk at the end of the rotor, which is rotating at an angular velocity Ω and precessing about Y and Z axes with amplitudes γ and β , respectively, as shown in figure 2.5. Hence γ and β correspond to slopes of bending in the $X-Y$ and $X-Z$ planes, respectively. At the instant of time shown, the rotor is also precessing with angular velocity $\dot{\beta}$ about a vertical axis OZ . The precessional frequency will thus correspond to whirling frequency ω rad/sec. If we consider the OY axis, it can be seen that the change in angular momentum over the time interval considered is $I_p \Omega \dot{\gamma}$, and so the gyroscopic moment which must be applied to produce this change, equal to the rate of change of angular momentum, is given by $I_p \Omega \dot{\gamma}$. The gyroscopic couple applied to the rotor $I_p \Omega \dot{\gamma}$, must act about the axis OY ,

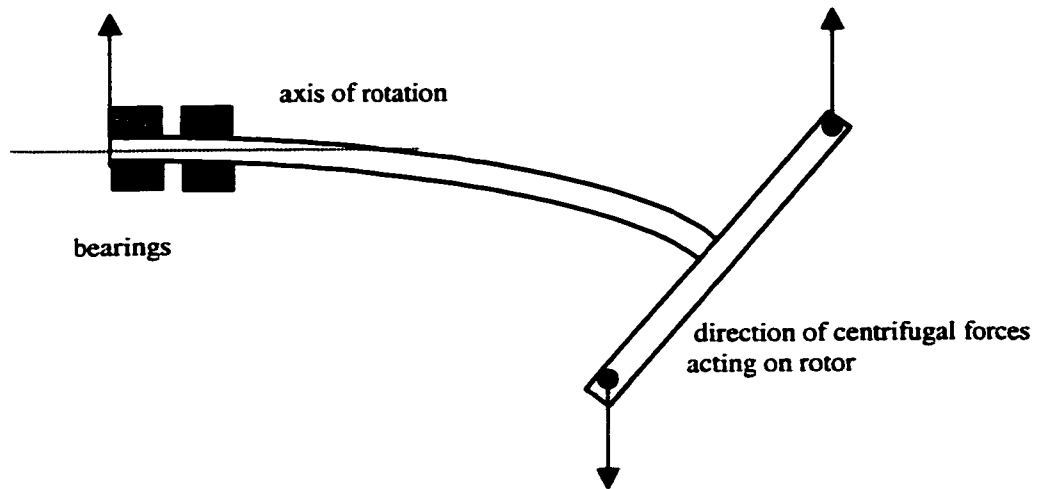


Figure 2.5a Overhung rotor mounted on a light flexible shaft

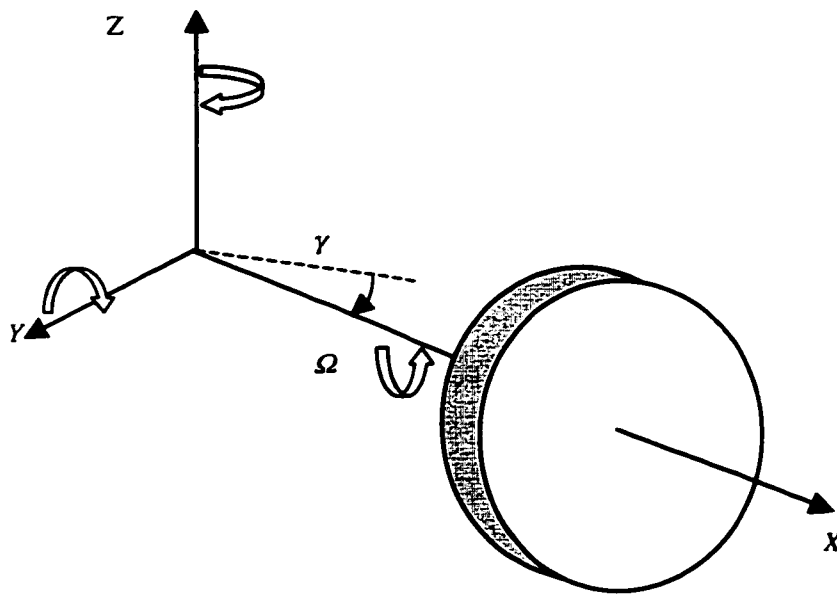


Figure 2.5b General angular motion of a rotor

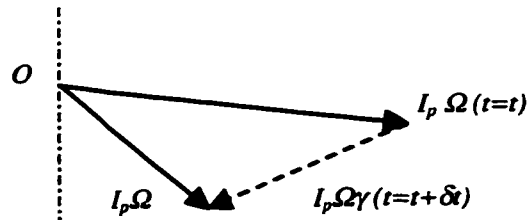


Figure 2.5c Angular momentum vectors for the system shown in figure (2.5b)

since this axis corresponds to the orientation of the vector $I_p \Omega \beta$ in figure (2.5c).

Moment M_y , which is applied to the rotor by the shaft can be written as

$$M_y = I_d \ddot{\beta} - I_p \Omega \dot{\gamma} \quad (2.50)$$

A similar expression may also be developed describing rotor motion in the XZ plane as

$$M_z = I_d \ddot{\gamma} + I_p \Omega \dot{\beta} \quad (2.51)$$

For free vibration we have

$$\begin{aligned} I_d \ddot{\gamma} + I_p \Omega \dot{\beta} &= 0 \\ I_d \ddot{\beta} - I_p \Omega \dot{\gamma} &= 0 \end{aligned} \quad (2.52)$$

For an isotropic shaft, considering no motion along the X-axis, the mass center of the disk has, in addition, deflections w (in Y) and v (in Z). With the complex notation $r = w+vi$, $\psi = \beta + \gamma i$, we have [62]

$$\begin{aligned} m_d \ddot{r} + k_{rr} r + k_{r\psi} \psi &= 0 \\ I_d \ddot{\psi} - i I_p \Omega \dot{\psi} + k_{r\psi} r + k_{\psi\psi} \psi &= 0 \end{aligned} \quad (2.53)$$

For $r = r_0 e^{i\omega t}$ the frequency equation is given for a rotor-bearing system as [62]

$$mI_d\omega_n^4 - mI_p\Omega\omega_n^3 - (mk_{\psi\psi} + I_p k_{rr})\omega_n^2 + k_{rr}I_p\Omega\omega_n + (k_{rr}k_{\psi\psi} - k_{r\psi}^2) = 0 \quad (2.54)$$

where k_{ij} , $i, j = r, \psi$, are stiffness influence coefficients. Different cases are analyzed below.

2.2.1 Approximate Solutions to Whirl Speeds

Case (i): Non-rotating uniform cantilever shaft with a non-rotating disk at the end

Rayleigh's Method

The fundamental frequency of a cantilever beam with a concentrated mass (disk) at the end can be calculated approximately using [63],

$$\omega = \sqrt{\frac{3EI}{(m_d + 0.23571M)L^3}} \quad (2.55)$$

where EI is the bending rigidity of the beam, M is the mass of the beam, L is the beam length and m_d is the mass of the disk.

Dunkerley's Method

The frequency equation for the beam uniformly loaded by itself is

$$\omega_{11} = \sqrt{\frac{3.515EI}{ML^3}} \quad (2.56)$$

For the concentrated mass by itself attached to a weightless cantilever beam, we have

$$\omega_{22} = \sqrt{\frac{3EI}{m_d L^3}} \quad (2.57)$$

By substituting into Dunkerley's formula [63] rearranged in the following form, the natural frequency of the system is determined as

$$\omega^2 = \frac{\omega_{11}^2 \omega_{22}^2}{\omega_{11}^2 + \omega_{22}^2} \quad (2.58)$$

The results are tabulated in Table 2.1.

Case(ii) Whirl speeds of a non-rotating uniform cantilever shaft with a rotating disk at the end (*Rayleigh's Method*)

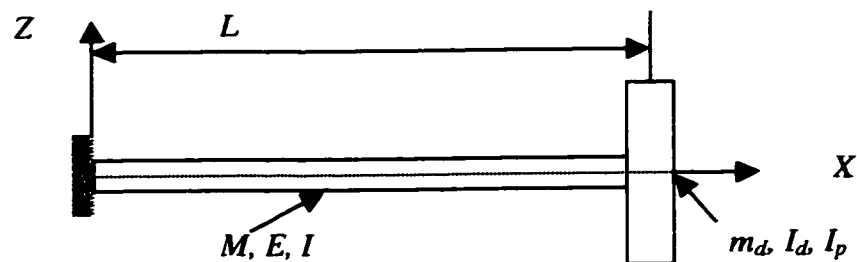


Figure 2.6 Approximate model of an overhung rotor

XYZ is the inertial frame, the rotor axis is along the X-axis, and the speed of

rotation Ω of the disk is constant (figure 2.6). For simplicity, only one degree of freedom is used for the displacements in Y and the Z directions. The rotor is fixed at the left end (cantilever beam) and the disk is situated at x .

The expressions for the displacements in the y and z directions are, respectively,

$$v(x,t) = f(x)q_1(t) = f(x)q_1 \quad (2.59)$$

$$w(x,t) = f(x)q_2(t) = f(x)q_2 \quad (2.60)$$

where q_1 and q_2 are generalized independent coordinates. Then the angular displacements will be

$$\beta = -\frac{\partial w}{\partial x} = -\frac{df(x)}{dx}q_2 = -g(x)q_2 \quad (2.61)$$

and

$$\gamma = \frac{\partial v}{\partial x} = \frac{df(x)}{dx}q_1 = g(x)q_1 \quad (2.62)$$

The second-order derivatives of v and w are necessary to express the strain energy; their expressions are

$$\frac{d^2v}{dx^2} = \frac{d^2f(x)}{dx^2}q_1 = h(x)q_1 \quad (2.63)$$

$$\frac{d^2w}{dx^2} = \frac{d^2f(x)}{dx^2}q_2 = h(x)q_2 \quad (2.64)$$

Displacement function:

The displacement function is chosen as the exact static deflection shape of a beam with constant cross-section subject to a tip load in bending; for one end fixed conditions; i.e.

$$f(x) = L \frac{x^2}{2} - \frac{x^3}{6} \quad (2.65)$$

Then

$$g(x) = Lx - \frac{x^2}{2} \quad (2.66)$$

$$h(x) = L - x \quad (2.67)$$

The disk

The kinetic energy T_D of the disk [64]

$$\begin{aligned} T_D &= \frac{1}{2} m_d f^2(L) (\dot{q}_1^2 + \dot{q}_2^2) + \frac{1}{2} I_d g^2(L) (\dot{q}_1^2 + \dot{q}_2^2) - I_p \Omega g^2(L) \dot{q}_1 q_2 \\ &= \frac{1}{2} (m_d f^2(L) + I_d g^2(L)) (\dot{q}_1^2 + \dot{q}_2^2) - I_p \Omega g^2(L) \dot{q}_1 q_2 \end{aligned} \quad (2.68)$$

The shaft

The kinetic energy T_S of the *non-rotating* shaft is

$$T_S = \frac{\rho A}{2} \int_0^L f^2(x) dx (\dot{q}_1^2 + \dot{q}_2^2) + \frac{\rho I}{2} \int_0^L g^2(x) dx (\dot{q}_1^2 + \dot{q}_2^2) \quad (2.79a)$$

and

$$T_S = \frac{1}{2} \left[\rho A \int_0^L f^2(x) dx + \rho I \int_0^L g^2(x) dx \right] (\dot{q}_1^2 + \dot{q}_2^2) \quad (2.69b)$$

Hence the kinetic energy of T of the disk-shaft assembly is

$$T = T_D + T_S \quad (2.70)$$

that is,

$$T = \frac{1}{2} \left[m_d \dot{f}^2(L) + I_d \dot{g}^2(L) + \rho A \int_0^L \dot{f}^2(x) dx + \rho I \int_0^L \dot{g}^2(x) dx \right] (\dot{q}_1^2 + \dot{q}_2^2) - \Omega [I_p g^2(L)] \dot{q}_1 q_2 \quad (2.71)$$

Equation (2.71) can be written in a more compact form as

$$T = \frac{1}{2} m (\dot{q}_1^2 + \dot{q}_2^2) - \Omega a \dot{q}_1 q_2 \quad (2.72)$$

The strain energy of the shaft U_S is given by

$$U_s = \frac{EI}{2} \int_0^L h^2(x) dx (q_1^2 + q_2^2) \quad (2.73)$$

Equation (2.73) can be written in a more compact form as

$$U_s = \frac{1}{2} k (q_1^2 + q_2^2) \quad (2.74)$$

The application of Lagrange's equations, with the kinetic energy given by equation (2.72) and the strain energy given by equation (2.74), gives the equations of motion as

$$\begin{bmatrix} m & 0 \\ 0 & m \end{bmatrix} \begin{bmatrix} \ddot{q}_1 \\ \ddot{q}_2 \end{bmatrix} + \begin{bmatrix} 0 & -a \\ a & 0 \end{bmatrix} \begin{bmatrix} \dot{q}_1 \\ \dot{q}_2 \end{bmatrix} + \begin{bmatrix} k & 0 \\ 0 & k \end{bmatrix} \begin{bmatrix} q_1 \\ q_2 \end{bmatrix} = 0 \quad (2.75)$$

The solutions of equation (2.75) have to be sought in the form

$$q_i = Q_i e^{r\tau} \quad \text{where } i = 1,2 \quad (2.76)$$

Substituting equation (2.76) in equation (2.75) gives two coupled homogeneous equations in Q_1 and Q_2 and the characteristic equation will be

$$(k + mr^2)^2 + a^2 \Omega^2 r^2 = 0 \quad (2.77a)$$

which can be written as

$$m^2 r^4 + (2km + a^2 \Omega^2) r^2 + k^2 = 0 \quad (2.77b)$$

When the disk is at rest ($\Omega = 0$) the angular frequencies are, ($r = \pm i\omega$)

$$\omega_{10} = \omega_{20} = \sqrt{\frac{k}{m}} \quad (2.78)$$

Under rotating conditions ($\Omega \neq 0$) the corresponding angular frequencies of equation (2.77) are ω_1 and ω_2 , where

$$\omega_1 = \sqrt{\omega_{10}^2 + \frac{a^2 \Omega^2}{2m^2} \left(1 - \sqrt{1 + \frac{4m^2 \omega_{10}^2}{a^2 \Omega^2}} \right)} \quad (2.79)$$

$$\omega_2 = \sqrt{\omega_{10}^2 + \frac{a^2 \Omega^2}{2m^2} \left(1 + \sqrt{1 + \frac{4m^2 \omega_{10}^2}{a^2 \Omega^2}} \right)} \quad (2.80)$$

The results are tabulated in Table 2.2.

2.2.2 Synchronous Whirl

Case (iii): Whirl speeds of a rotating uniform cantilever shaft with a rotating disk at the end (overhung rotor)

The critical speeds can be computed by substituting the condition $\omega_c = \Omega = \omega_n$, in equation (2.54), which yields the characteristic equation as [64]

$$mI_D \omega_c^4 + (mk_{vv} - I_D k_{rr}) \omega_c^2 - (k_{rr} k_{vv} - k_{rv}^2) = 0 \quad (2.81)$$

where $I_D = I_p - I_d$.

The critical speeds are:

$$\omega_{c,1,2} = \left\{ \frac{\left[-(mk_{vv} - I_D k_{rr}) \pm \left[(mk_{vv} - I_D k_{rr})^2 + 4mI_D (k_{rr} k_{vv} - k_{rv}^2) \right]^{1/2} \right]}{2mI_A} \right\}^{1/2} \quad (2.82)$$

Two more critical speeds can be computed from the condition $\omega_c = \Omega = -\omega_n$, which yields

$$\omega_{c,3,4} = \left\{ \frac{\left[(mk_{vv} - I_A k_{rr}) \pm \left[(mk_{vv} - I_A k_{rr})^2 + 4mI_A (k_{rr}k_{vv} - k_{rv}^2) \right]^{1/2} \right]}{2mI_A} \right\}^{1/2} \quad (2.83)$$

where $I_A = I_p + I_d$.

The four roots of the biquadratic equations (2.82) and (2.83) are the four critical speeds.

For an overhang rotor the equations (2.82) and (2.83) become

$$\frac{\omega_{c,1,2}}{\omega_n} = \left\{ \left(\frac{\beta_D}{\alpha_D} \right) \frac{[-(\alpha_D - 1) \pm [(\alpha_D - 1)^2 + 4\beta_D]^{1/2}]}{2} \right\}^{1/2} \quad (2.84)$$

$$\frac{\omega_{c,3,4}}{\omega_n} = \left\{ \left(\frac{\beta_A}{\alpha_A} \right) \frac{[(\alpha_A - 1) \pm [(\alpha_A - 1)^2 + 4\beta_A]^{1/2}]}{2} \right\}^{1/2} \quad (2.85)$$

where

$$\alpha_D = \frac{\left(\frac{L}{k_D} \right)^2}{3}, \quad \beta_D = \frac{\left(\frac{L}{k_D} \right)^2}{12}, \quad \alpha_A = \frac{\left(\frac{L}{k_A} \right)^2}{3}, \quad \beta_A = \frac{\left(\frac{L}{k_A} \right)^2}{12}$$

$$k_D = \sqrt{\frac{I_D}{m}}, \quad k_A = \sqrt{\frac{I_A}{m}}$$

The natural frequency is

$$\omega_n = \left[\frac{(k_{rr}k_{vv} - k_{rv}^2)}{mk_{vv}} \right]^{1/2} = \sqrt{\frac{3EI}{mL^3}} \text{ rad/s} \quad (2.86)$$

where

$$k_{rr} = \frac{12EI}{L^3}, \quad k_{vv} = \frac{4EI}{L}, \quad k_{rv} = \frac{6EI}{L^2} \quad (2.87)$$

Back substituting equation (2.87) in (2.81) the frequency equation for overhung rotor is

$$\omega^4 + \omega^2 \frac{12EI}{m_d I_d L^3} \left[\frac{m_d L^2}{3} - I_d \right] - \frac{12E^2 I^2}{m_d I_d L^4} = 0 \quad (2.88)$$

Let

$$\lambda = \omega_n \sqrt{\frac{m_d L^3}{EI}} \quad \text{frequency parameter} \quad (2.89)$$

and

$$\delta = \frac{I_d}{m_d L^2} \quad \text{disk parameter} \quad (2.90)$$

Then

$$\lambda^4 + \lambda^2 \left(\frac{4}{\delta} - 12 \right) - \frac{12}{\delta} = 0 \quad (2.91)$$

and

$$\lambda_{1,2}^2 = \left(6 - \frac{2}{\delta} \right) \pm \sqrt{\left(6 - \frac{2}{\delta} \right)^2 + \frac{12}{\delta}} = 0 \quad (2.92)$$

For real values of λ , the positive sign is to be considered in the above equation

and this root is plotted in figure 2.7.

For a lumped mass, $\delta = 0$ and the critical speed is given by

$$\omega_n^2 = \frac{3EI}{m_d L^3} \quad (2.93)$$

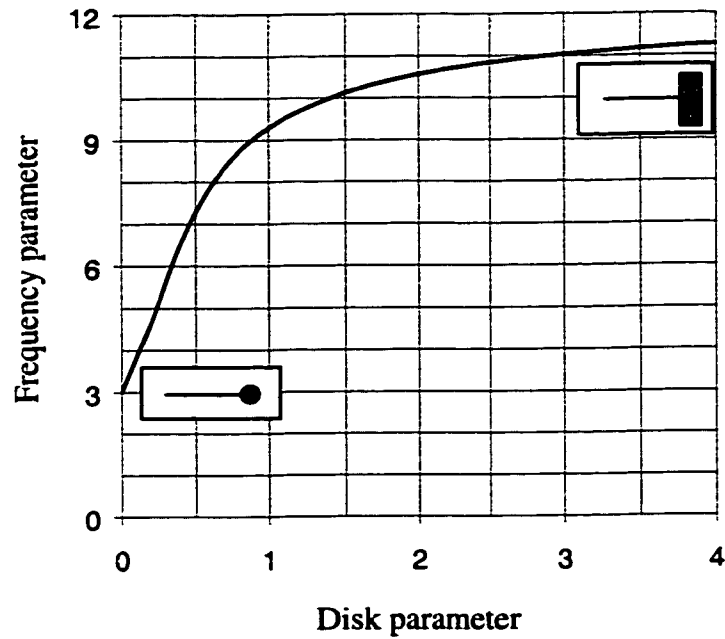


Figure 2.7 Effect of disk inertia on the critical speed of a simple overhung rotor

If $\delta = \infty$, i.e., $I_d = \infty$, which means that the disk mass is concentrated at a large radius, and hence no finite β is possible and the critical speed becomes

$$\omega_n^2 = \frac{12EI}{m_d L^3} \quad (2.94)$$

The effect of gyroscopic couple is to stiffen the rotor and to raise the critical speed as shown in figure 2.7.

If we use frequency equation (2.54) instead and then plot the roots ω_n we observe higher critical speeds. The intersection of $\omega_n = \Omega$ with the curves ω_{n1} and ω_{n2} gives the two critical speeds at which the whirl has the same direction (and angular velocity) with the rotation of the shaft. We call this forward precession. Line $\omega_n = -\Omega$ intersects the two negative roots ω_{n2} , and ω_{n4} . This indicates that critical speeds are possible with whirling angular velocity in a direction opposite to that of the shaft's rotation. We call this backward precession.

If at the speeds corresponding to the forward precession, we solve for the vibration modes, we shall observe modes such as the fundamental mode and it is the most dangerous one. The results for above calculations are tabulated in Table 2.3.

2.2.3 Finite Element Modeling

Case (iv) Whirl speeds and unbalance response of a non-uniform cantilever-sleeve rotor-bearing system with a non-rotating shaft and a rotating sleeve shaft and a rotating disk at the end

A general rotor dynamic system is composed of a large number of components, which typically include rigid and flexible disks, bearings, dampers, seals, couplings, and shaft segments. The finite element model can easily be utilized to model such rotor-bearing system for the purpose of determining critical speeds and unbalance response.

The present problem investigates the effect of gyroscopic moments, axial load and the rotary inertia on the dynamics of the system using finite element model. The cantilever-sleeve rotor used here is shown in figure 2.4. The rotor uses 12 shaft elements. Area of the 2-nd and 3-rd sections are same. The assembly procedure for shaft elements is described next.

The procedures of assembly of the system equations are conceptually equivalent for the fixed and rotating frames. In modeling the dynamic characteristics of a rotor dynamic system, several steps are required in the development of the equations of motion. The first step is to define one or more reference frames, which are useful for observing the motion of the system. The second step is to divide the real system into finite-degree-of-freedom model consisting of an interconnected set of discrete elements. The cantilever-sleeve rotor-bearing system shown in figure 2.8a is used here in presenting the various steps in developing a set of system equations of motion. One possible discrete model of the illustrative system is also shown. It consists of two shafts, one disk, two inter-shaft bearings (support structure), and twelve rotating shaft segments.

This discrete model includes twelve rotating assembly stations and six stationary assembly stations, each with two translations and two rotations. Separate reference systems can be used for each component; however, the common choice of the fixed XYZ reference for each component greatly simplifies the assembly process.

The third step in the modeling process is to choose a set of system coordinates. This is particularly simple if a common reference is used for all components and if this reference is also used as the system or global reference. For this choice, the system displacement vector consists of all the station displacements and is defined as

$$\{q\}_{\text{ext}} = \left[\underbrace{\{q_1\}, \dots, \{q_{13}\}}_{\text{shaft 1}}, \underbrace{\{q_1\}, \dots, \{q_7\}}_{\text{shaft 2}} \right] \quad (2.95)$$

Since shaft 2 is stationary and located inside shaft 1, we have given the same nodal numbers for shaft 2 as in shaft 1.

$$\{q_1\}, \dots, \{q_7\}_{\text{shaft-1}} = \{q_{14}\}, \dots, \{q_{20}\}_{\text{shaft-2}} \quad (2.96)$$

The fourth step is to define the connectivity of the discrete elements with the system displacement vector given in equation (2.96). The complete set of component coordinates constitutes a dependent set of coordinates, and the connectivity statements essentially represent geometric constraint relations between the component coordinates and the system coordinates.

The connectivity statements for the shaft segment between stations 1 and 14, 2 and 15, 3 and 16, 4 and 17, 5 and 18, 6 and 19 and the inter-shaft bearing between stations 7 and 20 will have the same nodal numbers as in shaft 1.

The equation of motion for the e -th typical element of the system is

$$[M^e] \{\ddot{q}^e\} + [G^e] \{\dot{q}^e\} + [K^e] \{q^e\} = \{Q^e\} \quad (2.97)$$

The system of equations are formally assembled by utilizing the principle of virtual displacements which states, "The work done by the external forces acting on the system and the work done by the internal forces must vanish for any virtual

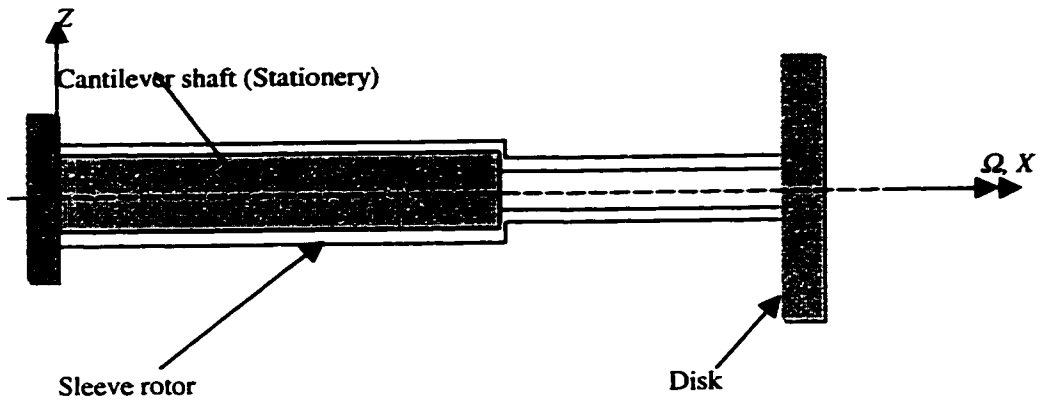


Figure 2.8a System Configuration

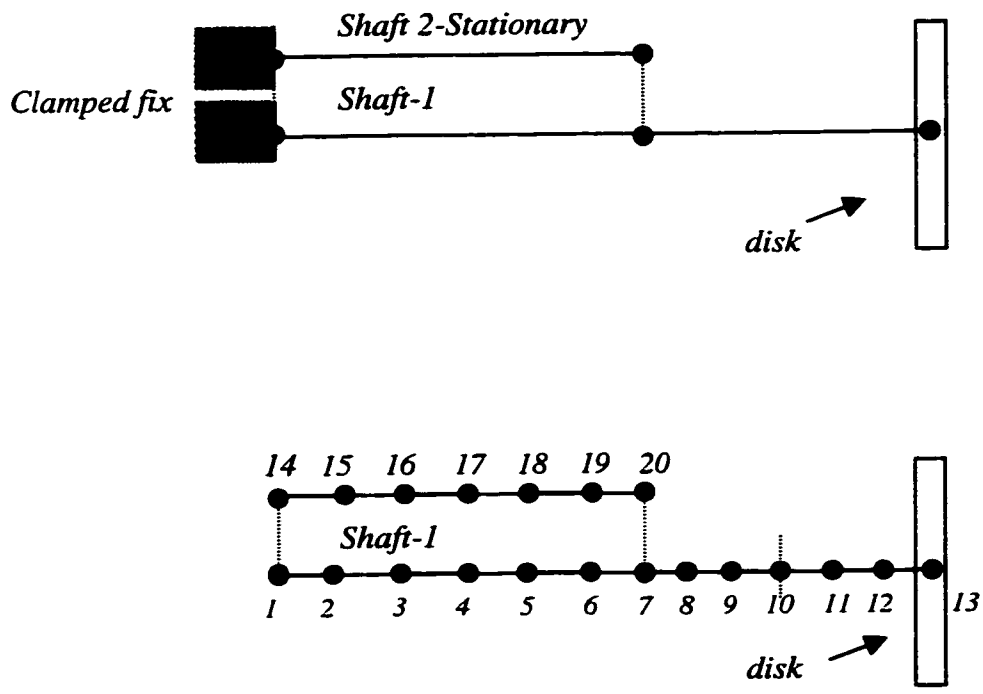


Figure 2.8b Cantilever-sleeve rotor bearing FEM model and schematic

displacement” [Oden, 1967], i.e.,

$$\delta W = 0 \quad (2.98)$$

This yields the following set of system equations of motion:

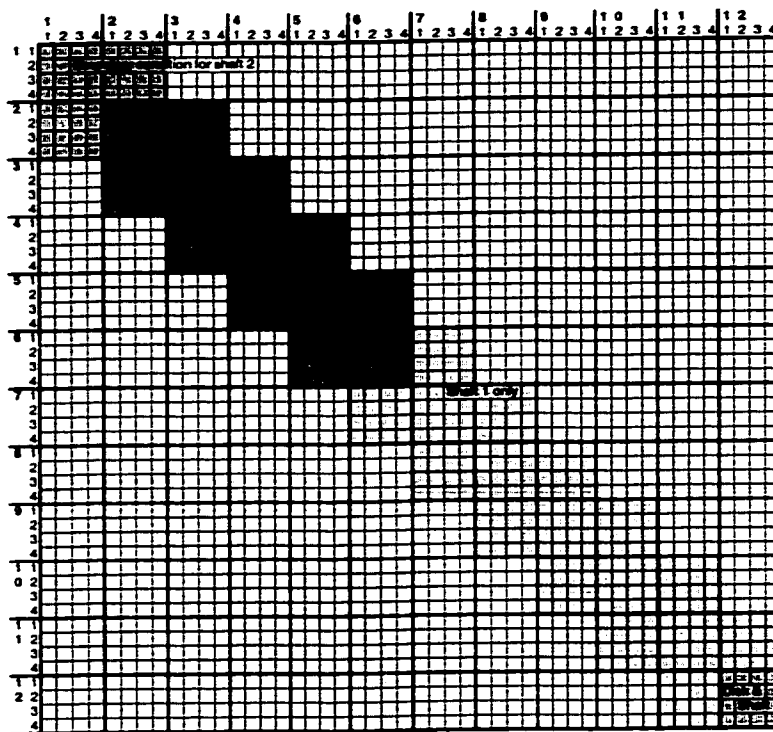
$$[M^s] \{\ddot{q}^s\} + [G^s] \{\dot{q}^s\} + [K^s] \{q^s\} = \{Q^s\} \quad (2.99)$$

The system mass matrix $[M]$ is symmetric and consists of contributions from the disks, and flexible shaft elements. The system gyroscopic matrix $[G]$ consists of contributions from the same components and is skew symmetric and spin-speed-dependent. The stiffness $[K]$ consists of symmetric arrays from the undamped shaft elements and contributions from the bearings and other components. The system applied force vector $\{Q\}$ includes rotating unbalance.

The forms of the system arrays of equation (2.99) are shown in figure 2.9 for the dual-shaft support structure example of figure 2.8b.

The system stiffness and inertia arrays are of order 52 with 4 degrees of freedom for each rotor station. The coordinate ordering in these system arrays is consistent with the displacement vector defined in the previous chapter for rotating assemblies. The form of the cosine and sine components of the system constant-speed unbalance force vector is

$$\{Q^s\} = \{Q_c^s\} \cos \Omega t + \{Q_s^s\} \sin \Omega t \quad (2.100)$$



Assemblage of mass matrix

Assemblage of stiffness matrix

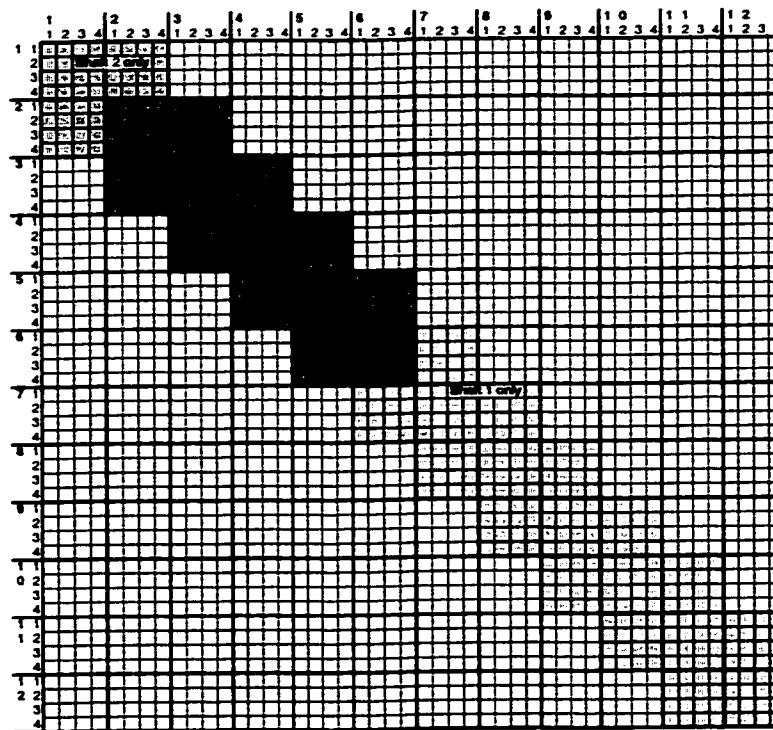


Figure 2.9 Forms of system arrays for the dual shaft support structure.

The unbalance response with the unbalance given in the data was computed for the speed of 15,000 rpm. The unbalance responses are plotted in figure 2.10 versus time. Plot of deflection and slope for the $XZ (w, \beta)$ plane is plotted in figure 2.11a and 2.11b. The critical speeds of a cantilever-sleeve rotor system calculated and are tabulated in Table 2.4.

2.2.4 Numerical Results

Shaft 2-Stationary

Diameter (d_1)	= 0.04445 m
Area = $(\pi d_1^2)/4$	= $1.552 \times 10^{-3} \text{ m}^2$
Mass Moment of Inertia ($I = \pi d_1^4/64$)	= $1.916 \times 10^{-7} \text{ m}^4$
Length	= 0.762 m
Density (ρ)	= 7800 kg/m^3
Young's modulus (E)	= $2 \times 10^{11} \text{ N/m}^2$

Shaft 1-Rotating

Inner diameter (d_2)	= 0.04445 m
Outer diameter (d_3)	= 0.0508 m
Area (A) = $\pi (d_3^2 - d_2^2)/4$	= $4.75 \times 10^{-4} \text{ m}^2$
Mass Moment of Inertia $I = \pi (d_3^4 - d_2^4)/64$	= $1.353 \times 10^{-7} \text{ m}^4$
Length	= 0.762 m
Density (ρ)	= 7800 kg/m^3
Young's modulus (E)	= $2 \times 10^{11} \text{ N/m}^2$

Tapered shaft

Inner diameter at the left (d_{LI})	= 0.0445 m
Inner diameter at right (d_{RI})	= 0.01905 m
Outer diameter at left (d_{LO})	= 0.0508 m
Outer diameter at right (d_{RO})	= 0.0254 m
Area = $(\pi d_{avg}^2)/4$	= $3.484 \times 10^{-4} \text{ m}^2$
Mass Moment of Inertia ($I_t = \pi d_{avg}^4/64$)	= $5.355 \times 10^{-8} \text{ m}^4$
Length	= 0.508 m
Density (ρ)	= 7800 kg/m^3
Young's module (E)	= $2 \times 10^{11} \text{ N/m}^2$

Data for the total shaft

Total shaft mass (M)	= 13.427 kg
Total shaft length (L)	= 1.27 m

Basic data for the disk

Mass of the disk (m_d)	= 9.08 kg
Outer diameter (d_D)	= 0.381 m
Thickness (h)	= 0.0254 m
Diametral Mass Moment of Inertia (I_d)	= 0.082 kg m^2
Polar Mass Moment of Inertia (I_P)	= 0.163 kg.m^2

Mass unbalance (disk)

Mass unbalance center	= (0.075, 0.065) m
-----------------------	--------------------

Mass eccentricities in Y and Z direction (constant cross section of the shaft)

Mass center eccentricity at $x = 0$	= (0.022225, 0.0254) m
-------------------------------------	------------------------

Mass center eccentricity at $x = r$ = (0.0254, 0.022225) m
 For tapered cross section mass center eccentricity = (0.01905, 0.05875) m
 Spin speed Ω = 15000 rpm

The shaft whirl ω may occur in the same direction or the opposite direction as the shaft spin Ω . These possibilities are termed positive or negative whirl, respectively, corresponding to positive or negative λ .

A spin speed Ω is termed a critical speed when it equals a natural frequency with respect to stationary axes. Hence critical speeds are represented by $\lambda = 1$ where $\omega = \Omega$. The case $\lambda = 0$ represents zero spin, for which $\omega_s = \omega$.

The study was conducted for a cantilever-sleeve rotor-bearing system using finite elements in order to establish a reference set of results for a particular number of finite elements used in the system model. It should be noted here that there is no closed form solution for a problem of this kind, and one must rely on the existing finite element method.

2.2.5 Comparison of Results and Discussion

The equations of motion for a uniform rotating shaft element have been formulated using shape functions that were originally developed for Euler-Bernoulli beam element. A finite element model including the effects of rotatory inertia, gyroscopic moments, and axial load has been presented in this chapter. The equations of motion of the elements are presented in both fixed and rotating frames of reference. The rotating frame equation is used to calculate the critical speeds since the two planes of

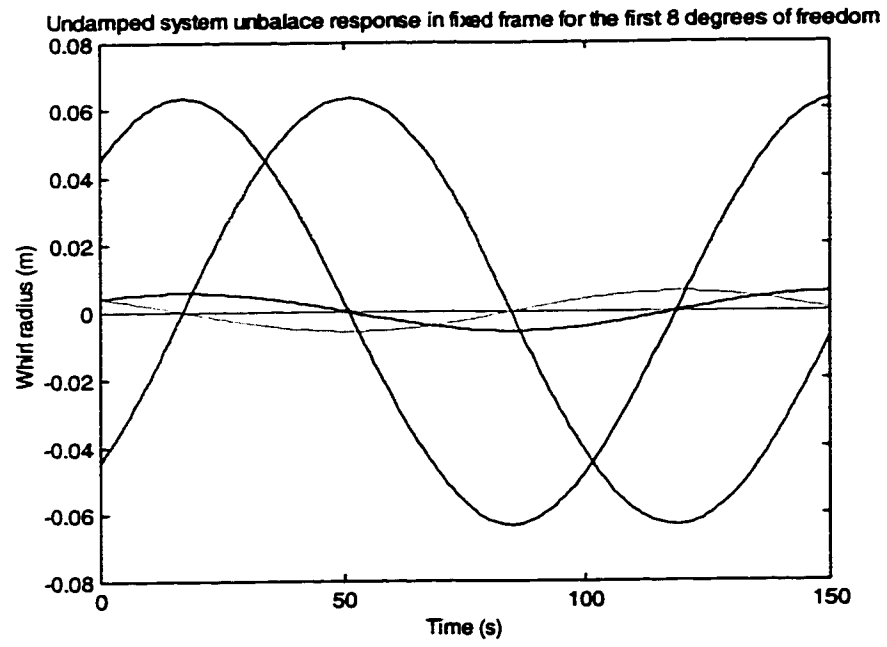


Figure 2.10 Unbalance response of cantilever-sleeve rotor bearing system for node 1 and node 2 in both plane

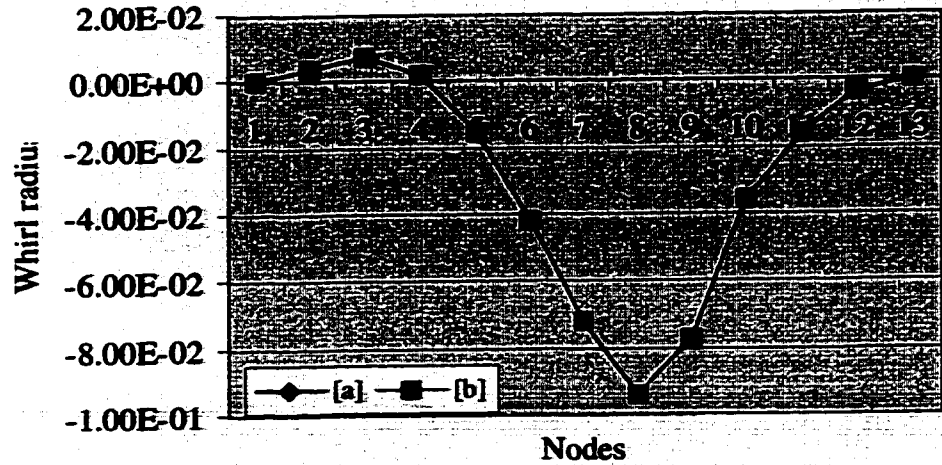


Figure 2.11a Steady state unbalance response in fixed frame coordinates. Plot of deflection v and w along the shaft for all the nodes.
 [a]- $\{v\} \cos \Omega t$, [b]- $\{w\} \sin \Omega t$

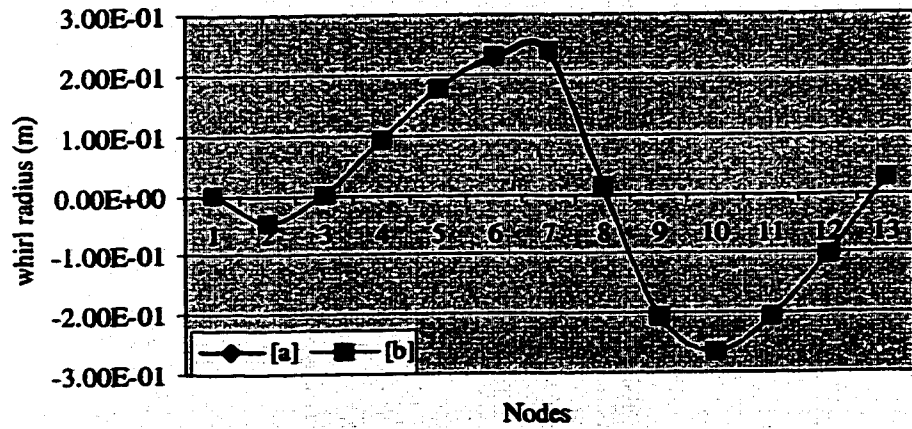


Figure 2.11b Steady state unbalance response in fixed frame coordinates. Plot of slope γ and β along the shaft for all the nodes.
 [a]- $\{\gamma\} \cos \Omega t$, [b]- $\{\beta\} \sin \Omega t$

Table 2.1 Critical speeds of a *non-rotating* uniform cantilever shaft with a *non-rotating* disk at the end

	Critical speeds (when $\Omega = 0$) rad/s			
	ω_1	ω_2	ω_3	ω_4
Solution obtained using Rayleigh's method, given by Eq. (2.55)	67.705	-	-	-
Finite element solution using two elements	66.109	543.638	1492.961	3307.748
Finite element solution using six elements	66.106	540.199	1435.345	2615.229

Table 2.2 Critical speeds of a *stationary* uniform cantilever shaft with a *rotating* disk at the end

	Critical speeds (when $\Omega = 15000$ rpm) rad/s			
	ω_1	ω_2	ω_3	ω_4
Closed form solution, given by Eq. (2.79 and 2.80)	66.161	-	-	-
Finite element solution using six elements	66.109	539.981	1435.579	2615.207
Finite element solutions using twelve elements	66.147	539.939	1434.075	2609.752

Table 2.3 Critical speeds of a *rotating* uniform cantilever shaft with a *rotating* disk at the end

	Critical speeds (when $\Omega = 15000$ rpm) rad/s			
	ω_1	ω_2	ω_3	ω_4
Closed form solution, given by Eq. (2.86)	78.619	-	-	-
Finite element solution using six elements	78.431	708.596	1969.571	3520.459
Finite element solution using twelve elements	78.432	708.466	1966.899	3510.578

Table 2.4 Critical speeds of a *cantilever-sleeve rotor bearing* system

	Critical speeds (when $\Omega = 15000$ rpm) rad/s			
	ω_1	ω_2	ω_3	ω_4
Finite element solution using six elements when $[G] = 0$	86.526	484.711	1103.156	2545.319
Finite element solution using twelve elements when $[G] = 0$	86.524	484.672	1102.824	2538.670
Finite element solutions using twelve elements when $[G] \neq 0$	86.527	484.850	1103.370	2538.712

Table 2.5 Comparison of critical speeds obtained using finite elements

	Critical speeds obtained using a mesh of six elements (when $\Omega = 15000$ rpm) rad/s			
	ω_1	ω_2	ω_3	ω_4
Finite element solutions for case (i): both shaft and disk <i>stationary</i>	66.106	540.199	1435.345	2615.229
Finite element solutions for case (ii): disk <i>rotating</i> and shaft <i>stationary</i>	66.109	539.981	1435.579	2615.207
Finite element solutions for case (iii): both shaft and disk <i>rotating</i>	78.431	708.596	1969.571	3520.459

Table 2.6 Critical speeds of a *stationary* uniform cantilever shaft with a *rotating* disk at the end

F = Forward precession critical speed,

B = Backward precession critical speed

	Critical speeds (when $\Omega = 15000$ rpm) rad/s			
	ω_n	$\omega_1 (F)$	$\omega_2 (B)$	$\omega_2 (B)$
Solution obtained using Rayleigh's method, given by Eq. (2.79 & 80)	66.161	53.083	85.41	-

Table 2.7 Critical speeds of a *rotating* uniform cantilever shaft with a *rotating* disk at the end

	Critical speeds (when $\Omega = 15000$ rpm) rad/s			
	ω_n	$\omega_1 (F)$	$\omega_2 (B)$	$\omega_2 (B)$
Closed form solution, given by Eq. (2.58, 2.85 and 2.86)	78.619	66.788	68.055	771.841

motion can be treated separately, while fixed frame equation are used to calculate the critical speeds with the gyroscopic effect. The solution of eigenvalue problem is obtained by the technique suggested by Meirovitch [60].

The finite rotor element was used to model a typical industrial cantilver-sleeve rotor system to obtain the critical speeds and unbalance response. The numerical results in this study includes the following four cases:

- (i) a non-rotating uniform cantilever shaft with a non-rotating disk at the end.
- (ii) a non-rotating uniform cantilever shaft with a rotating disk at the end.
- (iii) a rotating uniform cantilever shaft with a rotating disk at the end (overhung rotor).
- (iv) a non uniform cantilever-sleeve rotor bearing system with a non- rotating shaft, a rotating sleeve shaft and a rotating disk at the end.

For the system of case (i), the critical speeds that were calculated using two elements and a mesh of six elements are given in Table 2.1. In the same table, the first critical speed that was calculated using the Rayleigh's approximate method is also given. As can be seen, the finite element solutions and the approximate solution are in very good agreement.

For the system of case (ii), the critical speeds that were calculated using a mesh of six elements and using a mesh of twelve elements are given in Table 2.2. In the same table, the first critical speed that was calculated using the closed form solution is also given.

For the system of case (iii), the critical speeds that were calculated using a mesh of six elements and using a mesh of twelve elements are given in Table 2.3. In the same

table, the first critical speed that was calculated using the closed form solution is also given. As can be seen from these tables, the finite element solutions and the approximate solution are in very good agreement.

The finite element solutions for the cantilever sleeve rotor system of case (iv), are given in Table 2.4. The effects of gyroscopic moments are highlighted in this table. The effect of gyroscopic moment on the critical speeds of the system does not seem to be significant. Further the third natural frequency is close to the operating speed and hence a more accurate analysis is needed to determine the natural frequencies.

Based on the results presented in the above, a comparison is now made in Table 2.5 so as to bring out the effects of rotation of the shaft and the disk. The four critical speeds obtained using a mesh of six elements for each case are compared in Table 2.5. The effect of the rotation of the disk on the first critical speed is not so significant when compared with the effect of the rotation of the shaft on the first critical speed. The same conclusion holds good for all the other three critical speeds. However, all the critical speeds are significantly affected when both shaft and disk are rotating.

For the rotor-disk systems of case(ii) and case(iii), the first and second critical speeds were determined using closed form solutions. The calculated values are listed in Table 2.6 and Table 2.7. In case (ii) when both the rotor and disk are rotating, one forward precession critical speed at 66.788 rad/s, and two backward precession critical speeds at 68.055 rad/s and 771.841 rad/s were obtained.

Without the inclusion of gyroscopic moment, the critical speeds are comparable to the natural frequencies of vibration of the shaft-disk system. It is well known that the natural frequencies are significantly influenced by the boundary conditions of the system.

In the conventional finite element formulation, the basis functions are derived so as to include only the geometric (or essential) boundary conditions of the finite elements. The inclusion of boundary effects might yield a more precise finite element solution, and it can incorporate the free end conditions, which can not be satisfied by the conventional finite element method. If the basis functions are derived such that both the natural and essential boundary conditions are included in the element formulation, a more accurate result can be obtained using a coarser mesh. A coarser mesh saves the CPU time in the solution process. Therefore, inclusion of all boundary conditions in the element formulation will be advantageous. Such a formulation is developed in the next chapter.

CHAPTER 3

EFFICIENT BASIS FUNCTIONS FOR FINITE ELEMENT DYNAMIC ANALYSIS OF BEAMS

3.1 Bending of Beams

3.1.1 Euler-Bernoulli Beam Theory

The transverse deflection w of a beam is determined by solving the following fourth order differential equation of equilibrium [59]

$$\frac{d^2}{dx^2} \left[EI \frac{d^2 w}{dx^2} \right] = p(x) \quad (3.1)$$

where $p(x)$ is the distributed transverse load per unit length. Since the equation is of fourth order, the four constants of integration are determined by satisfying the four boundary conditions at the ends of the beam, defining the deflection, w , slope $\theta = \frac{dw}{dx}$,

bending moment $M = EI \frac{d^2 w}{dx^2}$, and the shear force $F = EI \frac{d^3 w}{dx^3}$. The sign convention

for the curvature is related to the orientation of the coordinate axes (figure 3.1). If x -axis is positive to the right, upward deflection is positive (see Appendix I). An integral formulation that is equivalent to the differential equation and natural boundary

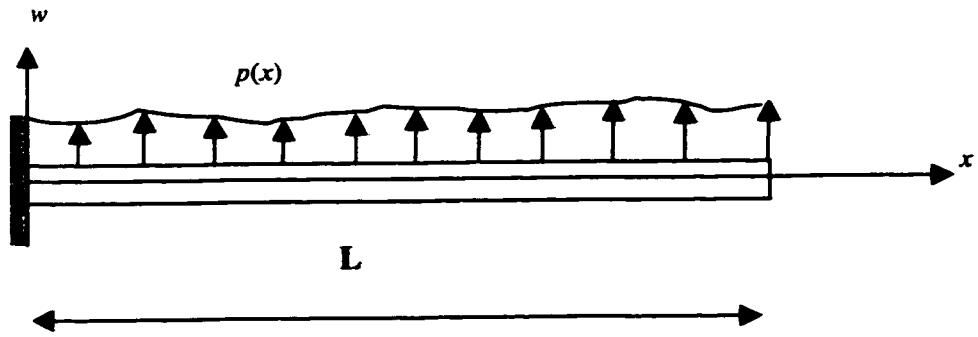


Figure 3.1 Bending of a beam

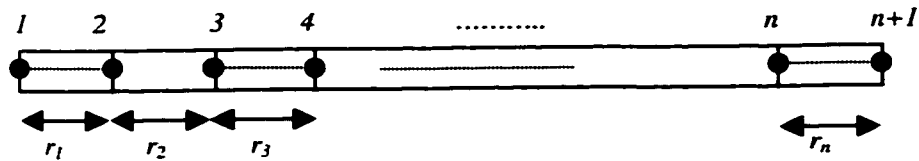


Figure 3.2 Discretization of the beam using Euler-Bernoulli beam elements

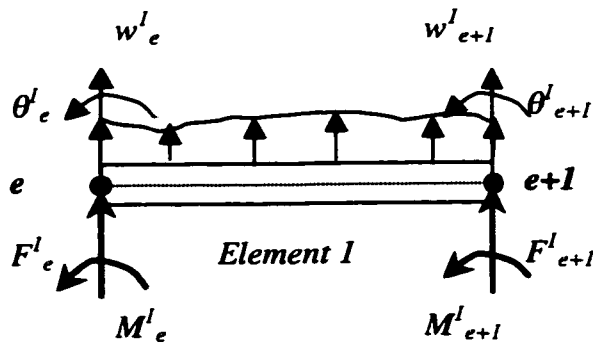


Figure 3.3 The generalized displacements and generalized forces are shown on a typical element.

conditions is needed in the finite element formulation.

3.1.2 Integral Formulation and Interpolation

Bending of beams leads to differential equation of fourth order. In the finite element formulation, first a functional is developed that corresponds to the fourth-order differential equation describing Euler-Bernoulli bending of beams with appropriate boundary conditions. The second derivative of transverse deflection is involved in the functional. Second, the element interpolation functions are chosen so as to satisfy conditions of compatibility and completeness. In this thesis new higher order interpolation functions are selected for the one dimensioned problem under consideration. Finally, the element coefficient matrices and load vector can be obtained. In this case, the stiffness and mass matrices will be derived as the element characteristic matrices.

3.2 Finite Element Model with Efficient Basis Functions

3.2.1 Governing Equation

The transverse deflection w of the beam is governed by the fourth-order differential equation for $0 < x < L$,

$$\frac{d^2}{dx^2} \left[b \frac{d^2 w}{dx^2} \right] - p(x) = 0 \quad (3.2)$$

where $b = b(x)$ and $p = p(x)$ are given functions of x and w is the dependent variable.

The sign convention used in the derivation of equation (3.1) is shown in figure (3.1). The function $b = EI$ is the product of the modulus of elasticity E and the moment of inertia I of the beam. In addition to satisfying the differential equation (3.1), w must also satisfy appropriate boundary conditions; since the equation is of fourth order, four boundary conditions are needed to solve it. The weak formulation of the equation will provide the form of these four boundary conditions. A step-by-step procedure for the finite-element analysis of equation (3.1) is presented next.

3.2.2 Domain Discretization

The first task in a finite element solution consists of discretizing the continuum by dividing it into a series of elements. Underlying the discretization process is the goal of achieving a good representation of the physical problem under study. In the method of finite elements we decompose the domain of the structure, in our case the length of the beam, into elements of small but finite lengths (figure 3.2). We consider the ends of the element as node points, each element having two end nodes as in figure (3.3). Various quantities at the node have physical significance, as follows:

$$\begin{aligned}\frac{dw}{dx} &= \theta = \text{slope} \\ EI \frac{d^2w}{dx^2} &= M = \text{bending moment} \\ -\frac{d}{dx} \left(EI \frac{d^2w}{dx^2} \right) &= -\frac{dM}{dx} = F = \text{shear force}\end{aligned}\tag{3.3}$$

The primary and secondary unknown variables and their forms at each node are dictated by the variational formulation of the differential equation, i.e., equation (3.1).

3.2.3 Derivation of Element Equations

We isolate a typical element $\Delta^e = (x_e, x_{e+1})$ (see figure 3.3) and construct the weak form of equation (3.1) over the element. The variational formulation provides the primary and secondary variables of the problem. Then suitable approximations for the primary variables are selected, interpolation functions are developed, and the element equations are derived.

3.2.3.1 Weak Form

The weak form of problems in solid mechanics can be developed either from the principle of virtual work (i.e., the principle of virtual displacements or virtual forces) or from the governing differential equations. Here we start with a given differential equation, using the three-step procedure [58] to obtain the weak form. Following the three-step procedure we write

$$0 = \int_{x_A}^{x_B} u \left[\frac{d^2}{dx^2} \left(b \frac{d^2 w}{dx^2} \right) - p \right] dx \quad (3.4a)$$

$$0 = \int_{x_A}^{x_B} \left[-\frac{du}{dx} \frac{d}{dx} \left(b \frac{d^2 w}{dx^2} \right) - up \right] dx + \left[u \frac{d}{dx} \left(b \frac{d^2 w}{dx^2} \right) \right]_{x_A}^{x_B} \quad (3.4b)$$

$$0 = \int_{x_A}^{x_B} \left(b \frac{d^2 u}{dx^2} \frac{d^2 w}{dx^2} - u p \right) dx + \left[u \frac{d}{dx} \left(b \frac{d^2 w}{dx^2} \right) - \frac{du}{dx} b \frac{d^2 w}{dx^2} \right]_{x_A}^{x_B} \quad (3.4c)$$

where $u(x)$ is a weight function that is twice differentiable with respect to x . “Weak” refers to the reduced (i.e., weakened) continuity of w , which is required to be twice-differentiable in the weighted-integral form.

In the present case, the first term of the equation is integrated twice by parts in order to trade two differentiations to the weight function u , with two derivatives of the dependent variable w : i.e., the differentiation is distributed equally between the weight function u and the dependent variable w . Because of the two integrations by parts, there appear two boundary expressions, which are to be evaluated at the two boundary points $x = x_A$ and $x = x_B$.

From the last line of the equation (3.4), it follows that the specification of w and dw/dx constitutes the essential (geometric and static) boundary conditions, and specification of

$$\frac{d}{dx} \left(b \frac{d^2 w}{dx^2} \right) = F \quad (\text{shear force}) \quad (3.5a)$$

and

$$b \left(\frac{d^2 w}{dx^2} \right) = M \quad (\text{bending moment}) \quad (3.5b)$$

constitutes the natural (or force) boundary conditions at the end points of the element.

Thus, there are two essential boundary conditions and two natural boundary

conditions; therefore, we must identify w and dw/dx as the primary variables at each node (so that the essential boundary conditions are included in the interpolation). The natural boundary conditions always remain in the weak form and end up on the right hand side (i.e., the source vector) of the matrix equation. For the sake of mathematical convenience, we introduce the following notation: $\theta = dw/dx$ and

$$\begin{aligned} Q_1^e &= \left[\frac{d}{dx} \left(b \frac{d^2 w}{dx^2} \right) \right]_{x_A}, & Q_3^e &= - \left[\frac{d}{dx} \left(b \frac{d^2 w}{dx^2} \right) \right]_{x_B} \\ Q_2^e &= - \left[\left(b \frac{d^2 w}{dx^2} \right) \right]_{x_A}, & Q_4^e &= \left[\left(b \frac{d^2 w}{dx^2} \right) \right]_{x_B} \end{aligned} \quad (3.6)$$

where Q_1^e and Q_3^e denote the shear forces, and Q_2^e and Q_4^e denote the bending moments. Since the quantities Q_2^e and Q_4^e contain bending moments, which can also be viewed as “bending forces,” the set $\{ Q_1^e, Q_2^e, Q_3^e, Q_4^e \}$ is often referred to as the generalized forces. The corresponding displacements and rotations are called the generalized displacements.

With the notation in equation (3.6), the weak form in equation (3.4), can be expressed as

$$\begin{aligned} 0 &= \int_{x_A}^{x_B} \left(b \frac{d^2 u}{dx^2} \frac{d^2 w}{dx^2} - up \right) dx - u(x_A) Q_1^e - \left(\frac{du}{dx} \right)_{x_A} Q_2^e - u(x_B) Q_3^e - \left(\frac{du}{dx} \right)_{x_B} Q_4^e \\ &\equiv B(u, w) - I(u) \end{aligned} \quad (3.7)$$

We can identify the bilinear and linear forms of the problem as

$$B(u, w) = \int_a^b b \frac{d^2 u}{dx^2} \frac{d^2 w}{dx^2} dx \quad (3.8)$$

$$I(u) = \int u p dx - u(x_a) Q_1' - \left(\frac{du}{dx} \right)_{x_a} Q_2' - u(x_b) Q_3' - \left(\frac{du}{dx} \right)_{x_b} Q_4'$$

Equation (3.8) is a statement of the principle of virtual displacements for the Euler-Bernoulli beam theory. The quadratic functional, known as the total potential energy of the beam element, is given by [58]

$$I_e(w) = \int \left[\frac{b}{2} \left(\frac{d^2 w}{dx^2} \right)^2 - w p \right] dx - w(x_a) Q_1' - \left(\frac{dw}{dx} \right)_{x_a} Q_2' - w(x_b) Q_3' - \left(\frac{dw}{dx} \right)_{x_b} Q_4' \quad (3.9)$$

Note that the key step in the derivation of the functional $I_e(w)$ from the weak form is the linearity and symmetry of the bilinear form $B(u, w)$. The relation $B(u, w) = \frac{1}{2} B(w, w)$ holds only if $B(u, w)$ is bilinear and symmetric in u and w . Thus, whenever $B(u, w)$ is bilinear and symmetric, and $I_e(w)$ is linear, the associated quadratic functional is given by

$$I_e(w) = \frac{1}{2} B(w, w) - I(w) \quad (3.10)$$

Other cases are discussed in the book by Reddy [65].

The first term in the square brackets represents the elastic strain energy due to bending, while the second is the work done by the distributed load: the remaining terms

account for the work done by the generalized forces Q_i^e in moving through the generalized displacements of the element.

3.2.3.2 Illustration Using a Beam Example

Consider the problem of finding the solution w to the differential equation of the beam

$$\frac{d^2}{dx^2} \left(b(x) \frac{d^2 w}{dx^2} \right) dx - p(x) = 0 \quad \text{for } 0 < x < L \quad (3.11)$$

subject to the boundary conditions

$$w(0) = \left(\frac{dw}{dx} \right) \Big|_{x=0} = 0, \quad \left(b \frac{d^2 w}{dx^2} \right) \Big|_{x=L} = M_0, \quad \left[\frac{d}{dx} \left(b \frac{d^2 w}{dx^2} \right) \right] \Big|_{x=L} = 0 \quad (3.12)$$

The solution w is the dependent variable of the problem, and all other quantities (L, b, p, M_0) that are known in advance are the data of the problem. Integrating twice the equation (3.11) after multiplying it with a weight function $u(x)$, will give us

$$0 = \int_{x_A}^{x_B} \left(b \frac{d^2 u}{dx^2} \frac{d^2 w}{dx^2} - u p \right) dx + \left[u \frac{d}{dx} \left(b \frac{d^2 w}{dx^2} \right) - \frac{du}{dx} b \frac{d^2 w}{dx^2} \right] \Big|_{x_A}^{x_B} \quad (3.13)$$

The boundary condition can be identified as in equation (3.13). In the present case, the specified essential boundary conditions are (because of the clamped condition)

$$w(0) = \left(\frac{dw}{dx} \right) \Big|_{x=0} = 0 \quad (3.14)$$

Hence, the weight function u is required to satisfy the conditions

$$u(0) = \left(\frac{du}{dx} \right) \Big|_{x=0} = 0 \quad (3.15)$$

The natural boundary conditions are

$$\left(b \frac{d^2 w}{dx^2} \right) \Big|_{x=L} = M_0, \quad \left[\frac{d}{dx} \left(b \frac{d^2 w}{dx^2} \right) \right] \Big|_{x=L} = 0 \quad (3.16)$$

Using equations (3.16) and (3.15) in (3.13), we obtain

$$0 = \int_0^L \left(b \frac{d^2 u}{dx^2} \frac{d^2 w}{dx^2} - up \right) dx - \left(\frac{du}{dx} \right) \Big|_{x=L} M_0 \quad (3.17a)$$

or

$$B(u, w) = I(u) \quad (3.17b)$$

where

$$B(u, w) = \int_0^L b \frac{d^2 u}{dx^2} \frac{d^2 w}{dx^2} dx \quad (3.18)$$

$$I(u) = \int_0^L up dx + \left(\frac{du}{dx} \right) \Big|_{x=L} M_0 \quad (3.19)$$

The quadratic form, commonly known as the total potential energy of the beam, is obtained using (3.17b), (3.18) and (3.19)

$$I(w) = \int \left[\frac{b}{2} \left(\frac{d^2 w}{dx^2} \right)^2 - wp \right] dx - \left(\frac{dw}{dx} \right) \Big|_{x=L} M_0 \quad (3.20)$$

As can be seen from the fourth order equation (3.20), the essential boundary conditions involve not only the dependent variable but also its first derivative. At the boundary point, only one of the two boundary conditions (essential or natural) can be specified since one is dependent on another. For example, if the transverse deflection is specified at a boundary point then one can not specify the shear force F at the same point, and vice versa. Similar situation applies to the slope dw/dx and the bending moment M . In the present case, w and dw/dx are the primary variables, and F and M are the secondary variables.

As can be seen from the static case the natural boundary condition is satisfied by including it in the weak form. In writing the final form of the variational or weak statement, we assume that all boundary conditions at the element level are of the natural type, so that they can be included in the variational statement. However in the dynamic case of free vibration, natural boundary conditions vanish in the weak form. In order to include the natural boundary conditions at the element level for a dynamic case of free vibration, a new set of efficient basis functions is developed next.

3.2.3.3 Interpolation Functions

To interpolate is to approximate the value of a function between known values by operating on the known values with a formula different from the function itself. The variational form in equation (3.7) requires that the interpolation functions of an element be continuous with nonzero derivatives up to order two. The approximation of the primary variables over a finite element should be such that it satisfies the interpolation properties (i.e., that it satisfies the essential and natural boundary conditions of the element:

$$w(x_A) = w_1 \quad w(x_B) = w_2 \quad \theta(x_A) = \theta_1 \quad \theta(x_B) = \theta_2 \quad (3.21a)$$

$$F(x_A) = F_1 \quad F(x_B) = F_2 \quad M(x_A) = M_1 \quad M(x_B) = M_2 \quad (3.21b)$$

In satisfying the essential and natural boundary conditions (equation (3.21)), the approximation automatically satisfies the continuity. Hence, we pay attention to the satisfaction of equation (3.21), which forms the basis for the interpolation procedure.

Since there are a total of eight conditions in an element (four per node), a eight-parameter polynomial is required to interpolate the end conditions. One must select w :

$$w(x) = c_0 + c_1x + c_2x^2 + c_3x^3 + c_4x^4 + c_5x^5 + c_6x^6 + c_7x^7 \quad (3.22)$$

Note that the continuity conditions (i.e., the existence of nonzero second and fourth derivatives of w in the element) are automatically met. The next step involves

expressing c_i in terms of the primary nodal variables (i.e., generalized displacements)

The boundary points $x = x_A = 0$ and $x = x_B = r$ are expressed in terms of local coordinates

$$\begin{aligned}\theta(x) &= \frac{dw(x)}{dx} = c_1 + 2c_2x + 3c_3x^2 + 4c_4x^3 + 5c_5x^4 + 6c_6x^5 + 7c_7x^6 \\ M(x) &= b \frac{d^2w(x)}{dx^2} = b(2c_2 + 6c_3x + 12c_4x^2 + 20c_5x^3 + 30c_6x^4 + 42c_7x^5) \\ F(x) &= -b \frac{d^3w(x)}{dx^3} = -b(6c_3 + 24c_4x + 60c_5x^2 + 120c_6x^3 + 210c_7x^4)\end{aligned}\quad (3.23)$$

such that the conditions in equation (3.22) are satisfied:

$$\begin{aligned}w_1 &= w(0) = c_0 \\ \theta_1 &= \theta(0) = c_1 \\ w_2 &= w(r) = c_0 + c_1r + c_2r^2 + c_3r^3 + c_4r^4 + c_5r^5 + c_6r^6 + c_7r^7 \\ \theta_2 &= \theta(r) = c_1 + 2c_2r + 3c_3r^2 + 4c_4r^3 + 5c_5r^4 + 6c_6r^5 + 7c_7r^6 \\ F_1 &= F(0) = -6bc_3 \\ M_1 &= M(0) = 2bc_2 \\ F_2 &= F(r) = -b(6c_3 + 24c_4r + 60c_5r^2 + 120c_6r^3 + 210c_7r^4) \\ M_2 &= M(r) = b(2c_2 + 6c_3r + 12c_4r^2 + 20c_5r^3 + 30c_6r^4 + 42c_7r^5)\end{aligned}\quad (3.24)$$

or

$$\begin{Bmatrix} w_1 \\ \theta_1 \\ w_2 \\ \theta_2 \\ F_1 \\ M_1 \\ F_2 \\ M_2 \end{Bmatrix} = \begin{bmatrix} 1 & 0 & 0 & 0 & 0 & 0 & 0 & 0 \\ 0 & 1 & 0 & 0 & 0 & 0 & 0 & 0 \\ 1 & r & r^2 & r^3 & r^4 & r^5 & r^6 & r^7 \\ 0 & 1 & 2r & 3r^2 & 4r^3 & 5r^4 & 6r^5 & 7r^6 \\ 0 & 0 & 0 & -6b & 0 & 0 & 0 & 0 \\ 0 & 0 & 2b & 0 & 0 & 0 & 0 & 0 \\ 0 & 0 & 0 & -6b & -24br & -60br^2 & -120br^3 & -210br^4 \\ 0 & 0 & 2b & 6br & 12br^2 & 20br^3 & 30br^4 & 42br^5 \end{bmatrix} \begin{Bmatrix} c_0 \\ c_1 \\ c_2 \\ c_3 \\ c_4 \\ c_5 \\ c_6 \\ c_7 \end{Bmatrix} \quad (3.25)$$

Inverting this matrix equation to express c_i in terms of $w_1, \theta_1, w_2, \theta_2, F_1, M_1, F_2$ and M_2 , and substituting the result into equation (3.22), we obtain

$$w(x) = N_1 w_1 + N_2 \theta_1 + N_3 w_2 + N_4 \theta_2 + N_5 F_1 + N_6 M_1 + N_7 F_2 + N_8 M_2 \quad (3.26)$$

where (with $x_A = 0, x_B = r$)

$$\begin{aligned} N_1^c(x) &= 1 - 35 \frac{x^4}{r^4} + 84 \frac{x^5}{r^5} - 70 \frac{x^6}{r^6} + 20 \frac{x^7}{r^7} \\ N_2^c(x) &= x - \frac{20x^4}{r^3} + \frac{45x^5}{r^4} - \frac{36x^6}{r^5} + \frac{10x^7}{r^6} \\ N_3^c(x) &= 35 \frac{x^4}{r^4} - 84 \frac{x^5}{r^5} + 70 \frac{x^6}{r^6} - 20 \frac{x^7}{r^7} \\ N_4^c(x) &= -15 \frac{x^4}{r^3} + 39 \frac{x^5}{r^4} - 34 \frac{x^6}{r^5} + 10 \frac{x^7}{r^6} \\ N_5^c(x) &= -\frac{x^3}{6b} + 2 \frac{x^4}{3br} - \frac{x^5}{br^2} + 2 \frac{x^6}{3br^3} - \frac{x^7}{6br^4} \\ N_6^c(x) &= \frac{x^2}{2b} - 5 \frac{x^4}{br^2} + 10 \frac{x^5}{br^3} - 15 \frac{x^6}{2br^4} + \frac{2x^7}{br^5} \\ N_7^c(x) &= \frac{x^4}{6br} - \frac{x^5}{2br^2} + \frac{x^6}{2br^3} - \frac{x^7}{6br^4} \\ N_8^c(x) &= 5 \frac{x^4}{2br^2} - 7 \frac{x^5}{br^3} + 13 \frac{x^6}{2br^4} - 2 \frac{x^7}{br} \end{aligned} \quad (3.27)$$

Note that interpolating w and its derivative at the nodes derives the 7-th order

interpolation functions in equation (3.26). N_1, \dots, N_8 in (3.27) are called interpolation functions.

The interpolation functions in equation (3.26) satisfy the following interpolation properties (see figure. (3.4), (3.5), (3.6) and (3.7)).

$$\begin{aligned}
 N_1|_{x=0} &= 1, & N_i|_{x=0} &= 0 \quad (i \neq 1) \\
 N_3|_{x=r} &= 1, & N_i|_{x=r} &= 0 \quad (i \neq 3) \\
 \frac{dN_2}{dx}|_{x=0} &= 1, & \frac{dN_i}{dx}|_{x=0} &= 0 \quad (i \neq 2) \\
 \frac{dN_4}{dx}|_{x=r} &= 1, & \frac{dN_i}{dx}|_{x=r} &= 0 \quad (i \neq 4)
 \end{aligned} \tag{3.28a}$$

$$\begin{aligned}
 b \frac{d^2 N_6}{dx^2}|_{x=0} &= 1, & b \frac{d^2 N_i}{dx^2}|_{x=0} &= 0 \quad (i \neq 6) \\
 b \frac{d^2 N_8}{dx^2}|_{x=r} &= 1, & b \frac{d^2 N_i}{dx^2}|_{x=r} &= 0 \quad (i \neq 8) \\
 \left[-b \frac{d^3 N_5}{dx^3} \right]_{x=0} &= 1, & \left[-b \frac{d^3 N_i}{dx^3} \right]_{x=0} &= 0 \quad (i \neq 5) \\
 \left[-b \frac{d^3 N_7}{dx^3} \right]_{x=r} &= 1, & \left[-b \frac{d^3 N_i}{dx^3} \right]_{x=r} &= 0 \quad (i \neq 7)
 \end{aligned} \tag{3.28b}$$

where $i = 1..8$.

It should be noted that the order of the interpolation functions derived above is the minimum required for the variational formulation (3.7).

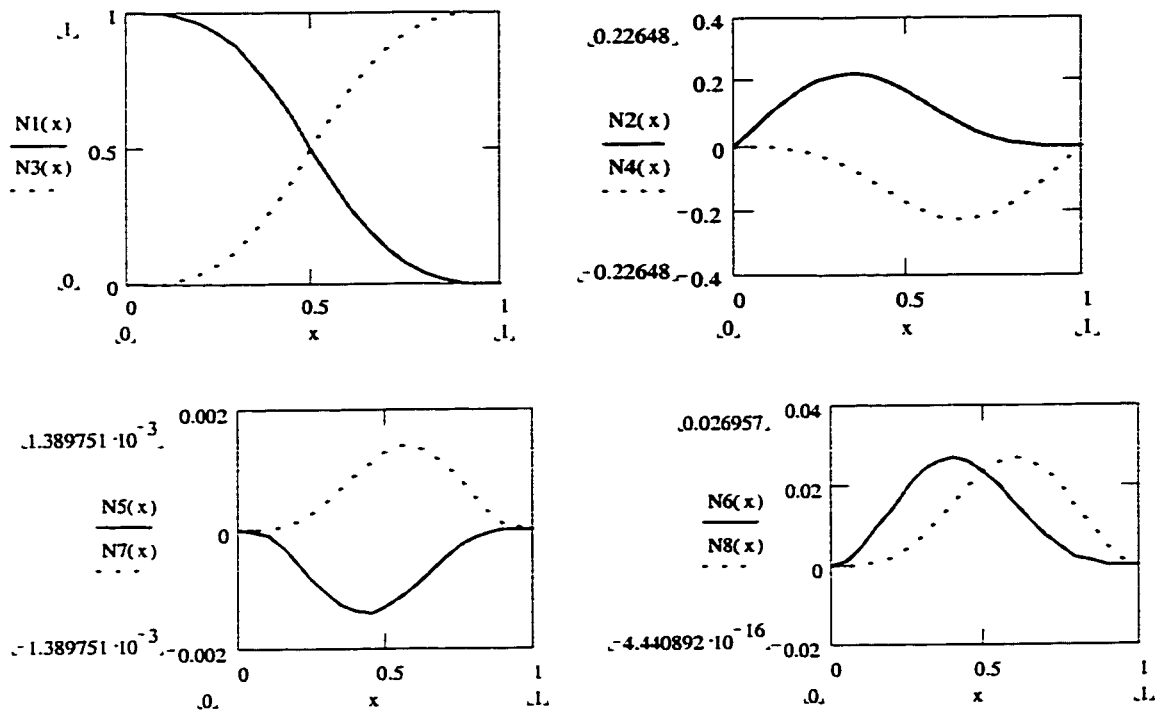


Figure 3.4 Interpolation functions N_i where $i = 1 \dots 8$

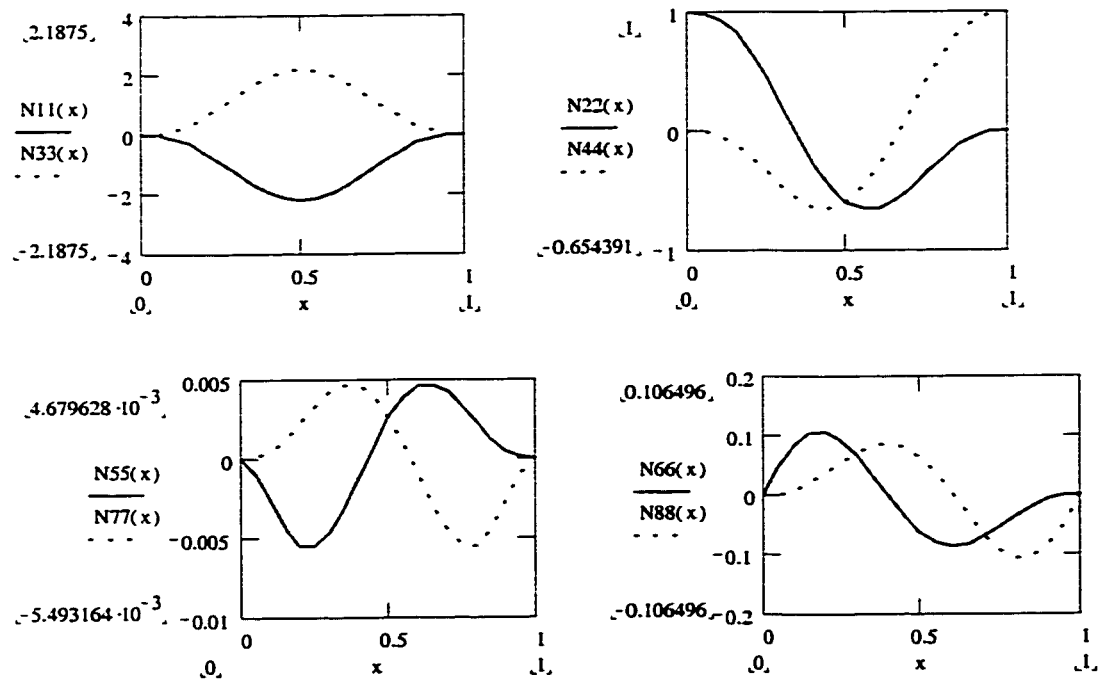


Figure 3.5 First derivatives of interpolation functions N_1 ($N11$) to N_8 ($N88$).

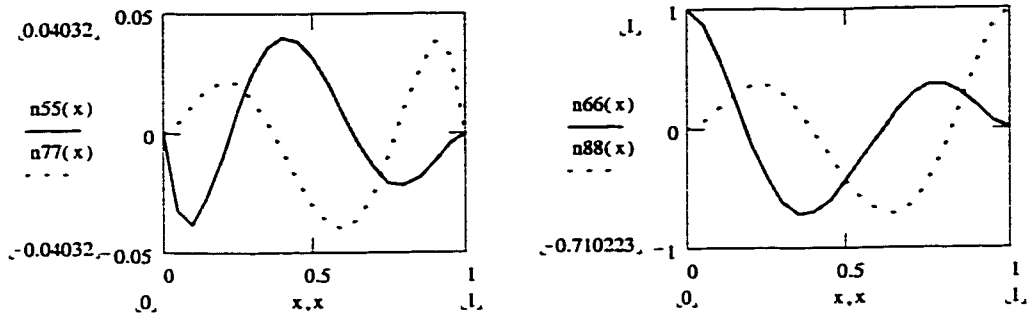


Figure 3.6 Second derivatives of interpolation functions N_5 ($n55$), N_6 ($n66$), N_7 ($n77$), and N_8 ($n88$).

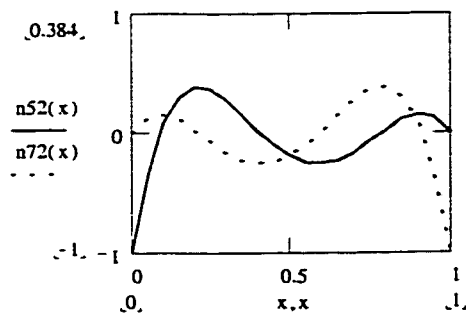


Figure 3.7 Third derivatives of interpolation function N_5 ($n52$) and N_7 ($n72$).

3.3 Formulation of the Eigenvalue Problem

3.3.1 Free Lateral Vibration of Beam

In practice it is found that when the lower natural frequencies of a machine component in the form of a beam coincide with the speed of operation of machinery, the component undergoes resonance. The bending oscillations of steel railway bridges and the bending oscillations of aircraft wings are examples, which have caused considerable concern in the past.

Thin beams with simple end conditions:

The sign convention adopted for the present analysis is shown in figure (3.8)

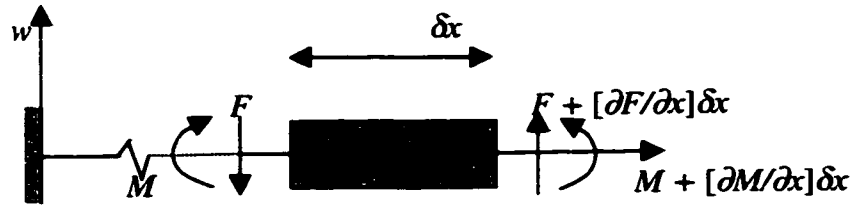


Figure 3.8 Sign convention for the beam

Apply Newton's law for the motion in the z direction of w:

$$\begin{aligned}
 -F + F + \frac{\partial F}{\partial x} \delta x &= \rho A \delta x \frac{\partial^2 w}{\partial t^2} \\
 \frac{\partial F}{\partial x} &= \rho A \frac{\partial^2 w}{\partial t^2}
 \end{aligned}
 \tag{3.29}$$

For rotational moment

$$\begin{aligned}
 -M + M + \frac{\partial M}{\partial x} \delta x + F \delta x &= 0 \\
 F &= -\frac{\partial M}{\partial x}
 \end{aligned}
 \tag{3.30}$$

Substituting value (3.30) in (3.29)

$$\frac{\partial^2 M}{\partial x^2} + \rho A \frac{\partial^2 w}{\partial t^2} = 0
 \tag{3.31}$$

We know that,

$$M = EI \frac{\partial^2 w}{\partial x^2} \quad (3.32)$$

Substituting (3.32) in equation (3.31) we will have

$$\frac{\partial^2}{\partial x^2} \left(EI \frac{\partial^2 w}{\partial x^2} \right) + \rho A \frac{\partial^2 w}{\partial t^2} = 0 \quad (3.33)$$

This is the differential equation of motion of the beam with no external load.

We employ a separation of variables approach by expressing w as the product of a function of x and a function of t , thus

$$w(x, t) = W(x) \tau(t) = W(x) e^{i\omega t} \quad (3.34)$$

where ω is the frequency of natural transverse motion and $W(x)$ is the mode shape of the transverse motion. Substituting equation (3.34) into equation (3.33) we get ordinary differential equations as follows:

$$\left[\frac{d^2}{dx^2} \left(EI \frac{d^2 W}{dx^2} \right) - \rho A \omega^2 W \right] e^{i\omega t} = 0 \quad (3.35)$$

or

$$\frac{d^2}{dx^2} \left(EI \frac{d^2 W}{dx^2} \right) - \lambda \rho A W = 0 \quad (3.36)$$

where $\lambda = \omega^2$.

Equation (3.36) is an eigenvalue problem, which involves determining the square of natural frequencies λ and mode shapes W .

3.3.2 Finite Element Model

An examination of the eigenvalue equation derived in the previous section shows that they are a special case of the equation for beam bending, as in equation (3.1). For example consider

$$\frac{d^2}{dx^2} \left(EI \frac{d^2 w}{dx^2} \right) - p(x) = 0 \quad (3.37)$$

The eigenvalue equation associated with this is

$$\frac{d^2}{dx^2} \left(EI \frac{d^2 W}{dx^2} \right) - \lambda \rho A W = 0 \quad (3.38)$$

This equation holds for a non-uniform beam. But for a uniform beam, the quantities ρ , A and EI are constants. Hence, the equation may be written in the following form

$$\frac{d^4 W}{dx^4} - \frac{\omega^2 \rho A}{EI} W = 0 \quad (3.39)$$

It is important to note that the spatial derivative operators of the static (i.e., non-time-dependent) and eigenvalue equations are the same. The difference between (3.36) and (3.37) is that, in place of the source term p , we have $\lambda \rho A W$ in the eigenvalue equations. This difference is responsible for another coefficient matrix, in addition to the coefficient matrix $[K]$, in the eigenvalue problems. The derivation of the finite element models of eigenvalue equations is presented next.

Over a typical element Δ^e , we seek a finite element approximation of W in the form

$$W = \sum_{j=1}^n v_j^e N_j^e(x) \quad (3.40)$$

The weak form of (3.38) is

$$0 = \int_{x_A}^{x_B} \left[EI \frac{d^2 u}{dx^2} \frac{d^2 W}{dx^2} - \lambda \rho A u W \right] dx - u(x_A) Q_1 - \frac{du}{dx} \Big|_{x_A} Q_2 - u(x_B) Q_3 - \frac{du}{dx} \Big|_{x_B} Q_4 \quad (3.41)$$

where $u(x)$ is the weight function, Q_n ($n = 1..4$) are usual secondary variables. Substituting the finite element approximation into the weak form gives the finite element model of the eigenvalue equation (3.38)

$$0 = \sum_{j=1}^n \int_{x_A}^{x_B} \left[EI \frac{d^2 N_i}{dx^2} \frac{d^2 N_j}{dx^2} dx - \lambda \rho A N_i N_j dx \right] v_j - Q_i \quad (3.42a)$$

or

$$[K^e] \{v^e\} - \lambda [M^e] \{v^e\} = \{Q^e\} \quad (3.42b)$$

where $\{v^e\}$ and $\{Q^e\}$ are the columns of nodal generalized displacement and force degrees of freedom of the Euler-Bernoulli beam element:

$$\{v^e\} = \begin{Bmatrix} w_1 \\ \theta_1 \\ w_2 \\ \theta_2 \\ F_1 \\ M_1 \\ F_2 \\ M \end{Bmatrix} \quad (3.43)$$

where the subscripts 1 and 2 refer to element nodes 1 and 2 (at $x = x_A$ and $x = x_B$). The $[K^e]$ and $[M^e]$, known as the stiffness and mass matrices, respectively, are defined by

$$K_{ij}^e = \int_{x_A}^{x_B} EI \frac{d^2 N_i}{dx^2} \frac{d^2 N_j}{dx^2} dx, \quad M_{ij}^e = \int_{x_A}^{x_B} \rho A N_i N_j dx \quad (3.44)$$

where N_i^e and N_j^e are the interpolation functions. The stiffness and mass matrices can be evaluated numerically for element-wise-constant value of EI , ρ and A and they are presented in equations (3.45) and (3.46).

$$\mathbf{K}_e = \frac{b}{r^3} \begin{bmatrix}
\frac{280}{11} & \frac{140}{11} \cdot r & \frac{-280}{11} & \frac{140}{11} \cdot r & -1 & \frac{40}{(33 \cdot b)} \cdot r^2 & -1 & \frac{40}{(33 \cdot b)} \cdot r^2 & -1 & \frac{40}{(33 \cdot b)} \cdot r^2 & -40 & \frac{40}{(33 \cdot b)} \cdot r^2 \\
\frac{140}{11} \cdot r & \frac{600}{77} \cdot r^2 & \frac{-140}{11} \cdot r & \frac{380}{77} \cdot r^2 & \frac{-8}{231} \cdot r^4 & \frac{379}{(462 \cdot b)} \cdot r^3 & \frac{-8}{231} \cdot r^4 & \frac{379}{(462 \cdot b)} \cdot r^3 & \frac{-5}{462} \cdot r^4 & \frac{379}{(462 \cdot b)} \cdot r^3 & -181 & \frac{-181}{(462 \cdot b)} \cdot r^3 \\
\frac{-280}{11} & \frac{-140}{11} \cdot r & \frac{280}{11} & \frac{-140}{11} \cdot r & \frac{1}{(22 \cdot b)} & \frac{280}{(33 \cdot b)} \cdot r^2 & \frac{1}{(22 \cdot b)} & \frac{280}{(33 \cdot b)} \cdot r^2 & \frac{1}{(22 \cdot b)} & \frac{280}{(33 \cdot b)} \cdot r^2 & \frac{40}{(33 \cdot b)} & \frac{40}{(33 \cdot b)} \cdot r^2 \\
\frac{140}{11} \cdot r & \frac{380}{77} \cdot r^2 & \frac{-140}{11} \cdot r & \frac{600}{77} \cdot r^2 & \frac{-5}{462} \cdot r^4 & \frac{181}{(462 \cdot b)} \cdot r^3 & \frac{-5}{462} \cdot r^4 & \frac{181}{(462 \cdot b)} \cdot r^3 & \frac{-8}{231} \cdot r^4 & \frac{181}{(462 \cdot b)} \cdot r^3 & -379 & \frac{-379}{(462 \cdot b)} \cdot r^3 \\
-1 & \frac{-8}{231} \cdot r^4 & \frac{1}{(22 \cdot b)} & \frac{-5}{462} \cdot r^4 & \frac{2}{(3465 \cdot b^2)} \cdot r^6 & \frac{-1}{(99 \cdot b^2)} \cdot r^5 & \frac{2}{(3465 \cdot b^2)} \cdot r^6 & \frac{-1}{(99 \cdot b^2)} \cdot r^5 & \frac{-1}{(4620 \cdot b^2)} \cdot r^6 & \frac{-1}{(4620 \cdot b^2)} \cdot r^5 & -5 & \frac{-5}{(2772 \cdot b^2)} \cdot r^5 \\
\frac{40}{(33 \cdot b)} \cdot r^2 & \frac{379}{(462 \cdot b)} \cdot r^3 & \frac{-40}{(33 \cdot b)} \cdot r^2 & \frac{181}{(462 \cdot b)} \cdot r^3 & \frac{-1}{(99 \cdot b^2)} \cdot r^5 & \frac{50}{(231 \cdot b^2)} \cdot r^4 & \frac{-1}{(99 \cdot b^2)} \cdot r^5 & \frac{50}{(231 \cdot b^2)} \cdot r^4 & \frac{5}{2772} \cdot r^5 & \frac{5}{2772} \cdot r^4 & -1 & \frac{-1}{(462 \cdot b^2)} \cdot r^4 \\
-1 & \frac{-5}{462} \cdot r^4 & \frac{1}{(22 \cdot b)} & \frac{-8}{231} \cdot r^4 & -1 & \frac{5}{2772} \cdot r^5 & -1 & \frac{5}{2772} \cdot r^5 & \frac{2}{(3465 \cdot b^2)} \cdot r^6 & \frac{2}{(3465 \cdot b^2)} \cdot r^5 & \frac{1}{(99 \cdot b^2)} & \frac{1}{(99 \cdot b^2)} \cdot r^5 \\
\frac{-40}{(33 \cdot b)} \cdot r^2 & \frac{-181}{(462 \cdot b)} \cdot r^3 & \frac{40}{(33 \cdot b)} \cdot r^2 & \frac{-379}{(462 \cdot b)} \cdot r^3 & \frac{-5}{(2772 \cdot b^2)} \cdot r^5 & \frac{-1}{(462 \cdot b^2)} \cdot r^4 & \frac{-5}{(2772 \cdot b^2)} \cdot r^5 & \frac{-1}{(462 \cdot b^2)} \cdot r^4 & \frac{1}{(99 \cdot b^2)} \cdot r^5 & \frac{1}{(99 \cdot b^2)} \cdot r^4 & 50 & \frac{50}{(231 \cdot b^2)} \cdot r^4
\end{bmatrix}$$

(3.45)

Finite element stiffness matrix

$$M^e = \frac{\rho \cdot A \cdot r}{420} \begin{bmatrix} \frac{72940}{429} & \frac{4530}{143} \cdot r & \frac{17150}{429} & -\frac{1905}{143} \cdot r & -\frac{383}{2574} r^3 & \frac{1370}{(429 \cdot b)} r^2 & \frac{521}{5148} r^3 & \frac{775}{(429 \cdot b)} r^2 \\ \frac{4530}{143} \cdot r & \frac{100}{13} r^2 & \frac{1905}{143} \cdot r & -\frac{1865}{429} r^2 & -\frac{6}{143} r^4 & \frac{245}{286} r^3 & \frac{5}{156} r^4 & \frac{995}{1716} r^3 \\ \frac{17150}{429} & \frac{1905}{143} \cdot r & \frac{72940}{429} & -\frac{4530}{143} \cdot r & -\frac{521}{5148} r^3 & \frac{775}{(429 \cdot b)} r^2 & \frac{383}{2574} r^3 & \frac{1370}{(429 \cdot b)} r^2 \\ -\frac{1905}{143} \cdot r & -\frac{1865}{429} r^2 & -\frac{4530}{143} \cdot r & \frac{100}{13} r^2 & \frac{5}{156} r^4 & -\frac{995}{1716} r^3 & -\frac{6}{143} r^4 & -\frac{245}{286} r^3 \\ -\frac{383}{2574} r^3 & \frac{100}{143} r^2 & -\frac{4530}{143} \cdot r & \frac{5}{156} r^4 & \frac{1}{3861} r^6 & -\frac{1}{198} r^5 & -\frac{7}{30888} r^6 & -\frac{43}{10296} r^5 \\ \frac{1370}{(429 \cdot b)} r^2 & \frac{245}{286} r^3 & \frac{775}{(429 \cdot b)} r^2 & -\frac{995}{1716} r^3 & -\frac{1}{198} r^5 & \frac{43}{429} r^4 & \frac{43}{10296} r^5 & \frac{131}{1716} r^4 \\ \frac{521}{5148} r^3 & \frac{5}{156} r^4 & \frac{383}{2574} r^3 & -\frac{6}{143} r^4 & \frac{7}{30888} r^6 & \frac{43}{10296} r^5 & \frac{1}{3861} r^6 & \frac{1}{198} r^5 \\ \frac{775}{(429 \cdot b)} r^2 & \frac{995}{1716} r^3 & \frac{1370}{(429 \cdot b)} r^2 & -\frac{245}{286} r^3 & -\frac{43}{10296} r^5 & \frac{131}{1716} r^4 & \frac{1}{198} r^5 & \frac{43}{429} r^4 \end{bmatrix} \quad (3.46)$$

Finite Element Mass Matrix

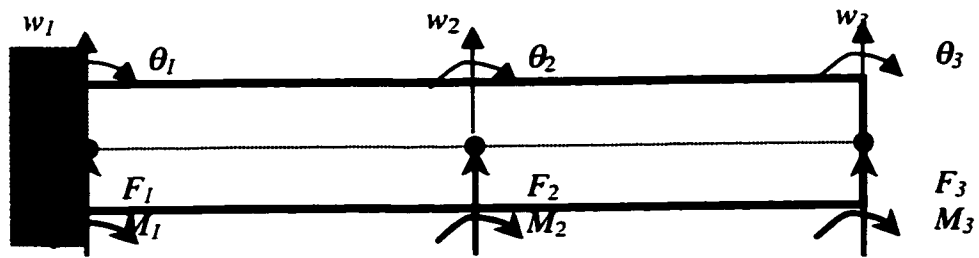


Figure 3.9a Two-element model of a Cantilever beam in global coordinates

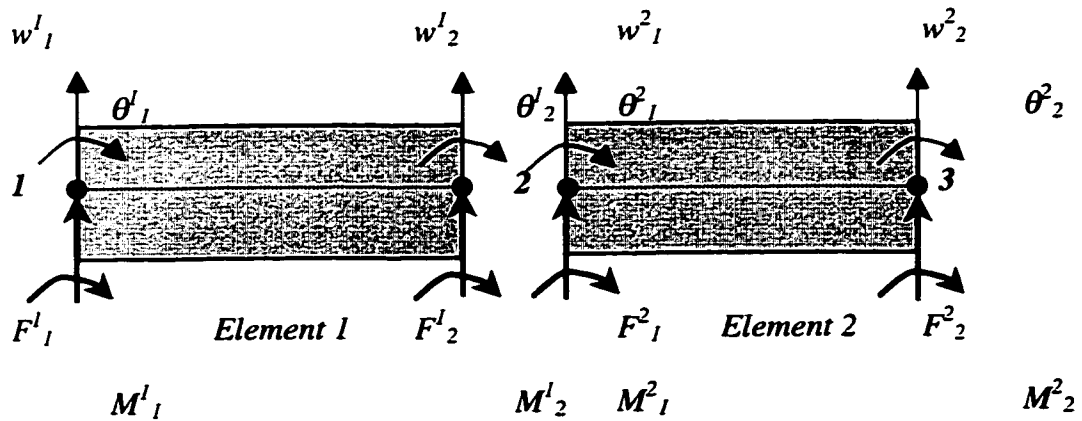


Figure 3.9b Assembly of two beam finite elements in local coordinates

3.3.3 Assembly of Element Equations

To demonstrate the assembly procedure, we select a two-element model (see figure. 3.9a). There are three global nodes and a total of twelve global degrees of freedom.

In deriving the element equations, we isolated a typical element (the e -th) from the mesh and formulated the variational problem (or weak form) and developed its finite element model. To solve the total problem, we must put the elements back into their original positions. In doing this before discretization, we impose the continuity of the primary variables at the connecting nodes between elements. Continuity of the primary variables refers here to single-valued nature of the solution. Thus, the assembly of elements is carried out by imposing the following two conditions:

1. Continuity of primary variables(deflection and slope, force and moment related derivatives at the corresponding point in the structure) at connecting nodes:

$$v_n^e = v_{l}^{e+1} \quad (3.47)$$

where

$$\{v^e\} = \begin{Bmatrix} w \\ \theta \\ F \\ M \end{Bmatrix}^e \quad (3.48)$$

i.e., the last nodal value of the elements Δ^e is the same as the first nodal value of the adjacent element Δ^{e+1} .

2. Balance of secondary variables(shear force and bending moment) at

connecting nodes:

$$Q_n^e + Q_{n+1}^{e+1} = 0 \quad \text{The boundary conditions are homogeneous} \quad (3.49)$$

In writing equation (3.47), it is assumed that elements are connected in a sequence. The continuity of primary variables $v_n^e = v_{n+1}^{e+1}$ for a mesh of linear elements is illustrated in figure (3.10).

The inter-element continuity of the primary variables is imposed by renaming the two variables v_n^e and v_{n+1}^{e+1} at $x = x_S$ as one and the same, namely the value of V at the global node S :

$$v_n^e = v_{n+1}^{e+1} = V_S \quad (3.50)$$

where $S = [(n-1)e+1]$ is the global node number corresponding to node n of the element Δ^e and node 1 of the element Δ^{e+1} . Similarly we can write for θ , F and M . For example, for the mesh of E linear finite elements ($n = 2$), we have (see figure (3.10))

$$\begin{aligned} v_1^1 &= V_1 \\ v_2^1 &= v_1^2 = V_2 \\ v_2^2 &= v_1^3 = V_3 \\ &\vdots \\ v_{2}^{E-1} &= v_1^E = V_E \\ v_2^E &= V_{E+1} \end{aligned} \quad (3.51)$$

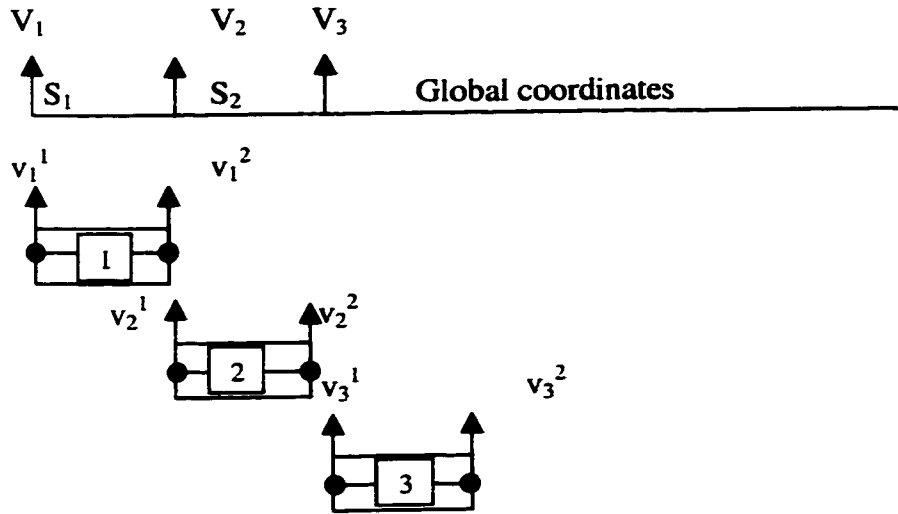


Figure 3.10 The inter-element continuity of nodal degrees of freedom

To obtain such expressions, we must add the n -th equation of the element Δ^e to the first equation of the element Δ^{e+1} ; that is, we add

$$\sum_{j=1}^n [K_{nj}^e - \lambda M_{nj}^e] \{v_j^e\} = 0$$

and

$$\sum_{j=1}^n [K_{1j}^{e+1} - \lambda M_{1j}^{e+1}] \{v_j^{e+1}\} = 0$$

to give

$$\sum_{j=1}^n [(K_{nj}^e v_j^e + K_{1j}^{e+1} v_j^{e+1}) - \lambda (M_{nj}^e v_j^e + M_{1j}^{e+1} v_j^{e+1})] = 0 \quad (3.52)$$

This process reduces the number of equations from $2E$ to $E+1$. The first equation of the first element and the last equation of the last element will remain unchanged, except for renaming of the primary variables. For a mesh of E linear elements ($n = 2$), we have 12 assembled equations. They contain the sum of coefficients and source terms at nodes common to two elements. Note that the numbering of the global equations corresponds to the numbering of the global primary degrees of freedom, V_i . This correspondence carries the symmetry of element matrices to the global matrix. In general, the assembled stiffness matrix for beam elements connected in series has the following form:(equation. 3.53).

$$\begin{bmatrix}
 K_{11}^1 & K_{12}^1 & K_{13}^1 & K_{14}^1 & 0 & 0 & K_{15}^1 & K_{16}^1 & K_{17}^1 & K_{18}^1 & 0 & 0 \\
 & K_{22}^1 & K_{23}^1 & K_{24}^1 & 0 & 0 & K_{25}^1 & K_{26}^1 & K_{27}^1 & K_{28}^1 & 0 & 0 \\
 & & K_{33}^1 + K_{11}^2 & K_{34}^1 + K_{12}^2 & K_{13}^2 & K_{14}^2 & K_{35}^1 & K_{36}^1 & K_{37}^1 + K_{15}^2 & K_{38}^1 + K_{16}^2 & K_{17}^2 & K_{18}^2 \\
 & & & K_{44}^1 + K_{22}^2 & K_{23}^2 & K_{24}^2 & K_{45}^1 & K_{46}^1 & K_{47}^1 + K_{25}^2 & K_{48}^1 + K_{26}^2 & K_{27}^2 & K_{28}^2 \\
 & & & & K_{33}^2 & K_{34}^2 & 0 & 0 & K_{35}^2 & K_{36}^2 & K_{37}^2 & K_{38}^2 \\
 & & & & & K_{44}^2 & 0 & 0 & K_{45}^2 & K_{46}^2 & K_{47}^2 & K_{48}^2 \\
 & & & & & & K_{55}^1 & K_{56}^1 & K_{57}^1 & K_{58}^1 & 0 & 0 \\
 & & & & & & & K_{66}^1 & K_{67}^1 & K_{68}^1 & 0 & 0 \\
 & & & & & & & & K_{77}^1 + K_{55}^2 & K_{78}^1 + K_{56}^2 & K_{57}^2 & K_{58}^2 \\
 & & & & & & & & & K_{88}^1 + K_{66}^2 & K_{67}^2 & K_{68}^2 \\
 & & & & & & & & & & K_{77}^2 & K_{78}^2 \\
 & & & & & & & & & & & K_{88}^2
 \end{bmatrix} - \lambda[M]$$

Symm.

$$\begin{bmatrix}
 w_1 \\
 \theta_1 \\
 w_2 \\
 \theta_2 \\
 w_3 \\
 \theta_3 \\
 F_1 \\
 M_1 \\
 F_2 \\
 M_2 \\
 F_3 \\
 M_3
 \end{bmatrix} = 0$$

(3.53)

3.3.4 Imposition of Boundary Conditions

At this stage in the analysis, we must specify the particular boundary conditions, i.e., geometric constraints and forces applied, of the problem to be analyzed. The type of essential (also known as geometric) boundary conditions for a specific beam problem depends on the nature of the geometric support. Table 3.1 contains a list of commonly used geometric supports for beams. The natural (also called force) boundary conditions involve the specification of generalized forces at the free end as well as the fixed ends. Here we consider a cantilever beam with free end of length L with the free end (see figure 3.9a).

First we write the natural (also called force) boundary conditions in this problem, at global node 3, corresponding to the free end, where the shear force and the bending moment are zero:

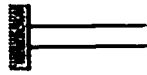

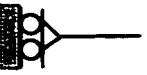
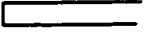
$$F_2^2 = M_2^2 = 0 \quad (3.54)$$

Next we identify and impose the specific generalized displacements. Since the beam is clamped at global node 1, it follows that the deflection w and the slope dw/dx are zero there, i.e.,

$$V_1^1 = w^1 = 0 \quad V_1^2 = \theta_1^1 = 0 \quad (3.55)$$

Using equations (3.54) and (3.55) in (3.53), we obtain

Table (3.1) Various Boundary Conditions of a Beam

<i>Various end cases</i>		<i>Boundary condition</i>	
		<i>Left,</i> $x = 0$	<i>Right,</i> $x = L$
Clamped (deflection, slope = 0)		$w(0,t) = 0$ $\frac{\partial w}{\partial x}(0,t) = 0$	$w(L,t) = 0$ $\frac{\partial w}{\partial x}(L,t) = 0$
Pinned (deflection, moment = 0)		$w(0,t) = 0$ $\frac{\partial^2 w}{\partial x^2}(0,t) = 0$	$w(L,t) = 0$ $\frac{\partial^2 w}{\partial x^2}(L,t) = 0$
Sliding (slope, shear = 0)		$\frac{\partial w}{\partial x}(0,t) = 0$ $\frac{\partial^3 w}{\partial x^3}(0,t) = 0$	$\frac{\partial w}{\partial x}(L,t) = 0$ $\frac{\partial^3 w}{\partial x^3}(L,t) = 0$
Free (moment, shear = 0)		$\frac{\partial^2 w}{\partial x^2}(0,t) = 0$ $\frac{\partial^3 w}{\partial x^3}(0,t) = 0$	$\frac{\partial^2 w}{\partial x^2}(L,t) = 0$ $\frac{\partial^3 w}{\partial x^3}(L,t) = 0$

$$V = \left\{ \begin{array}{l} w_1 = 0 \\ \theta_1 = 0 \\ w_2 \\ \theta_2 \\ w_3 \\ \theta_3 \\ F_1 \\ M_1 \\ F_2 \\ M_2 \\ F_3 = 0 \\ M_3 = 0 \end{array} \right\}, \quad (3.56)$$

3.3.5 Natural Frequencies of Uniform Beams with Various End Conditions

Two structures, identical in all respects except for boundary constraints, will have different natural modes and frequencies of vibration. As will be seen, there are cases in which the frequencies are identical but, in such cases, the mode shapes differ.

In this section we will summarize the natural frequencies for simple, uniform beams with various kinds of constraints at the ends. We shall be concerned with only the “natural” boundary conditions in which constraint forces at the ends do no work. For cases in which constraint forces do work on the beam, we must have information concerning the force-deflection properties of the attached structure, which react on these forces. This, in effect, requires that we extend the boundaries of our structure beyond those of the simple beam itself.

Constraints, which do no work on an arbitrary displacement of the beam, must be such that either the displacements at the constraints or the constraint forces are zero.

Here we use the terms displacement, rotation, force and moment. In beams, work at constraints might be computed from either or both of the products:

(Transverse Shear) x (Transverse Displacement)

(Bending Moment) x (Rotation)

For both products to be zero at the end of a beam, one term in each product must vanish. Thus, the boundary conditions must occur in pairs at each end. The possible four combinations are presented in Table (3.1).

Considering both ends, we have four boundary conditions, as we would expect to have in a problem governed by a differential equation of fourth order. Since any pair of conditions at one end may be combined with any one of the four pairs at the other end, we have ten possible combinations or ten beam types where the beam is uniform. Each one is typified by the unique eigenvalue and the natural frequencies can be expressed in terms of eigenvalues βL according to equation (3.57)

$$\omega = (\beta L)^2 \sqrt{\frac{EI}{\rho AL^4}} \quad (3.57)$$

3.3.5.1 Applications

Here we consider a couple of examples of eigenvalue problems to illustrate the concepts described in the previous section using higher order finite elements. We consider an example of free vibration of beams.

Consider a uniform beam of rectangular cross-section, L , width B , and height H . The beam is fixed at one end, say at $x = 0$, and free at the other, $x = L$. (figure3.1). We wish to determine the first four natural frequencies associated with the transverse deflection w . The finite element model of the beam theory is given (3.11). The number of eigenvalues we wish to determine dictates the minimum number of elements to be used.

One-Element Model:

The beam is considered as one element with 2 nodes. Each node has 4 degrees of freedom. $L = r$

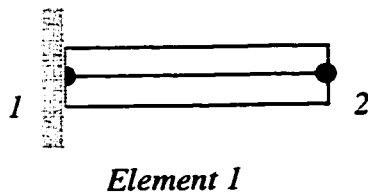


Figure (3.11) One-element model of a beam

$$\{v^e\} = \begin{Bmatrix} w_1 \\ \theta_1 \\ w_2 \\ \theta_2 \\ F_1 \\ M_1 \\ F_2 \\ M_2 \end{Bmatrix} \quad (3.58)$$

Essential boundary conditions at the fixed end:

$$w(0) = 0, \theta(0) = 0 \text{ or } w_1 = \theta_1 = 0 \quad (3.59)$$

Natural boundary conditions at the free end:

$$F(L) = 0, M(L) = 0 \text{ or } F_2 = M_2 = 0 \quad (3.60)$$

Because $w_l = \theta_l = 0$, the first two columns and rows of stiffness and mass matrices can be ignored, and further since it is a free end boundary at $x = L$, the last two columns and rows can be ignored. For a mesh of one element, with the set of boundary conditions at both ends, the condensed element equation becomes

$$[K] \{v\} - \lambda [M] \{v\} = 0 \quad (3.61)$$

where

$$\{v\} = \begin{Bmatrix} w_2 \\ \theta_2 \\ F_1 \\ M_1 \end{Bmatrix} \quad (3.62)$$

$$\left[\begin{array}{cccc} \frac{280}{11} & \frac{-140}{11}r & \frac{1}{(22b)}r^3 & \frac{-40}{(33b)}r^2 \\ \frac{-140}{11}r & \frac{600}{77}r^2 & \frac{-5}{462b}r^4 & \frac{181}{(462b)}r^3 \\ \frac{1}{(22b)}r^3 & \frac{-5}{462b}r^4 & \frac{2}{3465b^2}r^6 & \frac{-1}{99b^2}r^5 \\ \frac{-40}{(33b)}r^2 & \frac{181}{(462b)}r^3 & \frac{-1}{99b^2}r^5 & \frac{50}{231b^2}r^4 \end{array} \right] - \omega^2 \frac{\rho \cdot A \cdot r}{420} \left[\begin{array}{cccc} \frac{72940}{429} & \frac{-4530}{143} & \frac{-521}{(5148b)} & \frac{775}{(429b)} \\ \frac{-4530}{143} & \frac{100}{13} & \frac{5}{(156b)} & \frac{-995}{(1716b)} \\ \frac{-521}{(5148b)} & \frac{5}{(156b)} & \frac{1}{(3861b^2)} & \frac{-1}{(198b^2)} \\ \frac{775}{(429b)} & \frac{-995}{(1716b)} & \frac{-1}{(198b^2)} & \frac{43}{(429b^2)} \end{array} \right] \begin{Bmatrix} w_2 \\ \theta_2 \\ F_1 \\ M_1 \end{Bmatrix} = 0 \quad (3.63)$$

where

$$\lambda = \omega^2 \frac{\rho A r^4}{420b} \quad (3.64)$$

and

$$\omega_n = \frac{\beta_n}{r^2} \sqrt{\frac{b}{\rho A}} \quad (3.65)$$

where n = mode number. The solutions for equation (3.63) are given as

$$\beta_1 = 3.516, \beta_2 = 22.035, \beta_3 = 61.768 \text{ and } \beta_4 = 136.281$$

Two-Element Model:

The beam is modeled using two elements of equal length r ($L = 2r$), whose stiffness and mass matrices are given by equations (3.45) and (3.46). The nodal degrees of freedom for the two elements are:

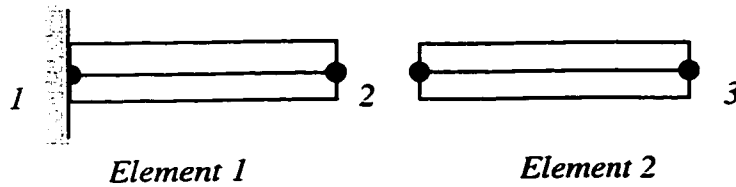


Figure 3.12 Two-element model of a beam

$$\{v_1^e\} = \begin{Bmatrix} w_1 \\ \theta_1 \\ w_2 \\ \theta_2 \\ F_1 \\ M_1 \\ F_2 \\ M_2 \end{Bmatrix} \quad \{v_2^e\} = \begin{Bmatrix} w_2 \\ \theta_2 \\ w_3 \\ \theta_3 \\ F_2 \\ M_2 \\ F_3 \\ M_3 \end{Bmatrix} \quad (3.66)$$

With the global coordinate coinciding with the beam axis, the system matrix is obtained by superimposing the preceding matrices for element one and two, into a 12 X

12 column matrix. We thus have

$$[K] \{v\} - \lambda [M] \{v\} = 0 \quad (3.67)$$

where

$$\{v\} = \{w_1 \quad \theta_1 \quad w_2 \quad \theta_2 \quad w_3 \quad \theta_3 \quad F_1 \quad M_1 \quad F_2 \quad M_2 \quad F_3 \quad M_3\}^T \quad (3.68)$$

After applying the boundary conditions at fixed and free ends the condensed equations are

$$[K^c] \{v^c\} - \lambda [M^c] \{v^c\} = 0 \quad (3.69)$$

where

$$\{v^c\} = \{w_2 \quad \theta_2 \quad w_3 \quad \theta_3 \quad F_1 \quad M_1 \quad F_2 \quad M_2\}^T \quad (3.70)$$

and the $[K^c]$ and $[M^c]$ matrices are given is equation (3.71) and (3.72).

$$K^c = \frac{b}{r^3} \begin{bmatrix} \frac{560}{11} \frac{b^2}{r^6} & 0 & -\frac{280}{11} \frac{b^2}{r^6} & \frac{140}{11} \frac{b^2}{r^5} & \frac{1}{22} \frac{b}{r^3} & -\frac{40}{33} \frac{b}{r^4} & 0 & \frac{80}{33} \frac{b}{r^4} \\ 0 & \frac{1200}{77} \frac{b^2}{r^4} & -\frac{140}{11} \frac{b^2}{r^5} & \frac{380}{77} \frac{b^2}{r^4} & -\frac{5}{462} \frac{b}{r^2} & \frac{181}{462} \frac{b}{r^3} & -\frac{16}{231} \frac{b}{r^2} & 0 \\ -\frac{280}{11} \frac{b^2}{r^6} & -\frac{140}{11} \frac{b^2}{r^5} & \frac{280}{11} \frac{b^2}{r^6} & -\frac{140}{11} \frac{b^2}{r^5} & 0 & 0 & \frac{1}{22} \frac{b}{r^3} & -\frac{40}{33} \frac{b}{r^4} \\ \frac{140}{11} \frac{b^2}{r^5} & \frac{380}{77} \frac{b^2}{r^4} & -\frac{140}{11} \frac{b^2}{r^5} & \frac{600}{77} \frac{b^2}{r^4} & 0 & 0 & -\frac{5}{462} \frac{b}{r^2} & \frac{181}{462} \frac{b}{r^3} \\ \frac{1}{22} \frac{b}{r^3} & -\frac{5}{462} \frac{b}{r^2} & 0 & 0 & \frac{2}{3465} & -\frac{1}{(99 \cdot r)} & -\frac{1}{4620} & -\frac{5}{(2772 \cdot r)} \\ -\frac{40}{33} \frac{b}{r^4} & \frac{181}{462} \frac{b}{r^3} & 0 & 0 & -\frac{1}{(99 \cdot r)} & \frac{50}{(231 \cdot r^2)} & \frac{5}{(2772 \cdot (r \cdot b))} & -\frac{1}{(462 \cdot r^2)} \\ 0 & -\frac{16}{231} \frac{b}{r^2} & \frac{1}{22} \frac{b}{r^3} & -\frac{5}{462} \frac{b}{r^2} & -\frac{1}{4620} & \frac{5}{(2772 \cdot (r \cdot b))} & \frac{4}{3465} & 0 \\ \frac{80}{33} \frac{b}{r^4} & 0 & -\frac{40}{33} \frac{b}{r^4} & \frac{181}{462} \frac{b}{r^3} & -\frac{5}{(2772 \cdot r)} & -\frac{1}{(462 \cdot r^2)} & 0 & \frac{100}{(231 \cdot r^2)} \end{bmatrix}$$

(3.71)

$$M^c = \frac{\rho \cdot A \cdot r}{420} \begin{bmatrix} \frac{145880}{429} & 0 & \frac{17150}{429} & -\frac{1905}{143} \cdot r & -\frac{521}{(5148 \cdot b)} \cdot r^3 & \frac{775}{(429 \cdot b)} \cdot r^2 & 0 & \frac{2740}{(429 \cdot b)} \cdot r^2 \\ 0 & \frac{200}{13} \cdot r^2 & \frac{1905}{143} \cdot r & -\frac{1865}{429} \cdot r^2 & \frac{5}{156} \frac{r^4}{b} & -\frac{995}{(1716 \cdot b)} \cdot r^3 & -\frac{12}{143} \frac{r^4}{b} & 0 \\ \frac{17150}{429} & \frac{1905}{143} \cdot r & \frac{72940}{429} & -\frac{4530}{143} \cdot r & 0 & 0 & -\frac{521}{(5148 \cdot b)} \cdot r^3 & \frac{775}{(429 \cdot b)} \cdot r^2 \\ -\frac{1905}{143} \cdot r & -\frac{1865}{429} \cdot r^2 & -\frac{4530}{143} \cdot r & \frac{100}{13} \cdot r^2 & 0 & 0 & \frac{5}{156} \frac{r^4}{b} & -\frac{995}{(1716 \cdot b)} \cdot r^3 \\ -\frac{521}{(5148 \cdot b)} \cdot r^3 & \frac{5}{156} \frac{r^4}{b} & 0 & 0 & \frac{1}{3861} \frac{r^6}{b^2} & -\frac{1}{198} \frac{r^5}{b^2} & -\frac{7}{30888} \frac{r^6}{b^2} & -\frac{43}{10296} \frac{r^5}{b^2} \\ \frac{775}{(429 \cdot b)} \cdot r^2 & -\frac{995}{(1716 \cdot b)} \cdot r^3 & 0 & 0 & -\frac{1}{198} \frac{r^5}{b^2} & \frac{43}{429} \frac{r^4}{b^2} & \frac{43}{10296} \frac{r^5}{b^2} & \frac{131}{1716} \frac{r^4}{b^2} \\ 0 & -\frac{12}{143} \frac{r^4}{b} & -\frac{521}{(5148 \cdot b)} \cdot r^3 & \frac{5}{156} \frac{r^4}{b} & -\frac{7}{30888} \frac{r^6}{b^2} & \frac{43}{10296} \frac{r^5}{b^2} & \frac{2}{3861} \frac{r^6}{b^2} & 0 \\ \frac{2740}{(429 \cdot b)} \cdot r^2 & 0 & \frac{775}{(429 \cdot b)} \cdot r^2 & -\frac{995}{(1716 \cdot b)} \cdot r^3 & -\frac{43}{10296} \frac{r^5}{b^2} & \frac{131}{1716} \frac{r^4}{b^2} & 0 & \frac{86}{429} \frac{r^4}{b^2} \end{bmatrix}$$

(3.72)

The solution for equation (3.69) then becomes

$$\beta_1 = 3.516, \beta_2 = 22.034, \beta_3 = 61.697 \text{ and } \beta_4 = 120.938.$$

The summary of the result is given in Table 3.2.

Table 3.2 Natural frequencies of a cantilever beam using meshes of one and two finite elements with efficient basis functions

No. of elements	Degrees of freedom	Natural frequencies: $\omega_n = \frac{\beta_n}{r^2} \sqrt{\frac{b}{\rho A}}$ rad/sec			
		β_1	β_2	β_3	β_4
1	4	3.516	22.035	61.768	136.281
2	8	3.516	22.034	61.697	120.938

In order to further illustrate the superiority of the present element, natural frequencies of the same cantilever beam are calculated using meshes of conventional cubic Hermitian finite elements. The results are presented in Table (3.3). Table (3.4) summarizes the total number of degrees of freedom (extracted from Table 3.3) that are needed to obtain the same accuracy in mesh of cubic Hermitian elements in the i -th natural frequency obtained with the 2 element model given in Table (3.2).

Table 3.3 Cantilever beam of length of r with free end using conventional finite elements

No. of elements	Degrees of freedom	Natural frequencies: $\omega_n = \frac{\beta_n}{r^2} \sqrt{\frac{b}{\rho A}}$			
		β_1	β_2	β_3	β_4
1	2	3.532	34.8069	-	-
2	4	3.517	22.221	75.157	218.138
3	6	3.516	22.1069	62.466	140.671
4	8	3.516	22.060	62.175	122.658
5	10	3.516	22.045	61.918	122.31
6	12	3.516	22.039	61.810	121.680
7	14	3.516	22.037	61.760	121.348
8	16	3.516	22.036	61.734	121.712
9	18	3.516	22.035	61.720	121.074
10	20	3.516	22.035	61.712	121.017
11	22	3.516	22.034	61.708	120.981
12	24	3.516	22.034	61.704	120.958
13	26	3.516	22.034	61.702	120.943
14	28	3.516	22.034	61.701	120.932
15	30	3.516	22.034	61.700	120.925
16	32	3.516	22.034	61.699	120.920

Table 3.4 Comparison of the results using the present method, with those using conventional finite elements.

Mode number	1	2	3	4
Degrees of freedom (present model)	8	8	8	8
Degrees of freedom (conventional FE)	6	28	32	28

3.4 Discussion of Results

As can be seen from Tables (3.2), (3.3) and (3.4), when 7-th order finite elements are employed more accurate results are obtained with fewer elements. It is to be noted that the result reported in Table (3.2) was obtained by employing 2 elements whereas the conventional finite element results are based on a higher number of elements to achieve the same result. The mesh with the 7-th order finite elements provides solutions that are closer to exact solutions; this is not the case when the mesh is made of conventional cubic Hermitian elements for the same number of degrees of freedom. As we can see a better correlation could be achieved by less number of elements with the present method. Table (3.5) indicates a satisfactory convergence trend in the solution. Hence, as the mesh size is reduced, that is as the number of elements is increased, we are ensured of monotonic convergence of the solution when efficient basis functions are used. Examples of this convergence are given in Tables (3.6) to (3.10). Convergence of a finite element solution based on the efficient basis functions for a cantilever beam is shown in Figure (3.10). The results are presented upto 10 elements for the case of a cantilever beam.

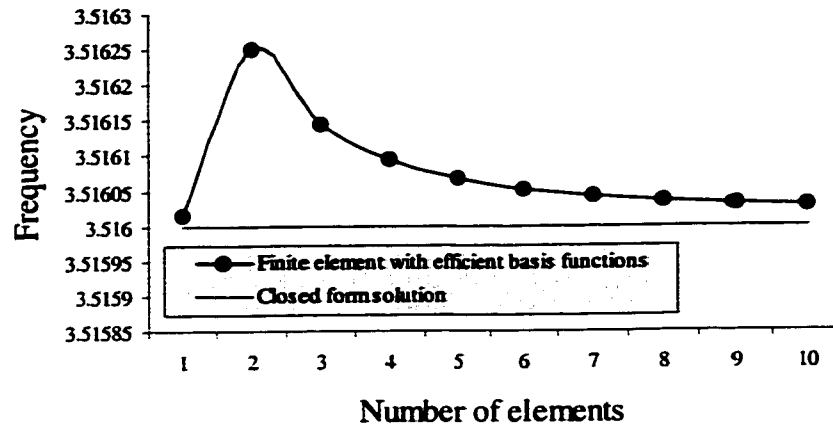


Figure 3.13 Convergence of a finite element solution based on the efficient basis function for a cantilever beam

We may readily solve for free vibrations of beams under different end conditions. For various end conditions the natural frequencies of the beam are calculated using the higher order finite element. Finite element solutions are obtained employing one to ten elements. The results are tabularized in Tables (3.5) to (3.11).

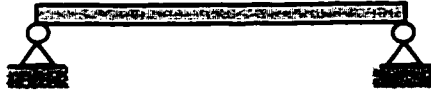
Chapter 4 discusses the use of the higher order finite elements using efficient basis functions to determine the critical speeds of rotors in general and the cantilever-sleeve rotor in particular.

Table 3.5 Natural frequencies of a cantilever beam using finite elements with efficient basis functions



No. of elements	Degrees of freedom	Natural frequencies: $\omega_n = \frac{\beta_n}{r^2} \sqrt{\frac{b}{\rho A}}$ rad/sec			
		β_1	β_2	β_3	β_4
1	4	3.516	22.035	61.768	136.281
2	8	3.516	22.037	61.697	120.938
3	12	3.516	22.037	61.692	120.698
4	16	3.516	22.037	61.696	120.884
5	20	3.516	22.036	61.700	120.888
6	24	3.516	22.036	61.702	120.901
7	28	3.516	22.036	61.702	120.907
8	32	3.516	22.035	61.701	120.909
10	40	3.516	22.035	61.700	120.909

Table 3.6 Natural frequencies of a simply-supported beam using finite elements with efficient basis functions and conventional finite elements



No. of elements	Degrees of freedom	Natural frequencies: $\omega_n = \frac{\beta_n}{r^2} \sqrt{\frac{b}{\rho A}}$			
		β_1	β_2	β_3	β_4
1	4	9.853	39.741	89.471	176.284
2	8	9.869	39.414	88.829	158.970
3	12	9.870	39.471	88.681	157.800
4	16	9.870	39.478	88.797	157.655
5	20	9.870	39.480	88.818	157.847
6	24	9.870	39.480	88.826	157.885
7	28	9.870	39.480	88.829	157.904
10	40	9.870	39.480	88.829	157.920
Natural frequencies obtained using conventional finite elements					
10	20	9.870	39.482	88.874	158.175
15	30	9.870	39.480	88.836	157.697
20	40	9.870	39.477	88.829	157.931
25	50	9.870	39.478	88.829	157.921
30	60	9.870	39.478	98.827	157.920

Table 3.7a Natural frequencies of a beam with both ends free, using conventional finite elements



No. of elements	Degrees of freedom	Natural frequencies: $\omega_n = \frac{\beta_n}{r^2} \sqrt{\frac{b}{\rho A}}$			
		$\beta_1, \text{ and } \beta_2$	β_3	β_4	β_5
1	4	0	26.833	91.652	
2	6	0	22.423	70.178	280.348
3	8	0	22.434	61.992	135.973
4	10	0	22.398	62.057	121.860
5	12	0	22.384	61.869	122.069
6	14	0	22.379	61.777	121.596
7	16	0	22.376	61.732	121.315
8	18	0	22.375	61.709	121.159
10	22	0	22.374	61.688	121.015

Table 3.7b Natural frequencies of a beam with both ends free, using finite elements with efficient basis functions

TABLE 3.7b

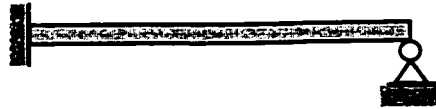
No. of elements	Degrees of freedom	Natural frequencies: $\omega_n = \frac{\beta_n}{r^2} \sqrt{\frac{b}{\rho A}}$			
		$\beta_1, \text{ and } \beta_2$	β_3	β_4	β_5
1	8	0	22.215	63.177	120.964
2	12	0	22.373	61.456	120.582
3	16	0	22.378	61.660	120.867
4	20	0	22.377	61.677	120.867
5	24	0	22.376	61.682	120.893
6	28	0	22.375	61.682	120.893
7	32	0	22.375	61.680	120.916
8	36	0	22.375	61.679	120.917
10	44	0	22.374	61.678	120.915

Table 3.8 Natural frequencies of a beam with one end pinned and the other free, using finite elements with efficient basis functions and conventional finite elements



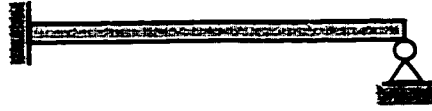
No. of elements	Degrees of freedom	Natural frequencies: $\omega_n = \frac{\beta_n}{r^2} \sqrt{\frac{b}{\rho A}}$			
		β_1	β_2	β_3	β_4
1	4	0	15.364	50.674	108.142
2	8	0	15.419	49.852	104.224
3	12	0	15.419	49.955	104.049
4	16	0	15.419	49.967	104.211
5	20	0	15.419	49.970	104.240
6	24	0	15.419	49.970	104.250
7	28	0	15.419	49.967	104.255
8	32	0	15.419	49.967	104.256
10	40	0	15.419	49.967	104.256
Natural frequencies obtained using conventional finite elements					
5	10	0	15.422	50.085	105.211
10	20	0	15.418	49.973	104.322
15	30	0	15.418	49.967	104.263
20	40	0	15.418	49.965	104.253

Table 3.9 Natural frequencies of a beam with one end fixed and the other pinned, using finite element with efficient basis functions



No. of elements	Degrees of freedom	Natural frequencies: $\omega_n = \frac{\beta_n}{r^2} \sqrt{\frac{b}{\rho A}}$			
		β_1	β_2	β_3	β_4
1	4	15.418	49.979	108.188	194.692
2	8	15.416	49.916	104.340	178.941
3	12	15.418	49.955	104.126	178.266
4	16	15.418	49.962	104.218	178.050
5	20	15.418	49.966	104.233	178.208
6	24	15.418	49.966	104.244	178.232
7	28	15.418	49.966	104.249	178.253
8	32	15.418	49.966	104.249	178.265
10	40	15.418	49.966	104.252	178.275

Table 3.10 Natural frequencies of a beam with one end fixed and the other pinned, using conventional finite elements



No. of elements	Degrees of freedom	Natural frequencies: $\omega_n = \frac{\beta_n}{r^2} \sqrt{\frac{b}{\rho A}}$			
		β_1	β_2	β_3	β_4
5	10	15.422	50.097	105.364	182.848
10	20	15.418	49.973	104.324	178.645
15	30	15.418	49.967	104.263	178.346
20	40	15.418	49.965	104.253	178.294
25	50	15.418	49.965	104.249	178.280

Table 3.11 Natural frequencies of a beam with both ends fixed, using finite elements with efficient basis functions and conventional finite elements



No. of elements	Degrees of freedom	Natural frequencies: $\omega_n = \frac{\beta_n}{r^2} \sqrt{\frac{b}{\rho A}}$			
		β_1	β_2	β_3	β_4
1	4	22.374	61.693	127.632	221.887
2	8	22.373	61.673	120.923	199.977
3	12	22.372	61.665	120.817	199.988
4	16	22.373	61.667	120.903	199.664
5	20	22.374	61.671	120.885	199.853
6	24	22.374	61.673	120.895	199.818
7	28	22.375	61.674	120.901	199.835
8	32	22.374	61.674	120.905	199.849
10	40	22.374	61.674	120.907	199.862
Natural frequencies obtained using conventional finite elements					
5	10	22.386	61.919	122.576	204.221
10	20	22.374	61.689	121.023	200.387
15	30	22.373	61.676	120.927	199.967
20	40	22.373	61.674	120.911	199.894
25	50	22.373	61.673	120.907	199.874

CHAPTER 4

DYNAMIC ANALYSIS OF ROTOR-BEARING SYSTEMS USING FINITE ELEMENTS WITH EFFICIENT HIGHER ORDER BASIS FUNCTIONS

4.1 Introduction

The finite element formulation with higher order polynomials as efficient basis functions is presented for the dynamic behavior of rotor-bearing systems. The higher order elements correctly account for all the boundary conditions at the free and fixed ends of the shaft. The accuracy of this formulation is demonstrated by numerical examples for the cases of a simply supported shaft with the disk at one third of the length and a cantilever-sleeve rotor system.

4.2 System Configuration and Coordinates

Two reference frames that are utilized in Chapter 2 to describe the motion have been used.

A typical cross section of the rotor in a deformed state is defined relative to the fixed frame \mathfrak{S} by the translation $V(s, t)$ and $W(s, t)$ in the Y and Z directions, respectively. In order to locate the elastic centerline further, the small angle rotations $B(s, t)$ and $\Gamma(s, t)$ about Y and Z -axes, respectively, are used, which aid to orient the plane of the cross-section. Forces $F(s, t)$ and $G(s, t)$ are in the directions of Y and Z axes,

respectively, and couples $M(s, t)$ and $N(s, t)$ are about Y and Z -axes, respectively. The cross section also spins normal to its face relative to \mathcal{S} . The abc : \mathcal{N} triad is attached to the cross-section with the “ a ” axis normal to the cross-section: \mathcal{N} is defined by the three successive rotations, as illustrated in figure (2.1) in chapter 2.

At a given node the rotor has eight degrees of freedom: two displacements v and w ; two slopes about the Y and Z -axes which are, respectively, β and γ ; two forces f and g and two moments about the Y and Z axes which are, respectively, m and n . The displacements $(V, W, B, \Gamma, F, G, M, N)$ of a typical cross-section relative to \mathcal{S} are transformed to corresponding displacements $(v, w, \beta, \gamma, f, g, m, n)$ relative to the rotating frame \mathcal{R} by the orthogonal transformation given by

$$\{q\} = [R] \{p\} \quad (4.1)$$

with

$$\{q\} = \begin{Bmatrix} V \\ W \\ B \\ \Gamma \\ F \\ G \\ M \\ N \end{Bmatrix}, \quad \{p\} = \begin{Bmatrix} v \\ w \\ \beta \\ \gamma \\ f \\ g \\ m \\ n \end{Bmatrix} \quad (4.1a)$$

$$R = \begin{bmatrix} \cos\omega t & -\sin\omega t & 0 & 0 & 0 & 0 & 0 & 0 \\ \sin\omega t & \cos\omega t & 0 & 0 & 0 & 0 & 0 & 0 \\ 0 & 0 & \cos\omega t & -\sin\omega t & 0 & 0 & 0 & 0 \\ 0 & 0 & \sin\omega t & \cos\omega t & 0 & 0 & 0 & 0 \\ 0 & 0 & 0 & 0 & \cos\omega t & -\sin\omega t & 0 & 0 \\ 0 & 0 & 0 & 0 & \sin\omega t & \cos\omega t & 0 & 0 \\ 0 & 0 & 0 & 0 & 0 & 0 & \cos\omega t & -\sin\omega t \\ 0 & 0 & 0 & 0 & 0 & 0 & \sin\omega t & \cos\omega t \end{bmatrix} \quad (4.1b)$$

and for later use the first two time derivatives of equation (4.1) are

$$\begin{aligned} \{\dot{q}\} &= \omega[S]\{p\} + [R]\{\dot{p}\} \\ \{\ddot{q}\} &= [R]\{\ddot{p}\} - \omega^2\{p\} + 2\omega[S]\{\dot{p}\} \end{aligned} \quad (4.2)$$

where

$$[dR/dt] = \omega [S] \quad (4.3a)$$

$$[d^2R/dt^2] = -\omega^2 [R] \quad (4.3b)$$

and

$$S := \begin{bmatrix} -\sin\omega t & -\cos\omega t & 0 & 0 & 0 & 0 & 0 & 0 \\ \cos\omega t & \sin\omega t & 0 & 0 & 0 & 0 & 0 & 0 \\ 0 & 0 & -\sin\omega t & -\cos\omega t & 0 & 0 & 0 & 0 \\ 0 & 0 & \cos\omega t & \sin\omega t & 0 & 0 & 0 & 0 \\ 0 & 0 & 0 & 0 & -\sin\omega t & -\cos\omega t & 0 & 0 \\ 0 & 0 & 0 & 0 & \cos\omega t & \sin\omega t & 0 & 0 \\ 0 & 0 & 0 & 0 & 0 & 0 & -\sin\omega t & -\cos\omega t \\ 0 & 0 & 0 & 0 & 0 & 0 & \cos\omega t & \sin\omega t \end{bmatrix} \quad (4.3c)$$

4.3 Component Equations

The typical rotor-bearing system has a set of interconnecting components consisting of rigid disk, rotor segments with distributed mass and elasticity, and linear bearings. For higher order finite element analysis of the rotor-bearing system, the rotor shaft segments are modeled by finite shaft elements with efficient basis functions, which include shaft rotation effects. Generally the axi-symmetric geometry of rotor elements gives the same mass and stiffness matrices in both the X-Y and the X-Z planes. The higher order finite rotor element equations of motion are developed in a manner analogous to the formulation in Chapter 2 by specifying spatial shape functions and then treating the rotor element as an integration of an infinite set of differential disks.

4.3.1 The Rigid Disk

The Lagrangian equation of motion of the rigid disk using equation (2.6b) and the constant spin speed restriction, $d\phi/dt = \Omega$, is

$$([M_T^d] + [M_R^d])\{\ddot{q}^d\} - \Omega[G^d]\{\dot{q}^d\} = \{Q^d\} \quad (4.4)$$

where

$$[M_T^d] = \begin{bmatrix} m_d & 0 & 0 & 0 & 0 & 0 & 0 & 0 \\ 0 & m_d & 0 & 0 & 0 & 0 & 0 & 0 \\ 0 & 0 & 0 & 0 & 0 & 0 & 0 & 0 \\ 0 & 0 & 0 & 0 & 0 & 0 & 0 & 0 \\ 0 & 0 & 0 & 0 & 0 & 0 & 0 & 0 \\ 0 & 0 & 0 & 0 & 0 & 0 & 0 & 0 \\ 0 & 0 & 0 & 0 & 0 & 0 & 0 & 0 \\ 0 & 0 & 0 & 0 & 0 & 0 & 0 & 0 \end{bmatrix}, \quad [M_R^d] = \begin{bmatrix} 0 & 0 & 0 & 0 & 0 & 0 & 0 & 0 \\ 0 & 0 & 0 & 0 & 0 & 0 & 0 & 0 \\ 0 & 0 & I_d & 0 & 0 & 0 & 0 & 0 \\ 0 & 0 & 0 & I_d & 0 & 0 & 0 & 0 \\ 0 & 0 & 0 & 0 & 0 & 0 & 0 & 0 \\ 0 & 0 & 0 & 0 & 0 & 0 & 0 & 0 \\ 0 & 0 & 0 & 0 & 0 & 0 & 0 & 0 \\ 0 & 0 & 0 & 0 & 0 & 0 & 0 & 0 \end{bmatrix} \quad (4.5a)$$

$$[G_d] = \begin{bmatrix} 0 & 0 & 0 & 0 & 0 & 0 & 0 & 0 \\ 0 & 0 & 0 & 0 & 0 & 0 & 0 & 0 \\ 0 & 0 & 0 & I_p & 0 & 0 & 0 & 0 \\ 0 & 0 & -I_p & 0 & 0 & 0 & 0 & 0 \\ 0 & 0 & 0 & 0 & 0 & 0 & 0 & 0 \\ 0 & 0 & 0 & 0 & 0 & 0 & 0 & 0 \\ 0 & 0 & 0 & 0 & 0 & 0 & 0 & 0 \\ 0 & 0 & 0 & 0 & 0 & 0 & 0 & 0 \end{bmatrix} \quad (4.5b)$$

Equation (4.4) is the equation of motion of the rigid disk referred to frame \mathcal{S} with the forcing term including mass unbalance, interconnection forces, and other external effects on the disk. For the disk mass center located at (η_d, ζ_d) relative to \mathcal{N} , the unbalance force in frame \mathcal{S} is

$$\begin{aligned}
\{Q^d\} &= \begin{Bmatrix} \eta_d \\ \zeta_d \\ 0 \\ 0 \\ 0 \\ 0 \\ 0 \\ 0 \end{Bmatrix} \cos \Omega t + \begin{Bmatrix} -\zeta_d \\ \eta_d \\ 0 \\ 0 \\ 0 \\ 0 \\ 0 \\ 0 \end{Bmatrix} \sin \Omega t \\
&= \{Q_c^d\} \cos \Omega t + \{Q_s^d\} \sin \Omega t
\end{aligned} \tag{4.6}$$

By using equations (4.1) and (4.2) and premultiplying by $[R]^T$, equation (4.4) yields an equation that is similar in form to equation (2.9). However the order of entries and the matrices are different.

4.3.2 Finite Shaft Element with Efficient Higher Order Basis Functions

A typical finite rotor element is illustrated in figure 4.1a. The shaft is modeled as a beam with a constant circular cross-section. It should be noted here that the element time-dependent cross section displacements (V , W , B , Γ , F , G , M and N) are also functions of position, x , along the axis of the element. The finite element used has two nodes, so the matrices are of sixteenth-order, including four displacements, four rotations, four shear forces and four moments. The rotations, forces and moments (B , Γ , F , G , M and N) are related to the displacements (V , W) by the equations

$$\begin{aligned}
B &= -\frac{\partial W}{\partial x} & (a) \\
\Gamma &= \frac{\partial V}{\partial x} & (b) \\
F &= -b \frac{\partial^3 V}{\partial x^3} = -\frac{\partial N}{\partial x} & (c) \\
G &= b \frac{\partial^3 W}{\partial x^3} = \frac{\partial M}{\partial x} & (d) \\
M &= b \frac{\partial^2 W}{\partial x} & (e) \\
N &= b \frac{\partial^2 V}{\partial x^2} & (f)
\end{aligned}
\tag{4.7}$$

and the nodal displacement vectors are

$$\{p_1^e\} = \begin{Bmatrix} v_1 \\ w_1 \\ \beta_1 \\ \gamma_1 \\ f_1 \\ g_1 \\ m_1 \\ n_1 \end{Bmatrix}, \quad \{p_2^e\} = \begin{Bmatrix} v_2 \\ w_2 \\ \beta_2 \\ \gamma_2 \\ f_2 \\ g_2 \\ m_2 \\ n_2 \end{Bmatrix}
\tag{4.8}$$

which includes the displacements $\{p_y\}$ and $\{p_z\}$ corresponding, respectively, to the motions in the Y and Z directions: that is

$$\{p_y^e\} = \{v_1, \gamma_1, f_1, n_1, v_2, \gamma_2, f_2, n_2\}^T
\tag{4.9a}$$

$$\{p_z^e\} = \{w_1, \beta_1, g_1, m_1, w_2, \beta_2, g_2, m_2\}^T
\tag{4.9b}$$

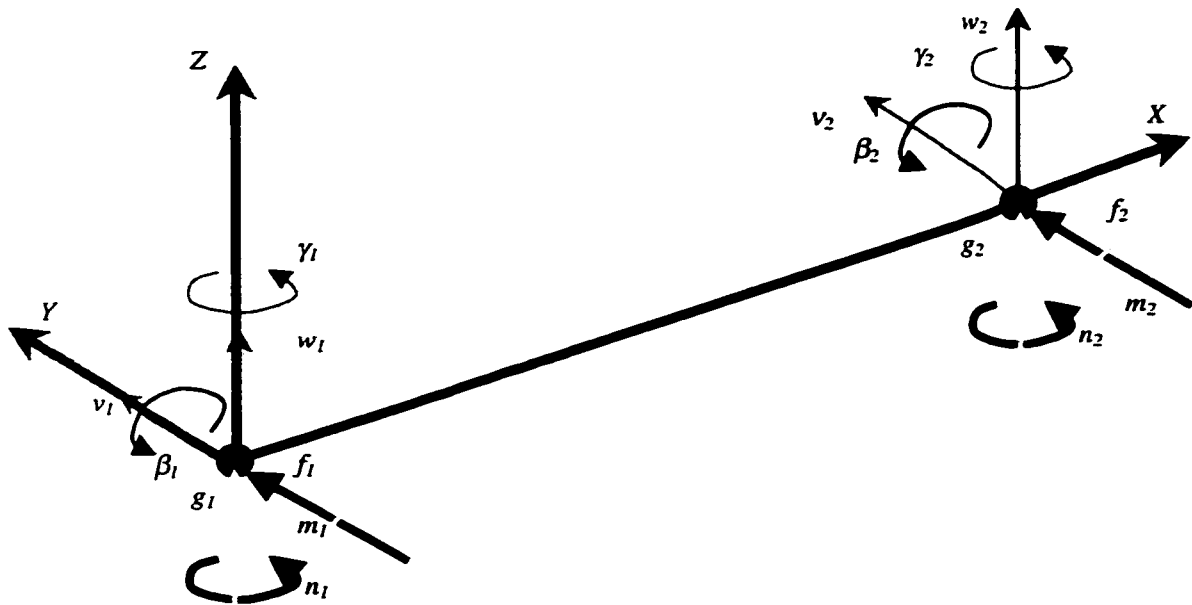


Figure (4.1a) Typical finite rotor element with eight degrees of freedom

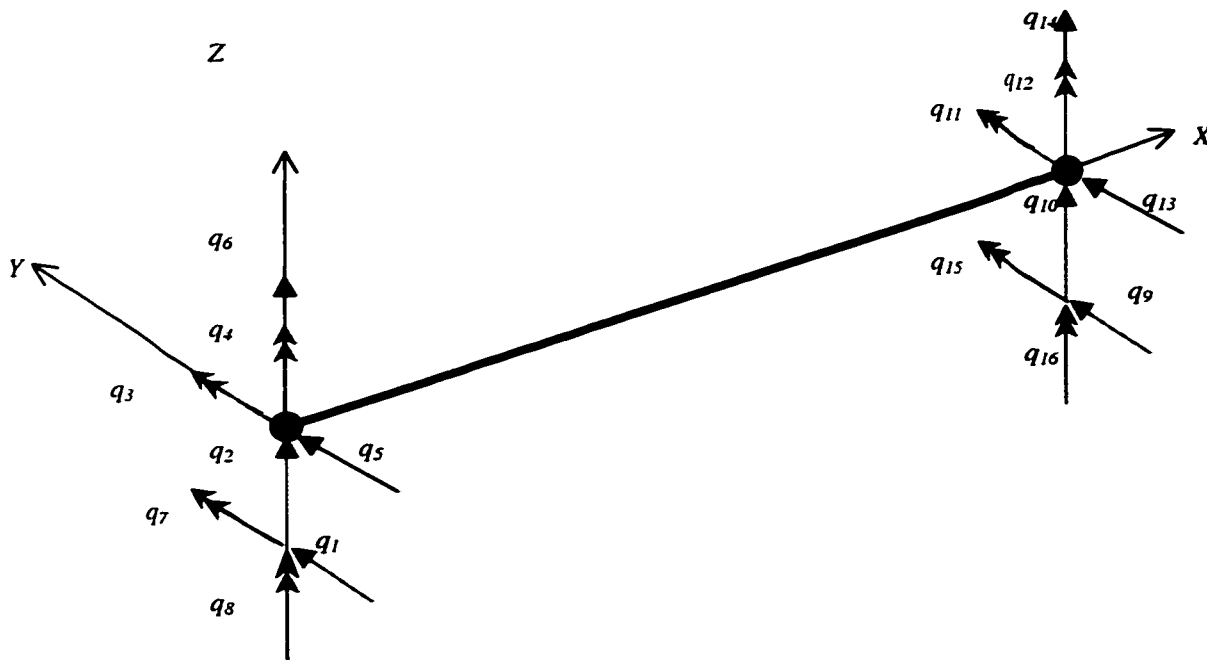


Figure (4.1b) Coordinates of a typical finite rotor element

The coordinates $(q_1^e, q_2^e, \dots, q_{16}^e)$ are the time-dependent end point degrees of freedom (translations, rotations, shear forces and moments) of the finite element and are indicated in figure (4.1b).

The translation of a typical point internal to the element is chosen to obey the relation

$$\begin{Bmatrix} V(x,t) \\ W(x,t) \end{Bmatrix} = [Y(x)]\{q^e(t)\} \quad (4.10)$$

where the spatial constraint matrix is given by

$$[Y] = \begin{bmatrix} N_1 & 0 & 0 & N_2 & N_3 & 0 & 0 & N_4 & N_5 & 0 & 0 & N_6 & N_7 & 0 & 0 & N_8 \\ 0 & N_1 & -N_2 & 0 & 0 & N_3 & -N_4 & 0 & 0 & N_5 & -N_6 & 0 & 0 & N_7 & -N_8 & 0 \end{bmatrix} \quad (4.11)$$

and is a matrix of displacement functions. In this case the individual functions represent the static displacement modes associated with a unit displacement of one of the end point coordinates with all others being constrained to zero displacement. These functions are

$$N_1^c(x) = 1 - 35 \frac{x^4}{r^4} + 84 \frac{x^5}{r^5} - 70 \frac{x^6}{r^6} + 20 \frac{x^7}{r^7}$$

$$N_2^c(x) = x - \frac{20x^4}{r^3} + \frac{45x^5}{r^4} - \frac{36x^6}{r^5} + \frac{10x^7}{r^6}$$

$$N_3^c(x) = 35 \frac{x^4}{r^4} - 84 \frac{x^5}{r^5} + 70 \frac{x^6}{r^6} - 20 \frac{x^7}{r^7}$$

$$N_4^c(x) = -15 \frac{x^4}{r^3} + 39 \frac{x^5}{r^4} - 34 \frac{x^6}{r^5} + 10 \frac{x^7}{r^6}$$

$$N_5^c(x) = -\frac{x^3}{6b} + 2 \frac{x^4}{3br} - \frac{x^5}{br^2} + 2 \frac{x^6}{3br^3} - \frac{x^7}{6br^4}$$

$$N_6^c(x) = \frac{x^2}{2b} - 5 \frac{x^4}{br^2} + 10 \frac{x^5}{br^3} - 15 \frac{x^6}{2br^4} + \frac{2x^7}{br^5}$$

$$N_7^c(x) = \frac{x^4}{6br} - \frac{x^5}{2br^2} + \frac{x^6}{2br^3} - \frac{x^7}{6br^4} \quad (4.12)$$

$$N_8^c(x) = 5 \frac{x^4}{2br^2} - 7 \frac{x^5}{br^3} + 13 \frac{x^6}{2br^4} - 2 \frac{x^7}{br}$$

From the equations (4.7) and (4.10) the rotations can be expressed in the form

$$\begin{Bmatrix} B \\ \Gamma \end{Bmatrix} = [\Phi] \{q^c\} \quad (4.13)$$

with

$$[\Phi] = \begin{bmatrix} [\Phi_B] \\ [\Phi_\Gamma] \end{bmatrix} \quad (4.14a)$$

or

$$[\Phi] = \begin{bmatrix} 0 & -N_1' & N_2' & 0 & 0 & -N_3' & N_4' & 0 & 0 & -N_5' & N_6' & 0 & 0 & -N_7' & N_8' & 0 \\ N_1' & 0 & 0 & N_2' & N_3' & 0 & 0 & N_4' & N_5' & 0 & 0 & N_6' & N_7' & 0 & 0 & N_8' \end{bmatrix} \quad (4.14b)$$

representing a matrix of rotation shape functions.

The energy of the complete element is obtained by integrating equation (2.19) over the length of the element to obtain

$$\begin{aligned} \mathcal{P}_B^e + \mathcal{P}_A^e + J^e = & \frac{1}{2} \{q^e\}^T ([K_B^e] - [K_A^e]) \{q^e\} + \frac{1}{2} \{\dot{q}^e\}^T ([M_T^e] + [M_R^e]) \{\dot{q}^e\} \\ & + \frac{1}{2} I_p^e \dot{\phi}^2 + \dot{\phi} \{\dot{q}^e\}^T [N^e] \{q^e\} \end{aligned} \quad (4.15)$$

where

$$\begin{aligned} [M_T^e] &= \int_0^L \mu [\Psi]^T [\Psi] ds \\ [M_R^e] &= \int_0^L \sigma_d [\Phi]^T [\Phi] ds \\ [N^e] &= \int_0^L \sigma_p [\Phi_r]^T [\Phi_B] ds \\ [K_B^e] &= \int_0^L EI [\Psi''']^T [\Psi'''] ds \\ [K_A^e] &= \int_0^L P [\Psi']^T [\Psi'] ds \end{aligned} \quad (4.16)$$

For the case of a uniform cross-section element under constant axial load P and with the identity $\sigma_p = 2\sigma_d = 2I$, the elements of the matrices of equations sets are obtained and given in equations set (4.17).

$$M_{R} = \frac{H}{420} \begin{bmatrix} \frac{72940}{429} & 0 & 0 & \frac{4530}{143} & \frac{383}{(2574b)} & 0 & 0 & \frac{1370}{(429b)} & 0 & 0 & \frac{775}{(429b)} & 0 & 0 & \frac{775}{(429b)} \\ 0 & \frac{72940}{429} & \frac{-4530}{143} & 0 & 0 & \frac{-383}{(2574b)} & \frac{-1370}{(429b)} & 0 & 0 & 0 & 0 & \frac{521}{(5148b)} & \frac{775}{(429b)} & 0 \\ 0 & \frac{-4530}{143} & \frac{100}{13} & 0 & 0 & \frac{6}{143b} & \frac{245}{(286b)} & 0 & 0 & 0 & 0 & \frac{-5}{156b} & \frac{995}{(1716b)} & 0 \\ \frac{4530}{143} & 0 & 0 & \frac{100}{13} & \frac{-6}{143b} & \frac{6}{143b} & 0 & 0 & \frac{245}{(286b)} & 0 & 0 & 0 & 0 & \frac{995}{(1716b)} \\ \frac{-383}{(2574b)} & 0 & 0 & \frac{-6}{143b} & \frac{1}{(3861b^2)} & \frac{1}{(3861b^2)} & 0 & 0 & 0 & 0 & 0 & \frac{-7}{(30888b^2)} & 0 & \frac{-43}{(10296b^2)} \\ 0 & \frac{-383}{(2574b)} & \frac{6}{143b} & 0 & 0 & \frac{1}{(3861b^2)} & \frac{1}{(98b^2)} & 0 & 0 & 0 & 0 & \frac{-7}{(30888b^2)} & \frac{43}{(10296b^2)} & 0 \\ 0 & \frac{-1370}{(429b)} & \frac{245}{(286b)} & 0 & 0 & \frac{1}{(98b^2)} & \frac{43}{(429b^2)} & 0 & 0 & 0 & 0 & \frac{-43}{(10296b^2)} & \frac{131}{(1716b^2)} & 0 \\ \frac{1370}{(429b)} & 0 & 0 & \frac{245}{(286b)} & \frac{-1}{(98b^2)} & 0 & 0 & \frac{43}{(429b^2)} & 0 & 0 & 0 & 0 & 0 & \frac{131}{(1716b^2)} \\ \frac{17150}{429} & 0 & 0 & \frac{1905}{143} & \frac{-521}{(5148b)} & 0 & 0 & \frac{775}{(429b)} & 0 & 0 & 0 & 0 & 0 & \frac{1370}{(429b)} \\ 0 & \frac{17150}{429} & \frac{-1905}{143} & 0 & 0 & \frac{-521}{(5148b)} & \frac{-775}{(429b)} & 0 & 0 & 0 & 0 & 0 & 0 & 0 \\ 0 & 0 & \frac{1905}{143} & \frac{-1865}{429} & 0 & 0 & \frac{-5}{156b} & \frac{-995}{(1716b)} & 0 & 0 & 0 & 0 & 0 & 0 \\ \frac{-1905}{143} & 0 & 0 & \frac{-1865}{429} & \frac{5}{156b} & 0 & 0 & \frac{-995}{(1716b)} & 0 & 0 & 0 & 0 & 0 & \frac{-245}{(286b)} \\ \frac{521}{(5148b)} & 0 & 0 & \frac{5}{156b} & \frac{-7}{(30888b^2)} & \frac{-6}{143b} & 0 & 0 & 0 & 0 & 0 & 0 & 0 & 0 \\ 0 & \frac{521}{(5148b)} & \frac{-5}{156b} & 0 & 0 & \frac{-7}{(30888b^2)} & \frac{-43}{(10296b^2)} & 0 & 0 & 0 & 0 & 0 & 0 & 0 \\ 0 & 0 & \frac{-775}{(429b)} & 0 & 0 & 0 & \frac{131}{(1716b^2)} & 0 & 0 & 0 & 0 & 0 & 0 & 0 \\ \frac{775}{(429b)} & 0 & 0 & \frac{995}{(1716b)} & \frac{-43}{(10296b^2)} & 0 & 0 & \frac{131}{(1716b^2)} & 0 & 0 & 0 & 0 & 0 & \frac{43}{(429b^2)} \end{bmatrix}$$

Finite shaft element characteristic translational mass matrix, where $M_R = [M_R]$

$$(4.17a)$$

$\frac{7000}{143}$	0	0	$\frac{1355}{143} r$	$\frac{-25}{(858b)} r^3$	0	0	$\frac{115}{(143b)} r^2$	$\frac{-7000}{143}$	0	0	$\frac{1355}{143} r$	$\frac{-25}{(858b)} r^3$	0	0	$\frac{-115}{(143b)} r^2$
0	$\frac{7000}{143}$	$\frac{-1355}{143} r$	0	0	$\frac{-25}{(858b)} r^3$	$\frac{-115}{(143b)} r^2$	0	0	$\frac{-7000}{143}$	$\frac{1355}{143} r$	0	0	$\frac{-25}{(858b)} r^3$	$\frac{115}{(143b)} r^2$	0
0	$\frac{-1355}{143} r$	$\frac{9000}{1001}$	0	0	$\frac{125}{3003} r^4$	$\frac{1845}{(2002b)} r^3$	0	0	$\frac{1355}{143}$	$\frac{485}{1001} r^2$	0	0	$\frac{-25}{2002} r^4$	$\frac{235}{(2002b)} r^3$	0
$\frac{1355}{143} r$	0	0	$\frac{9000}{1001}$	$\frac{-125}{3003} r^4$	$\frac{1845}{(2002b)} r^3$	0	$\frac{1845}{(2002b)} r^3$	$\frac{-1355}{143}$	0	0	$\frac{485}{1001} r^2$	$\frac{25}{2002} r^4$	$\frac{25}{2002} r^4$	0	$\frac{235}{(2002b)} r^3$
$\frac{-25}{(858b)} r^3$	0	0	$\frac{-125}{3003} r^4$	$\frac{1}{(3003b^2)} r^6$	0	0	$\frac{-37}{(6006b^2)} r^5$	$\frac{25}{(858b)}$	$\frac{25}{(858b)}$	$\frac{25}{2002} r^4$	$\frac{-5}{(24024b^2)} r^6$	0	0	0	$\frac{-73}{(24024b^2)} r^5$
0	$\frac{-25}{(858b)} r^3$	$\frac{125}{3003} r^4$	0	0	$\frac{1}{(3003b^2)} r^6$	$\frac{37}{(6006b^2)} r^5$	0	$\frac{25}{(858b)}$	$\frac{25}{(858b)}$	$\frac{-5}{(24024b^2)} r^6$	0	0	$\frac{-5}{(24024b^2)} r^6$	$\frac{73}{(24024b^2)} r^5$	0
0	$\frac{-115}{(143b)} r^2$	$\frac{1845}{(2002b)}$	0	0	$\frac{-37}{(6006b^2)} r^5$	$\frac{365}{(3003b^2)} r^4$	0	0	$\frac{115}{(143b)}$	$\frac{-235}{(2002b)}$	0	0	$\frac{-73}{(858b^2)} r^4$	0	0
$\frac{115}{(143b)} r^2$	0	0	$\frac{1845}{(2002b)}$	$\frac{-37}{(6006b^2)} r^5$	0	0	$\frac{365}{(3003b^2)} r^4$	$\frac{-115}{(143b)}$	0	0	$\frac{-235}{(2002b)}$	$\frac{73}{(24024b^2)} r^5$	0	0	$\frac{35}{(858b^2)} r^4$
$\frac{-7000}{143}$	0	0	$\frac{-1355}{143} r$	$\frac{25}{(858b)}$	0	0	0	$\frac{7000}{143}$	0	0	$\frac{-1355}{143} r$	$\frac{25}{(858b)}$	0	0	$\frac{115}{(143b)} r^2$
0	$\frac{-7000}{143}$	$\frac{1355}{143} r$	0	0	$\frac{25}{(858b)}$	$\frac{115}{(143b)} r^2$	0	0	$\frac{7000}{143}$	$\frac{1355}{143} r$	0	0	$\frac{25}{(858b)}$	$\frac{-115}{(143b)} r^2$	0
0	$\frac{-1355}{143} r$	$\frac{485}{1001}$	0	0	$\frac{-25}{2002} r^4$	$\frac{-235}{(2002b)}$	0	0	$\frac{1355}{143}$	$\frac{9000}{1001} r^2$	0	0	$\frac{125}{3003} r^4$	$\frac{-1845}{(2002b)}$	0
$\frac{1355}{143} r$	0	0	$\frac{485}{1001}$	0	0	0	0	0	$\frac{1355}{143}$	$\frac{9000}{1001} r^2$	0	0	$\frac{125}{3003} r^4$	$\frac{-1845}{(2002b)}$	0
$\frac{-25}{(858b)} r^3$	0	0	$\frac{25}{2002} r^4$	$\frac{-5}{(24024b^2)} r^6$	0	0	$\frac{73}{(24024b^2)} r^5$	$\frac{25}{(858b)}$	$\frac{25}{(858b)}$	$\frac{1}{3003} r^6$	0	0	$\frac{1}{3003} r^6$	0	$\frac{37}{(6006b^2)} r^5$
0	$\frac{-25}{(858b)} r^3$	$\frac{25}{2002} r^4$	0	0	$\frac{-5}{(24024b^2)} r^6$	$\frac{73}{(24024b^2)} r^5$	0	$\frac{25}{(858b)}$	$\frac{25}{(858b)}$	$\frac{1}{3003} r^6$	0	0	$\frac{1}{3003} r^6$	0	$\frac{37}{(6006b^2)} r^5$
$\frac{-115}{(143b)} r^2$	0	0	$\frac{235}{(2002b)}$	$\frac{-73}{(24024b^2)} r^5$	0	0	0	$\frac{-115}{(143b)}$	$\frac{-1355}{143} r$	$\frac{-125}{3003} r^4$	0	0	$\frac{-125}{3003} r^4$	0	$\frac{-1845}{(2002b)}$
$\frac{-115}{(143b)} r^2$	0	0	$\frac{235}{(2002b)}$	$\frac{-73}{(24024b^2)} r^5$	0	0	0	$\frac{-115}{(143b)}$	$\frac{-1355}{143} r$	$\frac{-125}{3003} r^4$	0	0	$\frac{-125}{3003} r^4$	0	$\frac{-1845}{(2002b)}$

$M_{R, 30r}^{m, \rho, I}$

Finite shaft element characteristic rotational mass matrix, where $M_R = [MR]$

(4.17b)

$$N_e := \frac{p-1}{15r} \begin{bmatrix} 0 & -\frac{3500}{143} & \frac{1355}{286}r & 0 & 0 & \frac{25}{(1716b)}r^3 & \frac{115}{(286b)}r^2 & 0 & 0 & \frac{3500}{143} & \frac{1355}{286}r & 0 & 0 & \frac{25}{(1716b)}r^3 & -\frac{115}{(286b)}r^2 & 0 \\ 0 & 0 & 0 & 0 & 0 & 0 & 0 & 0 & 0 & 0 & 0 & 0 & 0 & 0 & 0 & 0 \\ 0 & 0 & 0 & 0 & 0 & 0 & 0 & 0 & 0 & 0 & 0 & 0 & 0 & 0 & 0 & 0 \\ 0 & -\frac{1355}{286}r & \frac{4500}{1001}r^2 & 0 & 0 & \frac{125}{6006b}r^4 & \frac{1845}{(4004b)}r^3 & 0 & 0 & \frac{1355}{286}r & \frac{485}{2002}r^2 & 0 & 0 & -\frac{25}{4004b}r^4 & \frac{235}{(4004b)}r^3 & 0 \\ 0 & \frac{25}{(1716b)}r^3 & -\frac{125}{6006b}r^4 & 0 & 0 & \frac{-1}{(6006b^2)}r^6 & \frac{-37}{(12012b^2)}r^5 & 0 & 0 & \frac{-25}{(1716b)}r^3 & \frac{25}{4004b}r^4 & 0 & 0 & \frac{5}{(48048b^2)}r^6 & \frac{-73}{(48048b^2)}r^5 & 0 \\ 0 & 0 & 0 & 0 & 0 & 0 & 0 & 0 & 0 & 0 & 0 & 0 & 0 & 0 & 0 & 0 \\ 0 & 0 & 0 & 0 & 0 & 0 & 0 & 0 & 0 & 0 & 0 & 0 & 0 & 0 & 0 & 0 \\ 0 & -\frac{115}{(286b)}r^2 & \frac{1845}{(4004b)}r^3 & 0 & 0 & \frac{37}{(12012b^2)}r^5 & \frac{365}{(6006b^2)}r^4 & 0 & 0 & \frac{115}{(286b)}r^2 & -\frac{235}{(4004b)}r^3 & 0 & 0 & \frac{-73}{(48048b^2)}r^5 & \frac{35}{(1716b^2)}r^4 & 0 \\ 0 & \frac{3500}{143} & -\frac{1355}{286}r & 0 & 0 & \frac{-25}{(1716b)}r^3 & -\frac{115}{(286b)}r^2 & 0 & 0 & -\frac{3500}{143} & -\frac{1355}{286}r & 0 & 0 & \frac{-25}{(1716b)}r^3 & \frac{115}{(286b)}r^2 & 0 \\ 0 & 0 & 0 & 0 & 0 & 0 & 0 & 0 & 0 & 0 & 0 & 0 & 0 & 0 & 0 & 0 \\ 0 & 0 & 0 & 0 & 0 & 0 & 0 & 0 & 0 & 0 & 0 & 0 & 0 & 0 & 0 & 0 \\ 0 & -\frac{1355}{286}r & \frac{485}{2002}r^2 & 0 & 0 & \frac{-25}{4004b}r^4 & \frac{-235}{(4004b)}r^3 & 0 & 0 & \frac{1355}{286}r & \frac{4500}{1001}r^2 & 0 & 0 & \frac{125}{6006b}r^4 & -\frac{1845}{(4004b)}r^3 & 0 \\ 0 & \frac{25}{(1716b)}r^3 & \frac{25}{4004b}r^4 & 0 & 0 & \frac{5}{(48048b^2)}r^6 & \frac{73}{(48048b^2)}r^5 & 0 & 0 & \frac{-25}{(1716b)}r^3 & -\frac{125}{6006b}r^4 & 0 & 0 & \frac{-1}{(6006b^2)}r^6 & \frac{37}{(12012b^2)}r^5 & 0 \\ 0 & 0 & 0 & 0 & 0 & 0 & 0 & 0 & 0 & 0 & 0 & 0 & 0 & 0 & 0 & 0 \\ 0 & 0 & 0 & 0 & 0 & 0 & 0 & 0 & 0 & 0 & 0 & 0 & 0 & 0 & 0 & 0 \\ 0 & \frac{115}{(286b)}r^2 & \frac{235}{(4004b)}r^3 & 0 & 0 & \frac{73}{(48048b^2)}r^5 & \frac{35}{(1716b^2)}r^4 & 0 & 0 & -\frac{115}{(286b)}r^2 & -\frac{1845}{(4004b)}r^3 & 0 & 0 & \frac{-37}{(12012b^2)}r^5 & \frac{365}{(6006b^2)}r^4 & 0 \end{bmatrix}$$

Finite shaft element characteristic gyroscopic effect matrix, where $N_e = [N_e]$

(4.17c)

$$\mathbf{K}_B = \frac{b}{r^3} \begin{bmatrix}
 \frac{280}{11} & 0 & \frac{140}{11} & \frac{-1}{(22b)} r^3 & 0 & 0 & \frac{40}{(33b)} r^2 & \frac{-40}{(33b)} r^2 \\
 0 & \frac{280}{11} & \frac{-140}{11} & 0 & \frac{-1}{(22b)} r^3 & \frac{-40}{(33b)} r^2 & 0 & 0 \\
 0 & \frac{-140}{11} & \frac{600}{77} & 0 & \frac{8}{231b} r^4 & \frac{379}{(462b)} r^3 & 0 & 0 \\
 \frac{140}{11} & 0 & 0 & \frac{600}{77} & \frac{-8}{231b} r^4 & \frac{379}{(462b)} r^3 & \frac{379}{(462b)} r^3 & \frac{-181}{(462b)} r^3 \\
 \frac{-1}{(22b)} r^3 & 0 & 0 & \frac{-8}{231b} r^4 & \frac{2}{(3465b^2)} r^6 & 0 & \frac{-1}{(99b^2)} r^5 & \frac{-5}{(2773b^2)} r^5 \\
 0 & \frac{-1}{(22b)} r^3 & \frac{8}{231b} r^4 & 0 & 0 & \frac{2}{(3465b^2)} r^6 & \frac{1}{(99b^2)} r^5 & 0 \\
 0 & \frac{-40}{(33b)} r^2 & \frac{379}{(462b)} r^3 & 0 & 0 & \frac{1}{(99b^2)} r^5 & \frac{50}{(231b^2)} r^4 & 0 \\
 \frac{40}{(33b)} r^2 & 0 & 0 & \frac{379}{(462b)} r^3 & \frac{-1}{(99b^2)} r^5 & 0 & \frac{50}{(231b^2)} r^4 & \frac{-1}{(462b^2)} r^4 \\
 \frac{-280}{11} & 0 & \frac{-140}{11} & \frac{1}{(22b)} r^3 & 0 & 0 & \frac{-40}{(33b)} r^2 & \frac{40}{(33b)} r^2 \\
 0 & \frac{-280}{11} & \frac{140}{11} & 0 & \frac{1}{(22b)} r^3 & \frac{40}{(33b)} r^2 & 0 & 0 \\
 0 & \frac{-140}{11} & \frac{380}{77} & 0 & \frac{5}{462b} r^4 & \frac{181}{(462b)} r^3 & 0 & 0 \\
 \frac{140}{11} & 0 & 0 & \frac{380}{77} & \frac{-5}{462b} r^4 & \frac{181}{(462b)} r^3 & \frac{181}{(462b)} r^3 & \frac{-379}{(462b)} r^3 \\
 \frac{-1}{(22b)} r^3 & 0 & 0 & \frac{-5}{462b} r^4 & \frac{-1}{(4620b^2)} r^6 & 0 & \frac{-1}{(2773b^2)} r^5 & 0 \\
 0 & \frac{-1}{(22b)} r^3 & \frac{5}{462b} r^4 & 0 & 0 & \frac{-1}{(4620b^2)} r^6 & \frac{5}{(2773b^2)} r^5 & 0 \\
 0 & \frac{-40}{(33b)} r^2 & \frac{181}{(462b)} r^3 & 0 & 0 & \frac{-5}{(2773b^2)} r^5 & \frac{-1}{(462b^2)} r^4 & 0 \\
 \frac{-40}{(33b)} r^2 & 0 & 0 & \frac{181}{(462b)} r^3 & \frac{5}{(2773b^2)} r^5 & 0 & 0 & \frac{-1}{(462b^2)} r^4 \\
 \frac{280}{11} & 0 & 0 & \frac{-140}{11} & \frac{1}{(22b)} r^3 & 0 & 0 & \frac{40}{(33b)} r^2 \\
 0 & \frac{280}{11} & \frac{-140}{11} & 0 & \frac{1}{(22b)} r^3 & \frac{40}{(33b)} r^2 & 0 & 0 \\
 0 & \frac{-140}{11} & \frac{600}{77} & 0 & \frac{5}{462b} r^4 & \frac{181}{(462b)} r^3 & 0 & 0 \\
 \frac{-140}{11} & 0 & 0 & \frac{600}{77} & \frac{-8}{231b} r^4 & \frac{181}{(462b)} r^3 & \frac{181}{(462b)} r^3 & \frac{-379}{(462b)} r^3 \\
 \frac{1}{(22b)} r^3 & 0 & 0 & \frac{-5}{462b} r^4 & \frac{-1}{(4620b^2)} r^6 & 0 & \frac{2}{(3465b^2)} r^6 & 0 \\
 0 & \frac{1}{(22b)} r^3 & \frac{8}{231b} r^4 & 0 & 0 & \frac{-1}{(4620b^2)} r^6 & \frac{2}{(3465b^2)} r^6 & 0 \\
 0 & \frac{-40}{(33b)} r^2 & \frac{-379}{(462b)} r^3 & 0 & 0 & \frac{-40}{(33b)} r^2 & \frac{-379}{(462b)} r^3 & 0 \\
 \frac{40}{(33b)} r^2 & 0 & 0 & \frac{-379}{(462b)} r^3 & \frac{1}{(99b^2)} r^5 & 0 & 0 & \frac{50}{(231b^2)} r^4
 \end{bmatrix}$$

Finite shaft element characteristic bending stiffness matrix, where $K_B = [K_B]$

$$(4.17d)$$

$\frac{7000}{143}$	0	0	$\frac{1355}{143}r$	$\frac{-25}{(858b)}r^3$	0	0	$\frac{115}{(143b)}r^2$	$\frac{-7000}{143}$	0	0	$\frac{1355}{143}r$	$\frac{-25}{(858b)}r^3$	0	0	$\frac{-115}{(143b)}r^2$
0	$\frac{7000}{143}$	$\frac{-1355}{143}r$	0	0	$\frac{-25}{(858b)}r^3$	$\frac{-115}{(143b)}r^2$	0	0	$\frac{7000}{143}$	$\frac{-1355}{143}r$	0	0	$\frac{-25}{(858b)}r^3$	$\frac{-115}{(143b)}r^2$	0
0	$\frac{-1355}{143}r$	$\frac{9000}{1001}$	0	0	0	$\frac{1845}{(2002b)}$	0	0	$\frac{1355}{143}$	$\frac{485}{1001}r^2$	0	0	$\frac{-25}{2002b}r^4$	$\frac{235}{(2002b)}$	0
$\frac{1355}{143}r$	0	0	$\frac{9000}{1001}$	$\frac{-125}{3003b}r^4$	0	0	$\frac{1845}{(2002b)}$	$\frac{-1355}{143}r$	0	0	$\frac{485}{1001}r^2$	$\frac{25}{2002b}r^4$	0	0	$\frac{235}{(2002b)}$
$\frac{-25}{(858b)}r^3$	0	0	$\frac{-125}{3003b}r^4$	$\frac{1}{(3003b^2)}$	$\frac{1}{3003b^6}$	0	$\frac{-37}{(6006b^2)}$	$\frac{25}{(858b)}$	0	0	$\frac{25}{2002b}$	$\frac{-5}{(24024b^2)}$	0	0	$\frac{-73}{(24024b^2)}$
0	$\frac{-25}{(858b)}r^3$	$\frac{125}{3003b}r^4$	0	0	$\frac{1}{(3003b^2)}$	$\frac{37}{(6006b^2)}$	0	0	$\frac{25}{(858b)}$	$\frac{125}{3003b}r^4$	0	0	$\frac{-5}{(24024b^2)}$	$\frac{73}{(24024b^2)}$	0
0	$\frac{-115}{(143b)}r^2$	$\frac{1845}{(2002b)}$	0	0	0	$\frac{365}{(3003b^2)}$	0	0	$\frac{115}{(143b)}$	$\frac{-235}{(2002b)}$	0	0	$\frac{-73}{(24024b^2)}$	$\frac{35}{(858b^2)}$	0
$\frac{115}{(143b)}r^2$	0	0	$\frac{1845}{(2002b)}$	$\frac{-37}{(6006b^2)}$	0	0	$\frac{365}{(3003b^2)}$	$\frac{-115}{(143b)}$	0	0	$\frac{-235}{(2002b)}$	$\frac{73}{(24024b^2)}$	0	0	$\frac{35}{(858b^2)}$
$\frac{-7000}{143}$	0	0	$\frac{-1355}{143}r$	$\frac{25}{(858b)}$	0	0	$\frac{-115}{(143b)}$	$\frac{7000}{143}$	0	0	$\frac{-1355}{143}r$	$\frac{25}{(858b)}$	0	0	$\frac{115}{(143b)}$
0	$\frac{-7000}{143}$	$\frac{1355}{143}r$	0	0	$\frac{25}{(858b)}$	$\frac{115}{(143b)}$	0	0	0	0	0	0	0	0	0
0	$\frac{-1355}{143}r$	$\frac{485}{1001}r^2$	0	0	$\frac{-25}{2002b}r^4$	$\frac{-235}{(2002b)}$	0	0	$\frac{7000}{143}$	$\frac{1355}{143}r$	0	0	$\frac{25}{(858b)}$	$\frac{-115}{(143b)}$	0
$\frac{1355}{143}r$	0	0	$\frac{485}{1001}r^2$	0	0	$\frac{-235}{(2002b)}$	0	0	0	0	0	0	$\frac{25}{(858b)}$	$\frac{-115}{(143b)}$	0
$\frac{-25}{(858b)}r^3$	0	0	$\frac{25}{2002b}r^4$	$\frac{-5}{(24024b^2)}$	0	0	$\frac{73}{(24024b^2)}$	$\frac{-1355}{143}r$	0	0	$\frac{9000}{1001}$	$\frac{-125}{3003b}r^4$	0	0	$\frac{-1845}{(2002b)}$
0	$\frac{-25}{(858b)}r^3$	$\frac{-25}{2002b}r^4$	0	0	$\frac{-5}{(24024b^2)}$	0	$\frac{73}{(24024b^2)}$	$\frac{-1355}{143}r$	0	0	$\frac{9000}{1001}$	$\frac{-125}{3003b}r^4$	0	0	$\frac{-1845}{(2002b)}$
$\frac{-115}{(143b)}r^2$	0	0	$\frac{235}{(2002b)}$	$\frac{-73}{(24024b^2)}$	0	0	$\frac{365}{(3003b^2)}$	$\frac{115}{(143b)}$	0	0	$\frac{-1845}{(2002b)}$	$\frac{37}{(6006b^2)}$	0	0	$\frac{365}{(3003b^2)}$
$\frac{115}{(143b)}r^2$	0	0	$\frac{235}{(2002b)}$	$\frac{-73}{(24024b^2)}$	0	0	$\frac{365}{(3003b^2)}$	$\frac{115}{(143b)}$	0	0	$\frac{-1845}{(2002b)}$	$\frac{37}{(6006b^2)}$	0	0	$\frac{365}{(3003b^2)}$

$K_A = \frac{P}{30r}$

Finite shaft element characteristic axial load stiffness matrix, where $K_A = [K_A]$

(4.17e)

The Lagrangian equation of motion for the finite rotor element using equation (4.15) and the constant spin speed restriction, $d\phi/dt = \Omega$, is

$$([M_r^c] + [M_k^c])\{\ddot{q}^c\} - \Omega [G^c]\{\dot{q}^c\} + ([K_b^c] - [K_a^c])\{q^c\} = \{Q^c\} \quad (4.18)$$

with

$$[G^c] = ([N^c] - [N^c] \Gamma) \quad (4.19)$$

and it is referred to the fixed frame coordinates.

$$G_c = \frac{0.1}{15r} \begin{bmatrix} 0 & -\frac{3500}{143} & \frac{1355}{286}r & 0 & 0 & \frac{25}{(1716b)}r^3 & \frac{115}{(286b)}r^2 & 0 & 0 & \frac{25}{(1716b)}r^3 & \frac{115}{(286b)}r^2 & 0 \\ 3500 & 143 & 0 & \frac{1355}{286}r & 0 & \frac{25}{(1716b)}r^3 & \frac{115}{(286b)}r^2 & 0 & 0 & 0 & 0 & 0 \\ 143 & 0 & 0 & \frac{1355}{286}r & 0 & \frac{25}{(1716b)}r^3 & \frac{115}{(286b)}r^2 & 0 & 0 & \frac{25}{(1716b)}r^3 & \frac{115}{(286b)}r^2 & 0 \\ -\frac{1355}{286}r & 0 & 0 & -\frac{4500}{1001}r^2 & \frac{125}{6006b}r^4 & 0 & 0 & 0 & 0 & 0 & 0 & -\frac{235}{(4004b)}r^3 \\ 0 & -\frac{1355}{286}r & \frac{4500}{1001}r^2 & 0 & 0 & \frac{125}{6006b}r^4 & 0 & 0 & 0 & -\frac{25}{4004b}r^4 & \frac{235}{(4004b)}r^3 & 0 \\ 0 & \frac{25}{(1716b)}r^3 & \frac{125}{6006b}r^4 & 0 & 0 & -\frac{1}{(6006b^2)}r^6 & -\frac{37}{(12012b^2)}r^5 & 0 & 0 & \frac{5}{(48048b^2)}r^6 & -\frac{73}{(48048b^2)}r^5 & 0 \\ -\frac{25}{(1716b)}r^3 & 0 & 0 & -\frac{125}{6006b}r^4 & \frac{1}{(6006b^2)}r^6 & 0 & 0 & -\frac{37}{(12012b^2)}r^5 & 0 & 0 & 0 & -\frac{73}{(48048b^2)}r^4 \\ -\frac{115}{(286b)}r^2 & 0 & 0 & -\frac{1845}{(4004b)}r^3 & \frac{37}{(12012b^2)}r^5 & 0 & 0 & -\frac{365}{(6006b^2)}r^4 & 0 & 0 & 0 & -\frac{35}{(1716b^2)}r^3 \\ 0 & -\frac{115}{(286b)}r^2 & \frac{1845}{(4004b)}r^3 & 0 & 0 & \frac{37}{(12012b^2)}r^5 & \frac{365}{(6006b^2)}r^4 & 0 & 0 & -\frac{73}{(48048b^2)}r^5 & \frac{35}{(1716b^2)}r^4 & 0 \\ 0 & \frac{3500}{143} & 0 & \frac{1355}{286}r & 0 & 0 & 0 & 0 & 0 & 0 & 0 & 0 \\ 3500 & 143 & 0 & \frac{1355}{286}r & 0 & 0 & 0 & 0 & 0 & 0 & 0 & 0 \\ 143 & 0 & 0 & \frac{1355}{286}r & 0 & 0 & 0 & 0 & 0 & 0 & 0 & 0 \\ -\frac{1355}{286}r & 0 & 0 & -\frac{485}{2002}r^2 & \frac{25}{4004b}r^4 & 0 & 0 & 0 & 0 & 0 & 0 & -\frac{115}{(286b)}r^2 \\ 0 & -\frac{1355}{286}r & \frac{485}{2002}r^2 & 0 & 0 & \frac{25}{4004b}r^4 & 0 & 0 & 0 & 0 & 0 & 0 \\ 0 & \frac{25}{(1716b)}r^3 & \frac{125}{6006b}r^4 & 0 & 0 & -\frac{1}{(6006b^2)}r^6 & -\frac{37}{(12012b^2)}r^5 & 0 & 0 & \frac{5}{(48048b^2)}r^6 & -\frac{73}{(48048b^2)}r^5 & 0 \\ -\frac{25}{(1716b)}r^3 & 0 & 0 & -\frac{125}{6006b}r^4 & \frac{1}{(6006b^2)}r^6 & 0 & 0 & -\frac{37}{(12012b^2)}r^5 & 0 & 0 & 0 & -\frac{73}{(48048b^2)}r^4 \\ -\frac{115}{(286b)}r^2 & 0 & 0 & -\frac{1845}{(4004b)}r^3 & \frac{37}{(12012b^2)}r^5 & 0 & 0 & -\frac{365}{(6006b^2)}r^4 & 0 & 0 & 0 & -\frac{35}{(1716b^2)}r^3 \\ 0 & -\frac{115}{(286b)}r^2 & \frac{1845}{(4004b)}r^3 & 0 & 0 & \frac{37}{(12012b^2)}r^5 & \frac{365}{(6006b^2)}r^4 & 0 & 0 & -\frac{73}{(48048b^2)}r^5 & \frac{35}{(1716b^2)}r^4 & 0 \\ 0 & \frac{3500}{143} & 0 & \frac{1355}{286}r & 0 & 0 & 0 & 0 & 0 & 0 & 0 & 0 \\ 3500 & 143 & 0 & \frac{1355}{286}r & 0 & 0 & 0 & 0 & 0 & 0 & 0 & 0 \\ 143 & 0 & 0 & \frac{1355}{286}r & 0 & 0 & 0 & 0 & 0 & 0 & 0 & 0 \\ -\frac{1355}{286}r & 0 & 0 & -\frac{485}{2002}r^2 & \frac{25}{4004b}r^4 & 0 & 0 & 0 & 0 & 0 & 0 & -\frac{115}{(286b)}r^2 \\ 0 & -\frac{1355}{286}r & \frac{485}{2002}r^2 & 0 & 0 & \frac{25}{4004b}r^4 & 0 & 0 & 0 & 0 & 0 & 0 \\ 0 & \frac{25}{(1716b)}r^3 & \frac{125}{6006b}r^4 & 0 & 0 & -\frac{1}{(6006b^2)}r^6 & -\frac{37}{(12012b^2)}r^5 & 0 & 0 & \frac{5}{(48048b^2)}r^6 & -\frac{73}{(48048b^2)}r^5 & 0 \\ -\frac{25}{(1716b)}r^3 & 0 & 0 & -\frac{125}{6006b}r^4 & \frac{1}{(6006b^2)}r^6 & 0 & 0 & -\frac{37}{(12012b^2)}r^5 & 0 & 0 & 0 & -\frac{73}{(48048b^2)}r^4 \\ -\frac{115}{(286b)}r^2 & 0 & 0 & -\frac{1845}{(4004b)}r^3 & \frac{37}{(12012b^2)}r^5 & 0 & 0 & -\frac{365}{(6006b^2)}r^4 & 0 & 0 & 0 & -\frac{35}{(1716b^2)}r^3 \\ 0 & -\frac{115}{(286b)}r^2 & \frac{1845}{(4004b)}r^3 & 0 & 0 & \frac{37}{(12012b^2)}r^5 & \frac{365}{(6006b^2)}r^4 & 0 & 0 & -\frac{73}{(48048b^2)}r^5 & \frac{35}{(1716b^2)}r^4 & 0 \end{bmatrix}$$

Finite shaft element characteristic gyroscopic matrix, where $G_c = [G_c]$

(4.20)

All the matrices of equation (4.18) are symmetric except the gyroscopic matrix $[G]$ of equation (4.20), which is skew symmetric. The force vector $\{Q\}$ includes mass unbalance, interconnection forces, and other element external effects. For the element with distributed mass center eccentricity $(\eta(x), \zeta(x))$, utilizing the consistent matrix approach the equivalent unbalance force is

$$\begin{aligned} \{Q^e\} &= \int \rho A \Omega^2 [Y] \left(\begin{Bmatrix} \eta(x) \\ \zeta(x) \end{Bmatrix} \cos \Omega t + \begin{Bmatrix} -\zeta(x) \\ \eta(x) \end{Bmatrix} \sin \Omega t \right) \\ &= \{Q_c^e\} \cos \Omega t + \{Q_s^e\} \sin \Omega t \end{aligned} \quad (4.21)$$

By assuming a linear distribution of the mass center locations in the finite rotor segment, the mass eccentricities in Y and Z directions measured at $t = 0$ for a differential disk located at distance x , a linear mass unbalance distribution over the element, can be represented by the expressions,

$$\begin{aligned} \eta(x) &= \eta_L \left(1 - \frac{x}{r}\right) + \eta_R \left(\frac{x}{r}\right) \\ \zeta(x) &= \zeta_L \left(1 - \frac{x}{r}\right) + \zeta_R \left(\frac{x}{r}\right) \end{aligned} \quad (4.22)$$

with (η_L, ζ_L) and (η_R, ζ_R) denoting the mass center eccentricity at $x = 0$ (left end) and $x = r$ (right end) in Y and Z directions, respectively. The equivalent unbalance force from equation (4.21) is presented as equation (4.23).

$$\begin{aligned}
Q_c &:= \rho \cdot A \cdot \Omega^2 \cdot \left[\begin{array}{l} \frac{1}{36} \cdot r \cdot (5 \cdot \eta_2 + 13 \cdot \eta_1) \\ \frac{1}{36} \cdot r \cdot (5 \cdot \zeta_2 + 13 \cdot \zeta_1) \\ \frac{-1}{252} \cdot r^2 \cdot (17 \cdot \zeta_1 + 10 \cdot \zeta_2) \\ \frac{1}{252} \cdot r^2 \cdot (17 \cdot \eta_1 + 10 \cdot \eta_2) \\ \frac{-1}{15120} \cdot r^4 \cdot \frac{(4 \cdot \eta_2 + 5 \cdot \eta_1)}{b} \\ \frac{-1}{15120} \cdot r^4 \cdot \frac{(5 \cdot \zeta_1 + 4 \cdot \zeta_2)}{b} \\ \frac{-1}{1008} \cdot r^3 \cdot \frac{(5 \cdot \zeta_2 + 7 \cdot \zeta_1)}{b} \\ \frac{1}{1008} \cdot r^3 \cdot \frac{(7 \cdot \eta_1 + 5 \cdot \eta_2)}{b} \\ \frac{1}{36} \cdot r \cdot (13 \cdot \eta_2 + 5 \cdot \eta_1) \\ \frac{1}{36} \cdot r \cdot (5 \cdot \zeta_1 + 13 \cdot \zeta_2) \\ \frac{1}{252} \cdot r^2 \cdot (17 \cdot \zeta_2 + 10 \cdot \zeta_1) \\ \frac{-1}{252} \cdot r^2 \cdot (10 \cdot \eta_1 + 17 \cdot \eta_2) \\ \frac{1}{15120} \cdot r^4 \cdot \frac{(5 \cdot \eta_2 + 4 \cdot \eta_1)}{b} \\ \frac{1}{15120} \cdot r^4 \cdot \frac{(5 \cdot \zeta_2 + 4 \cdot \zeta_1)}{b} \\ \frac{-1}{1008} \cdot r^3 \cdot \frac{(7 \cdot \zeta_2 + 5 \cdot \zeta_1)}{b} \\ \frac{1}{1008} \cdot r^3 \cdot \frac{(5 \cdot \eta_1 + 7 \cdot \eta_2)}{b} \end{array} \right] \\
Q_s &:= \rho \cdot A \cdot \Omega^2 \cdot \left[\begin{array}{l} \frac{-1}{36} \cdot r \cdot (5 \cdot \zeta_2 + 13 \cdot \zeta_1) \\ \frac{1}{36} \cdot r \cdot (5 \cdot \eta_2 + 13 \cdot \eta_1) \\ \frac{-1}{252} \cdot r^2 \cdot (17 \cdot \eta_1 + 10 \cdot \eta_2) \\ \frac{-1}{252} \cdot r^2 \cdot (17 \cdot \zeta_1 + 10 \cdot \zeta_2) \\ \frac{1}{15120} \cdot r^4 \cdot \frac{(5 \cdot \zeta_1 + 4 \cdot \zeta_2)}{b} \\ \frac{-1}{15120} \cdot r^4 \cdot \frac{(4 \cdot \eta_2 + 5 \cdot \eta_1)}{b} \\ \frac{-1}{1008} \cdot r^3 \cdot \frac{(7 \cdot \eta_1 + 5 \cdot \eta_2)}{b} \\ \frac{-1}{1008} \cdot r^3 \cdot \frac{(5 \cdot \zeta_2 + 7 \cdot \zeta_1)}{b} \\ \frac{-1}{36} \cdot r \cdot (5 \cdot \zeta_1 + 13 \cdot \zeta_2) \\ \frac{1}{36} \cdot r \cdot (13 \cdot \eta_2 + 5 \cdot \eta_1) \\ \frac{1}{252} \cdot r^2 \cdot (10 \cdot \eta_1 + 17 \cdot \eta_2) \\ \frac{1}{252} \cdot r^2 \cdot (17 \cdot \zeta_2 + 10 \cdot \zeta_1) \\ \frac{-1}{15120} \cdot r^4 \cdot \frac{(5 \cdot \zeta_2 + 4 \cdot \zeta_1)}{b} \\ \frac{1}{15120} \cdot r^4 \cdot \frac{(5 \cdot \eta_2 + 4 \cdot \eta_1)}{b} \\ \frac{-1}{1008} \cdot r^3 \cdot \frac{(5 \cdot \eta_1 + 7 \cdot \eta_2)}{b} \\ \frac{-1}{1008} \cdot r^3 \cdot \frac{(7 \cdot \zeta_2 + 5 \cdot \zeta_1)}{b} \end{array} \right]
\end{aligned}$$

(4.23)

Equation (4.23) gives us the element components of the unbalance force vector, where 1 and 2 represents the left (L) and right (R) nodes of the mass center eccentricity.

Equation (4.18) is transformed to whirl frame coordinates by using equations (4.1), (4.2) and (4.3) extended to include eight coordinates (four coordinates in each direction) at each end of the element and then premultiplying by $[R]^T$.

$$\begin{aligned} & \left([M_T^c] + [M_R^c] \right) \left\{ \ddot{P}^c \right\} + \omega \left(2[\hat{M}_T^c] + (1-\lambda)[G^c] \right) \left\{ \dot{P}^c \right\} \\ & + \left(([K_B^c] - [K_A^c]) - \omega^2 ([M_T^c] + (1-2\lambda)[M_R^c]) \right) \left\{ P^c \right\} = \left\{ P^c \right\} \end{aligned} \quad (4.24)$$

In addition, since $\sigma_P = 2 \sigma_d$,

$$[R]^T [M_R^c] [S] = \frac{1}{2} [G^c] \quad (4.25)$$

where $\Omega/\omega = \lambda$, and

$$[\hat{M}_T^c] = [R]^T [M_T^c] [S] \quad (4.26)$$

4.4 Bearings

The coupling between forces and displacements, and between slopes and bending moments are neglected here. The equations are limited to those which obey the governing equation given as equation (2.32).

4.5 System Equations of Motion

For a specified set of shaft spin speeds the assembled undamped system equations

of motion, consisting of component equations of the form of equations (4.4), (4.18) and (2.32), are of the form

$$[M^r] \{ \ddot{q}^r \} - \Omega [G^r] \{ \dot{q}^r \} + [K^r] \{ q^r \} = \{ Q^r \} \quad (4.27)$$

for fixed frame coordinates. The boundary conditions are then imposed at the left and right boundary points of each shaft. Boundary conditions for typical end conditions for the XZ plane are given in Table 3.1. For an overhung rotor fixed at the left end, the end conditions are as follows:

Left end (fixed) $w = \beta = 0$ (displacement and slope)

Right end (free) $F = M = 0$ (force and moment)

The matrices have banded structure with an overlapping of the element matrices.

The mass matrix is symmetric as in the case of non-rotating structures, and describes the translatory and rotary inertial behavior of the rotor. However the gyroscopic matrix is skew-symmetric. The stiffness matrix is symmetric. For computational purpose equation (4.27) can be written as first order differential equations in a matrix form as given in equation (2.36).

4.5.1 Whirl Speed Analysis

The free vibration solutions of equation (4.27) are of the form of equation (2.41) and when substituted into the homogeneous form of equation (4.27), they provide the

eigenvalue problem in the form of an equation that is similar in form to equation (2.42).

For whirl frame coordinates equation (4.27) transforms to the form

$$[M^s] \left\{ \ddot{p}^s \right\} + \omega (2[\hat{M}^s] - \lambda [G^s]) \left\{ \dot{p}^s \right\} + ([K^s] - \omega^2 ([M^s] + \lambda [\hat{G}^s])) \left\{ p^s \right\} = \left\{ P^s \right\} \quad (4.28)$$

8n x 1

The natural circular whirl speeds and mode shapes can be obtained from the homogeneous form of equation (4.28), if we assume a constant solution $\{p^s\} = \{p_0\} = \text{const}$. The associated eigenvalue problem is

$$[K^s] \{p_0\} = \omega^2 ([M^s] + \lambda [G^s]) \{p_0\} \quad (4.29)$$

where matrix $\{p_0\}$ is of $4n \times 1$. The $4n$ eigenvalues are real and the positive values, ω_i , with associated vectors $\{p_0\}^i$ represent natural circular whirl speeds and mode shapes relative to R at the specified whirl ratio λ .

4.6 Industrial Applications

4.6.1 Simple Rotor Model

4.6.1.1 Determination of the Model

The frame \mathfrak{S} (XYZ) is the inertial frame, the rotor axis is along the X -axis, and the

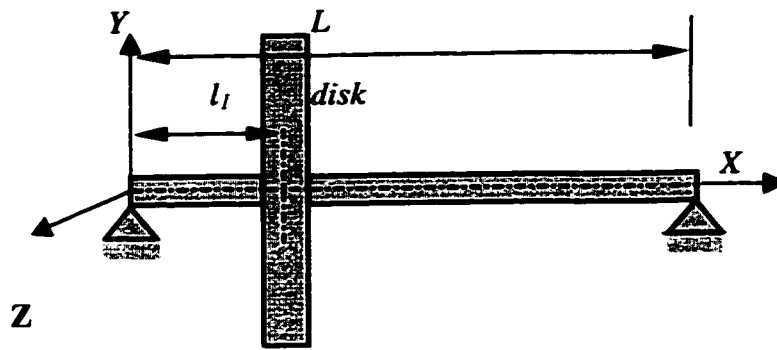


Figure 4.2. Model of the rotor

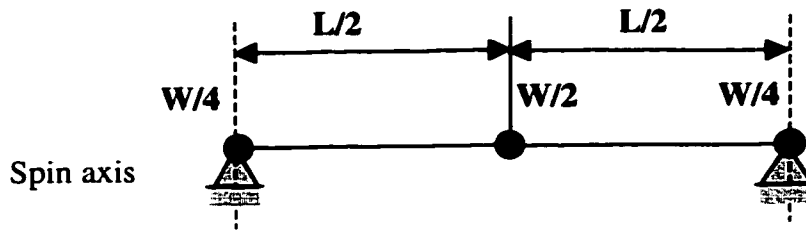


Figure 4.3 Uniform beam represented as a three-stations lumped-mass model

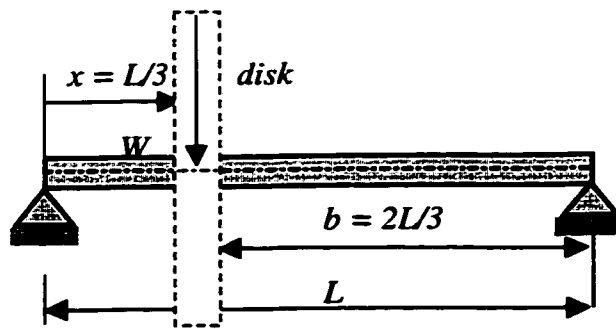


Figure 4.4 Equal lumped mass model

speed of rotation Ω is constant (Figure 4.2). In order to make hand calculations, only one degree of freedom is used for the displacements in the Y and the Z directions. The rotor is simply supported at both ends. It consists of

a symmetric shaft of length L ;

a symmetric disk, situated at $x = l_1 = L/3$;

Numerical Data

Basic data for the disk

Inner radius $R_1 = 0.01\text{m}$

Outer radius $R_2 = 0.15\text{m}$

Thickness $h = 0.03\text{ m}$

Density $\rho = 7800\text{ kg/m}^3$

Length $l_1 = L/3$

Then M_d , I_d and I_p are obtained. These quantities are

$$M_d = \pi (R_2^2 - R_1^2) h \rho = 16.47\text{ kg}$$

$$I_d = M_d/12 (3 R_2^2 - 3 R_1^2 + h^2) = 9.347 \times 10^{-2}\text{ kg m}^2$$

$$I_p = M_d/2 (R_1^2 + R_2^2) = 0.1861\text{ kg m}^2$$

Basic data for the shaft

Length $L = 0.4\text{ m}$

Cross-sectional radius $R_1 = 0.01\text{ m}$

Density $\rho = 7800\text{ kg/m}^3$

Young's modulus $E = 2 \times 10^{11} \text{ N/m}^2$

Operating speed $\Omega = 15000 \text{ rpm}$

The cross-sectional area A and area moment of inertia I are obtained as

$$A = \pi R^2 = 3.142 \times 10^{-4} \text{ m}^2$$

$$I = \pi R^4/4 = 7.854 \times 10^{-9} \text{ m}^4$$

4.6.1.2 Critical Speeds of a Uniform Shaft

Figure 4.2 represents a uniform beam of length L and cross-sectional radius R . The lumped mass model of this rotor is illustrated in Figure 4.3. Let us introduce some concepts of continuum to a lumped-mass stiffness rotor model.

The beam natural frequencies (considering ideal simply supported boundaries) are given by

$$\omega_n = (n\pi)^2 \sqrt{\frac{EI}{ML^3}} \quad \text{rad/sec} \quad (4.30)$$

where $\omega_n = n$ -th natural frequency and $M =$ total shaft mass. Corresponding to each natural frequency (or eigenvalue) is a mode shape or eigenvector. The eigenvectors for a uniform beam are given by

$$\phi(x) = \sin \frac{n\pi x}{L} \quad (4.31)$$

The displacement mode shape does not represent the actual shaft deflection but represents a normalized shape that the shaft assumes at the corresponding frequency. If the uniform shaft is rotated about its axis, then any residual unbalance or shaft bow will cause the shaft to bow outward as the rotor speed approaches the shaft critical speed.

The actual whirl radius of the shaft will be dependent on the magnitude of unbalance, the relationship of the rotor speed to the critical speed, and the amount of damping present in the system.

Computation of the critical speeds of a uniform steel shaft:

Total shaft mass $M = \rho A L = 7800 \times 3.142 \times 10^{-4} \times 0.4 = 0.9803 \text{ kg}$

$$\begin{aligned}\omega_1 &= (1\pi)^2 \sqrt{\frac{2 \times 10^{11} \times 7.854 \times 10^{-9}}{0.9803 \times 0.4^3}} = 1561.68 \\ \omega_2 &= (2\pi)^2 \sqrt{\frac{2 \times 10^{11} \times 7.854 \times 10^{-9}}{0.9803 \times 0.4^3}} = 6246.70 \\ \omega_3 &= (3\pi)^2 \sqrt{\frac{2 \times 10^{11} \times 7.854 \times 10^{-9}}{0.9803 \times 0.4^3}} = 14055.08 \\ \omega_4 &= (4\pi)^2 \sqrt{\frac{2 \times 10^{11} \times 7.854 \times 10^{-9}}{0.9803 \times 0.4^3}} = 24986.80\end{aligned}$$

rad/sec

Computation of the critical speed of a lumped mass shaft:

A proper lumped-mass model to represent the rotor for the first critical speed requires three stations (see figure 4.3). Weights of $W/4$ at the ends of the rotor and $W/2$ at the center of the shaft (assuming the weight distribution of $W/3$ at each station leads to an improper lumped-mass model). For the assumption of rigid bearings at the ends of the shaft, we arrive at a Jeffcott rotor simulating a uniform shaft by placing half of the total

shaft weight at the middle of the bearing span. Note, however, that this lumped-mass model is valid only for motion through the rotor's critical speeds in the fundamental mode region.

Since the shaft stiffness of a uniform beam with simple supports at the center span is given by

$$K_{shaft} = \frac{48EI}{L^3} \quad (4.32)$$

$$K = \frac{48 \times 2 \times 10^{11} \times 7.854 \times 10^{-9}}{(0.4)^3} = 11.8 \times 10^5 \text{ kg/m}$$

$$\omega_1 = \sqrt{\frac{11.8 \times 10^5}{0.9803/2}} = 1551.59 \text{ rad/sec}$$

Computation of the critical speed of a lumped mass shaft-disk system using Rayleigh's method:

Let us calculate the first approximation to the fundamental frequency of lateral vibration for the system shown in figure (4.4). We see that the deflection of the beam at any point x from the left end due to a single load W at a distance b from the right end is

$$w(x) = \frac{Wbx}{6EIL} (L^2 - x^2 - b^2) \quad (4.33)$$

Then the frequency equation is

$$\omega^2 = \frac{g \sum_i M_i w_i}{\sum_i M_i w_i^2} \quad (4.34)$$

Due to 16.54-kg mass the deflection at the corresponding point is

$$\begin{aligned}
 w\left(\frac{L}{3}\right) &= \frac{m_d g \frac{L}{3}}{6EI} \left(L^2 - \frac{L^2}{9} - \frac{4L^2}{9} \right) \\
 &= \frac{8}{481} \frac{m_d g L^3}{EI}
 \end{aligned} \tag{4.35}$$

By substituting into equation (4.34) the first approximation to the fundamental frequency is

$$\begin{aligned}
 \omega_1 &= \sqrt{\frac{481}{8} \frac{EI}{m_d L^3}} \quad \text{rad/s} \\
 &= \sqrt{\frac{8 \times 2 \times 10^{11} \times 7.854 \times 10^{-9}}{8 \times 16.47 \times 0.4^3}} = 299.331
 \end{aligned} \tag{4.36}$$

Critical speed calculation of rotating shaft-disk system using closed form solution:

For a rotor system with a disk at one third of its length, the natural frequency is given from the equations (2.54) and (2.86)

$$\omega = \sqrt{\frac{243}{4} \frac{EI}{m_d L^3}} \tag{4.37a}$$

Then the natural frequency will be 300.882 rad/s. From the equation (2.82) and (2.83) one forward critical speed and two backward critical speeds of a rotor on rigid bearings including gyroscopic effect will be 311.6 rad/s, 257.432 rad/s and 508.947 rad/s.

where

$$k_{rr} = \frac{3EIL}{a^3b^3}(a^2 - ab + b^2), \quad k_{\psi\psi} = \frac{3EIL}{ab}, \quad k_{r\psi} = \frac{3EIL}{a^2b^2}(a - b) \quad (3.37b)$$

where $a = L/3$ and $b = 2L/3$. Based on the results presented above, a comparison is now made in Table 4.1.

Table 4.1 Critical speed of a simply supported, non-rotating uniform steel shaft-disk system.

	ω_n (rad/s)
critical speed of a uniform steel shaft using closed form solution	1561.68
critical speed of a lumped mass steel shaft	1551.59
critical speed of a steel shaft-disk system using Rayleigh's method	299.331
critical speed of a steel shaft-disk system using closed form solution	300.882

Calculation of the static buckling load:

The critical buckling load for a shaft is given by

$$P_{cr} = \frac{\pi^2 EI}{L^2} \quad (4.38)$$

Critical buckling load for a shaft given above will be

$$P_{cr} = \frac{\pi^2 \times 2 \times 10^{11} \times 7.854 \times 10^{-9}}{0.4^2} = 96894.84 \text{ N}$$

In the following examples, an axial force equal to 10 % of this buckling load is taken into consideration.

4.6.2 Finite Element Model

4.6.2.1 Conventional Finite Element Model

In order to evaluate the accuracy of finite rotating shaft element with efficient basis functions, as the first example, a simply supported rotor-disk system is considered, using conventional finite elements. Critical speeds of the system were computed using three and six finite elements (Figure 4.5). The results of various conditions are listed in Tables 4.2 to 4.6. Computed first critical speeds were compared with well-established closed form analyses, which are tabulated in Table 4.1.

4.6.2.2 Finite Element with Efficient higher Order Basis Functions

As the first example, the non-rotating simply supported rotor-disk system is considered. Critical speeds of the system were computed using one, two and three finite elements (Figure 4.6). The results of various conditions are listed in Tables 4.7 to 4.10.

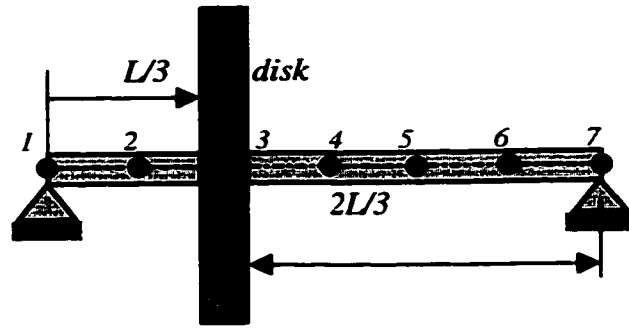


Figure 4.5 Six-element finite element model

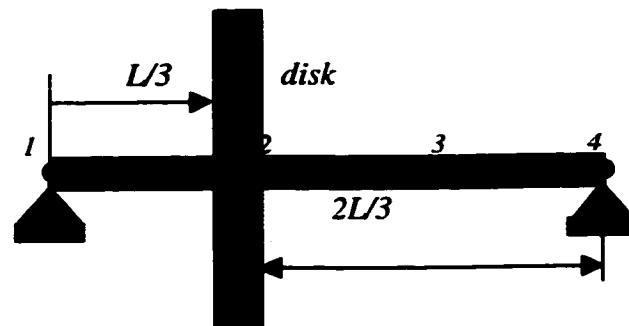


Figure 4.6 Three-element finite element model

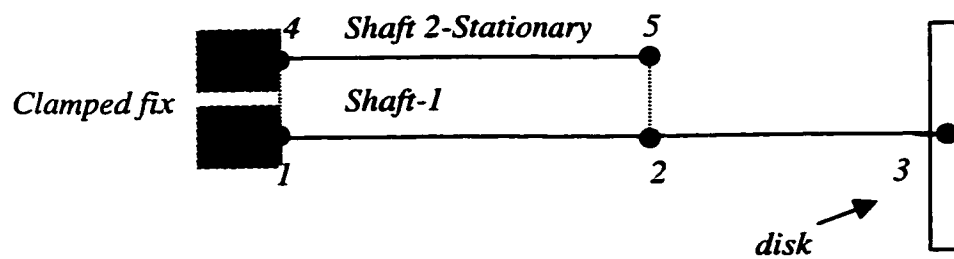


Figure 4.7 Cantilever-sleeve rotor-bearing system using finite element with efficient basis functions

As a second example, a cantilever-sleeve rotor system is considered. Figure 4.7 shows the finite element model of cantilever-sleeve rotor-bearing system used in Chapter 2. The shaft cross-sections are constant up to node 3 and then are tapered towards node 5. No damping is included in this model. The finite element model includes 1 stationary shaft element, 2 rotating shaft elements, a disk at node 3 and two rigid bearings at the fixed end. Displacement of the rotating sleeve shaft and stationary cantilever shaft at nodes 1 and 2 are the same. Assembly procedures are same as discussed in Chapters 2 and 3. The results obtained using finite elements with efficient basis functions are shown in Tables 4.13 and 4.14.

Table 4.2 Critical speeds of a simply supported rotor system with no disk, zero compressive load or bearing pressure and zero bearing spring constant, using conventional finite elements

	Critical speeds (rad/sec)			
	ω_1	ω_2	ω_3	ω_4
Finite element solution using three elements	1560.97	6252.48	14214.17	27394.70
Finite element solution using six elements	1560.65	6232.95	14014.45	24976.92

Table 4.3 Critical speeds of a simply supported rotor-disk system including the Mass of the disk using conventional finite elements; $M_d = 16.47$ kg

	Critical speeds (rad/sec)			
	ω_1	ω_2	ω_3	ω_4
Finite element solution using six elements	295.75	4532.20	14014.46	19721.49

Table 4.4 Critical speeds of a simply supported rotor-disk system including the mass moment of inertia of the disk using conventional finite elements; $M_d = 16.47$ kg, $I_d = 9.427 \times 10^{-2}$ kgm² and $I_p = 0.1861$ kgm²

	Critical speeds (rad/sec)			
	ω_1	ω_2	ω_3	ω_4
Finite element solution using three elements	283.05	781.72	5579.79	20659.19
Finite element solution using six elements	283.05	781.72	5532.23	17801.27

Table 4.5 Critical speeds of a simply supported rotor-shaft system including the mass moments of inertia of the disk using conventional finite elements; $M_d = 16.47$ kg, $I_d = 0.09427$ kgm², $I_p = 0.1861$ kgm², $k = 10^7$ N/m and $P = 9689.48$ N

	Critical speeds (rad/sec)			
	ω_1	ω_2	ω_3	ω_4
Finite element solution using three elements	281.68	781.20	5574.02	20652.93
Finite element solution using six elements	281.69	781.19	5526.56	17794.65

Table 4.6 Critical speeds of a simply supported rotor-shaft system including the mass moments of inertia of the disk, bearing spring constant and compressive load using conventional finite elements with gyroscopic effect; $M_d = 16.47$ kg, $I_d = 0.09427$ kgm² and $I_p = 0.1861$ kgm², $k = 10^7$ N/m and $P = 9689.48$ N

	Critical speeds (rad/sec)			
	ω_1	ω_2	ω_3	ω_4
Finite element solution using six elements	302.116	1066.750	5528.117	17798.405
Finite element solution using twelve elements	301.392	1066.995	5524.849	17695.644

Table 4.7 Critical speeds of a simply supported rotor system with no disk, zero compressive load or bearing pressure and zero bearing spring constant, using finite elements with efficient basis functions

	Critical speeds (rad/sec)			
	ω_1	ω_2	ω_3	ω_4
Finite elements with efficient basis functions using one element	1558.01	6269.02	14063.14	27510.75
Finite elements with efficient basis functions using two elements	1560.57	5956.80	13959.73	24998.37

Table 4.8 Critical speeds of a simply supported rotor-disk system including the mass of the disk using finite elements with efficient basis functions; $M_d = 16.47$ kg

	Critical speeds (rad/sec)			
	ω_1	ω_2	ω_3	ω_4
Finite elements with efficient basis functions using three elements	248.49	4274.34	13536.98	19381.06

Table 4.9 Critical speeds of a simply supported rotor-disk system including the mass moment of inertia of the disk using finite elements with efficient basis functions; $M_d = 16.47$ kg and $I_d = 0.09427$ kgm²

	Critical speeds (rad/sec)			
	ω_1	ω_2	ω_3	ω_4
Finite elements with efficient basis functions using three elements	236.92	894.52	5530.63	17735.92

Table 4.10 Critical speeds of a simply supported rotor-shaft system including the mass moments of inertia of the disk using finite elements with efficient basis functions; $M_d = 16.47$ kg, $I_d = 0.09427$ kgm², $I_p = 0.1861$ kgm², $k = 10^7$ N/m and $P = 9689.48$ N

	Critical speeds (rad/sec)			
	ω_1	ω_2	ω_3	ω_4
Finite elements with efficient basis functions using three elements	236.92	894.52	5530.63	17735.92

Table 4.11 Critical speeds of a simply supported rotor system with no disk, zero compressive load or bearing pressure and zero bearing spring constant, using beam theory, conventional finite element method and finite element with efficient basis functions, respectively

(both plane)	Critical speeds (rad/sec)			
	ω_1	ω_2	ω_3	ω_4
Beam theory (closed form solution), given by equation (4.30)	1561.68	6246.70	14055.08	24986.80
Solutions using six conventional finite elements	1560.65	6232.95	14014.46	24976.92
Solutions using two finite elements with efficient basis functions	1560.57	5956.80	13959.73	24998.37

Table 4.12 Critical speeds of a simply supported rotor-shaft system including the mass moments of inertia of the disk using a mesh of six conventional finite elements and a mesh of three finite elements with efficient basis functions; $M_d = 16.47$ kg, $I_d = 0.09427$ kgm², $I_p = 0.1861$ kgm², $k = 10^7$ N/m and $P = 9689.48$ N

(both planes)	Critical speeds (rad/sec)			
	ω_1	ω_2	ω_3	ω_4
Solutions using six conventional finite elements	281.69	781.19	5526.56	17794.65
Solution using three finite elements with efficient basis functions	241.19	838.98	4164.31	17487.81

Table (4.13) Critical speeds of a non-rotating cantilever-sleeve rotor-bearing system using mesh of two elements using finite elements with efficient basis functions

	Critical speeds (rad/sec)			
	ω_1	ω_2	ω_3	ω_4
Solution using two finite elements with efficient basis functions	86.525	491.377	1280.675	2713.964

Table (4.14) Critical speeds of a non-rotating cantilever-sleeve rotor-bearing system using a mesh of twelve conventional finite elements and a mesh of two finite elements with efficient basis functions

	Critical speeds (rad/sec)			
	ω_1	ω_2	ω_3	ω_4
Solution using twelve conventional finite elements	86.524	484.672	1102.825	2538.669
Solution using two finite elements with efficient basis functions	86.525	491.377	1280.675	2713.964

4.7. Numerical Results and Discussions

The equations of motion for a uniform rotating shaft element have been formulated using efficient higher order basis functions that were developed in chapter 3. The model includes the effects of rotational inertia, gyroscopic moments and axial load. The equations of motion for the elements are presented in both fixed and rotating frames of reference. The rotating frame equation is used to calculate the critical speeds since the two planes of motion can be treated separately. However, the fixed frame equation is used to calculate the influence of the gyroscopic effect on the critical speeds.

For the simply supported shaft, the critical speeds that were calculated using meshes of three and six finite elements, respectively, are given in Table 4.2. For the simply supported shaft with a disk at one third of its length, the critical speeds that were calculated using a mesh of six finite elements are given in Table 4.3. For the same shaft-disk system the critical speeds that were calculated after adding mass moment of inertia, polar moment of inertia, spring constant and axial load and using meshes of three and six finite elements, respectively, are given in Table 4.4 and Table 4.5. The effect of gyroscopic moments is highlighted in Table 4.6.

For the simply supported shaft, the critical speeds that were calculated using meshes of one and two finite elements with effective basis functions are given in Table 4.7. For the simply supported shaft with a disk at one third of its length, the critical speeds that were calculated using a mesh of three finite elements with effective basis functions are given in Table 4.8. For the same shaft-disk system the critical speeds that were calculated after adding mass moment of inertia, polar moment of inertia, spring

constant and axial load and using a mesh of three finite elements with efficient basis functions are given in Table 4.9 and Table 4.10.

The natural frequencies of a uniform non-rotating simply supported beam obtained using beam theory (closed form solution), conventional finite element method and finite elements with efficient basis functions are compared in Table 4.11. Results by all the three methods agree quite well.

The natural frequencies of a uniform rotating simply supported beam with the disk at one third of its length, obtained using conventional finite element method and finite elements with efficient basis functions are listed in Table 4.12. The results by using the efficient higher order basis functions are superior.

It may be noted that a mesh of two or three finite elements with efficient basis functions have been used in the above numerical study so that the total number of degrees of freedom is the same in the meshes of conventional and the newly developed finite elements. As can be seen, the boundary conditions significantly influence the dynamic response of the system. The newly developed finite element model provides better results using smaller number of elements compared to the case of conventional finite element model.

For non-rotating cantilever-sleeve rotor-bearing system, the critical speeds that were calculated using a mesh of two newly developed finite elements are given in Table 4.13.

A comparison of critical speeds of a non-rotating cantilever-sleeve rotor-bearing system with the disk at the end using the newly developed finite elements is made with those obtained for the case of conventional finite elements. The results of this

comparison are listed in Table 4.14. The second natural frequency obtained using efficient higher order basis functions is higher than that obtained by using conventional finite elements. This may be due to the smaller number of elements (three) used in the case of efficient higher order basis functions, which could not effectively represent the second mode. Moreover, the third natural frequency is close to the operating speed and needs more accurate determination.

The numerical results indicate that the new finite element with efficient higher order basis functions developed in this thesis provides a more accurate representation of the rotating shaft dynamics. The inclusion of the effect of both natural and essential boundary conditions yields a more precise finite element model than the conventional finite element model. Moreover, the new modeling can be programmed easily and also the entire solution process requires less CPU time.

The next chapter-5 provides a summary and the conclusions drawn based on the analysis and the results obtained in this thesis.

CHAPTER 5

SUMMARY AND CONCLUSIONS

In this thesis a finite element simulation of a cantilever-sleeve rotor-bearing system is presented using conventional finite elements and using newly developed finite elements with efficient higher order basis functions. The effects of rotary inertia, gyroscopic moment and axial force are included in the analysis. The critical speeds are obtained for the following configurations:

- (i) a non-rotating uniform cantilever shaft with a non-rotating disk at the end.
- (ii) a non-rotating uniform cantilever shaft with a rotating disk at the end.
- (iii) a rotating uniform cantilever shaft with a rotating disk at the end (overhung rotor).
- (iv) a non uniform cantilever-sleeve rotor-bearing system with a non- rotating shaft and a rotating sleeve shaft and a rotating disk.

The numerical examples that demonstrate the effect of gyroscopic moment on the critical speeds are provided. The solution of eigenvalue problem is obtained by using the first order of equations of motion as suggested by Meirovitch [60]. The comparisons with the closed form solutions for the cases (i), (ii) and (iii) were made to illustrate the accuracy of the modeling. Very close agreement was obtained in all the cases. The unbalance response for the cantilever-sleeve rotor system is also obtained.

Several investigators have presented in the past various finite element models for the vibration of Euler-Bernoulli beam-shaft structure. However a finite element model

that can include in the basis functions the effects of all the boundary conditions of the beam, has not so far been developed. Such a finite element model has been developed in this thesis and further its applications to beam vibrations and rotor dynamics have been made.

In the finite element model, four degrees of freedom per node are considered so as to satisfy all the boundary conditions. The four degrees of freedom at a node of the element are the displacement, slope, bending moment and shear force. Thus, this element can adequately represent all the physical situations involved in any combination of boundary conditions. The superiority of this element is illustrated by comparing the results of vibration analysis with that obtained using existing finite element modeling and that obtained using closed form solutions. The mass and stiffness matrices of beam finite element with efficient higher order basis functions for vibration analysis are developed.

The newly developed beam finite element is used to develop the finite shaft element with efficient higher order basis functions for the dynamic analysis of rotor-bearing systems.

The finite element model for the rotor-bearing system is developed including the effects of rotary inertia, gyroscopic moments and axial load. The equations of motion are presented in both fixed and rotating frames of reference. The dynamic behavior of a simple rotor system and a cantilever-sleeve rotor-bearing system is studied using finite elements with efficient higher order basis functions. Natural frequencies and whirl speeds were calculated by using both the fixed and rotating frame formulations. A set of comparisons was made with the results obtained using the conventional finite elements.

5.1 The conclusions of the present investigation

Based on the analysis and the numerical results forecasted in this thesis, the principal conclusions that be drawn are:

- 1) A finite element with efficient higher order basis functions can satisfy the entire essential and natural boundary conditions of a beam and a rotor shaft, right in the element formulation. Thus, this element adequately represents all the physical situations involved in any combination of displacement, rotation, bending moment and shearing force.
- 2) For complex rotor systems such as the cantilever-sleeve rotor systems considered here, it is necessary to use better analysis methods in order to calculate natural frequencies of the system. This will help to design and operate the rotor system such that the operating speeds are away from any natural frequencies. In the numerical example provided, the third natural frequency needs to be analyzed more accurately since it is close to the operating speed.
- 3) More accurate results are obtained using fewer numbers of elements that have increased degrees of freedom and efficient higher order basis functions rather than using larger number of elements that have fewer degrees of freedom. Further, no errors are introduced during post processing for stresses, strain, etc.

The larger the number of degrees of freedom involved in the model the greater are

the advantages of the present approach. Thus present model requires smaller number of elements to obtain the same results that would be obtained using larger number of conventional finite elements. The eigenvalues obtained by using beam finite element with efficient higher order basis functions converge more rapidly to the exact solution.

5.2 Recommendations for Future Work

Some suggestions for the possible future work are given below:

- (i) The finite element with efficient higher order basis functions obtained in the present investigation can be applied to the stress analysis of tapered beams and plates.
- (ii) Analysis of rotor-bearing system using finite non-rotating and rotating shaft elements with efficient higher order basis functions based on Timoshenko beam theory can be developed for thick beams and shafts.

REFERENCES

1. H. H. JEFFCOTT 1919 *Phil. Mag., Series 6*, **37**, 304. The Lateral Vibrations of Loaded Shafts in the Neighborhood of a Whirling Speed-The Effect of Want of Balance.
2. R. G. GREEN 1948 *Journal of Applied Mechanics*, **70**, 369-376. Gyroscopic Effects on the Critical Speeds of Flexible Rotors.
3. R. L. RUHL 1970 *Ph.D. Thesis, Cornell University, Ithaca, N.Y.*, Dynamics of Distributed Parameter Turborotor Systems Transfer Matrix and Finite Element Techniques.
4. T. THORKILDSEN 1972 *MSE Engineering Report, Arizona University*. Solution of a Distributed Mass and Unbalanced Rotor System Using a Consistent Mass Matrix Approach.
5. S. R. POLK 1974 *MSE Engineering report, Arizona University*. Finite Element Formulation and Solution of Flexible Rotor Rigid Disk Systems for Natural Frequencies and Critical Speeds.
6. J. THOMAS and J. DOKUMACI 1974 *Aeronautical Quarterly* **25**, 109-18. Simple Finite Elements for Pre-twisted Blading Vibrations.
7. A. KRISHNA MURTY 1974 *Proc. Int. Conf. Finite Element Methods Engineering., Coimbatore Institute of Technology, India* Finite Element Analysis of Rotating Structural Elements.
8. D. R. CHIVENS and H. D. NELSON 1975 *Trans. ASME Journal of Engineering for Industry* **97** 881-886. The Natural Frequencies and Critical Speeds of a

Rotating, Flexible Shaft-Disk System.

9. H.D NELSON and J. M. McVAUGH 1976 *Trans. ASME Journal of Engineering for Industry* **98**, 593-600. The Dynamics of Rotor-Bearing Systems Using Finite Elements.
10. E. S. ZORZI and H. D. NELSON 1977 *Trans. ASME Journal of Engineering for Industry* **99**, 71-79. Finite Element Simulation of Rotor-Bearing Systems Using Finite Elements.
11. A. V. KRISHA MURTY and S. SRIDHARA MURTY 1977 *Mechanism and Machine Theory* **12**, 311-322. Finite Element Analysis of Rotors.
12. E. S. ZORZI and H. D. NELSON 1980 *Journal of mechanical design* **102**, 158-161. The Dynamics of Rotor Bearing Systems with Axial Torque-A Finite Element Approach.
13. H. D. NELSON 1980 *Journal of mechanical design* **102**, 793-803. A Finite Rotating Shaft Element Using Timoshenko Beam Theory.
14. H. N. OZGUVEN 1984 *Journal of vibration, acoustics, stress, and reliability in design* **106** 72-79. Whirl Speeds and Unbalance Response of Multi-Bearing Rotors Using Finite Elements.
15. H. N. OZGUVEN 1984 *Journal of vibration acoustics, stress, and reliability in design* **106** 59-61. On the Critical Speeds of Continuous Shaft-Disk Systems.
16. H. D. NELSON, W. L. MEACHAM, D. P. FLEMING and A. KASCAK 1983 *Journal of Engineering for Power, Transactions ASME* **105(3)**, 606-614. Nonlinear Analysis of Rotor-Bearing Systems Using Components Mode Synthesis.

17. J. PADOVAN and M. ADAMS 1984 *Computers and Structures* **18(4)**, 629-634. Non-linear Transient Finite Element Analysis of Rotor-Bearing Systems Using Component Mode Synthesis.
18. N. O. MYKLESTAD 1944 *Journal of Aeronautical Science* **11(2)**, 153-162. A New Method of Calculating Natural Modes of Uncoupled Bending Vibration of Airplane Wings and Other Types of Beam.
19. M. A. PROHL 1945 *Transactions ASME Journal of Applied Mechanics* **67** A142-A148. A General Method for Calculating Critical Speeds of Flexible Rotors.
20. J. W. LUND 1967 *Journal of Engineering for Industry, Transactions ASME* **89(4)**, 785-796. Calculating the Experiments on the Unbalance Response of Flexible Rotor.
21. K. KIKUCHI 1970 *Bulletin of JSME* **13**, 61. Analysis of Unbalance Vibration of Rotating Shaft System with Many Bearing and Disks.
22. J. S. RAO 1985 *Proceedings of 1985 Bently Rotor Dynamics Research Corporation Symposium, June, Carson City, Nevada*. Time Marching Transfer Matrix Techniques for Transient Analysis of Rotors.
23. B. T. MURPHY and J. M. VANCE 1983 *Journal of Engineering for Power, Transactions ASME* **105(3)**, 591-595. An Improved Method for Calculating Critical Speeds and Rotor Dynamics Stability of Turbo-Machinery.
24. E. J. GUNTER, K. C. CHOY and P. E. ALLAIRE 1978 *Journal of the Frankling Institute* **4**, 305. Modal Analysis of Turbo-Rotors Using Planar Modes-Theory.
25. P. BERTHIER, G. FERRARIS and M. LALANNE 1983 *Shock and Vibration Bulletin* **53** part 4, 103-111. Prediction of Critical Speed, Unbalance and Non-

Synchronous Forced Response of Rotor.

26. D. A. GLASGOW and H. D. NELSON 1980 *Journal of Mechanical Design, Trans. ASME* **102**, 352-359. Stability Analysis of Rotor Bearing Systems Using Component Mode Synthesis.
27. R. B. BHAT 1982 *Proceedings of the 1st International Modal Analysis Conference, Orlando* 648. Unbalance Response of a Single Mass Rotor on Fluid Film Bearings Using Modal Analysis.
28. LORD RAYLEIGH 1877 *Theory of Sound*. London: Macmillan and Co.
29. S. TIMOSHENKO 1921 *Philosophical Magazine* **41**, 744-746. On The Correction for Shear of the Differential Equations for Transverse Vibration of Prismatic Bars.
30. J. PRESCOTT 1942 *Philosophical Magazine* **33**, 703-754. Elastic Waves and Vibrations of Thin Rods.
31. E. VOLTERRA 1961 *International Journal of Mechanical Science* **3**,47-67. Second Approximations of Method of Internal Constraint and Its Applications.
32. J. SUTHERLAND and L. GOODMAN 1951 *Department of Civil Engineering, University of Illinois, Urbana, Illinois Report*. Vibration of Prismatic Bars Including Rotary Inertia and Shear Corrections.
33. T. HUANG 1958 *Proceedings of the Third U.S. National Congress of Applied Mechanics*, 189-194. Effect of Rotary Inertia on the Vibration of Beams Treated by the Approximate Methods of Ritz and Galerkin.
34. R. ANDERSON 1953 *Journal of Applied Mechanics, Transactions of the American Society Mechanical Engineers* **20**, 504-510. Flexural Vibrations in

Uniform Beams According to Timoshenko Theory.

35. C. DOLPH 1954 *Quarterly of Applied Mathematics* **12**, 175-178. On the Timoshenko Theory for Transverse Beam Vibrations.
36. T. HUANG 1961 *Journal of Applied Mechanics, Transactions of the American Society of Mechanical Engineers* **83**, 579-584. The Effect of Rotary Inertia and Shear Deformation on the Frequency as Normal Mode Equations of Uniform Beams with Simple End Conditions.
37. J. THOMAS 1968, *Ph.D. Thesis, University of London*. Vibration Characteristics of Tapered Cantilever Beams.
38. R. MCCALLEY 1963 *General Electric Company, Schenectady, New York, and Report No. DIG/SA 63-73*. Rotary Inertia Correction for Mass Matrices.
39. J. ARCHER 1965 *American Institute of Aeronautics and Astronautics Journal* **3**, 1910—1918. Consistent Matrix Formulations for Structural Analysis Using Finite-Element Techniques.
40. K. KAPUR 1966 *Journal of the Acoustical Society of America* **40**, 1058—1063. Vibrations of Timoshenko Beam Using a Finite Element Approach.
41. W. CARNEGIE, J. THOMAS and E. DOKUMACI 1969 *Aeronautical Quarterly* **20**, 321-332. An Improved Method of Matrix Displacement Analysis in Vibration Problems.
42. D. EGGLE 1969 *NASA CR-1317*. An Approximate Theory for Transverse Shear Deformation and Rotary Inertia Effects in Vibrating Beams.
43. R. NICKEL and G. SECOR 1972 *International Journal of Numerical Methods in Engineering* **5**, 243-253. Convergence of Consistently Derived Timoshenko

Beam Finite Elements.

44. R. DAIS, R. D. HENSHELL and G. B. WARBURTON 1972 *Journal of Sound and Vibration* **22**, 475-487. A Timoshenko Beam Element.
45. J. THOMAS and B. A. H. ABBAS 1975 *Journal of Sound and Vibration* **41**(3), 291-299. Finite Element Model for Dynamic Analysis of Timoshenko Beam.
46. T. Y. YANG and C. T. SUN 1973 *Journal of Sound and Vibration* **27**, 297-311. Finite Elements for the Vibration of Framed Shear Walls.
47. C. T. SUN and S. N. HUANG 1975 *Computers and Structures* **5**, 297-303. Transverse Impact Problems by Higher Order Beam Finite Element.
48. I. FRIED 1971 *American Institute of Aeronautics and Astronautics Journal* **9**, 2071-2073. Discretization and Computational Errors in High-Order Finite Element.
49. C. W. S. TO 1979 *Journal of Sound and Vibration* **63**, 33-50. Higher Order Tapered Beam Finite Elements for Vibration Analysis.
50. Y. C. HOU, C. H. Tseng and S. F. Ling 1996 *Journal of Sound and Vibration* **191**, 91-106. A New High-Order Non-Uniform Timoshenko Beam Finite Element on Variable Two-parameter Foundations for Vibration Analysis.
51. A. HOUMAT 1995 *Journal of Sound and Vibration* **187**, 841-849. Vibrations of Timoshenko Beams by Variable Order Finite Elements.
52. D. J. DAWE 1978 *Journal of Sound and Vibration* **60**, 11-20. A Finite Element for the Vibration Analysis of Timoshenko Beams.
53. K.N HANDA 1970 *Ph.D. Thesis, University of Southampton*. The Response of Tall Structures to Atmospheric Turbulence.

54. J. THOMAS and E. DOKUMACI 1973 *Aeronautical Quarterly* **24**, 39-46.
Improved Finite Elements for Vibration Analysis of Tapered Beam.
55. E. C. PESTEL 1965 *Proceeding of conference on matrix methods in structural mechanics, Wright Patterson Air force base, Ohio, U. S. A., October 1965.*
Dynamic Stiffness Matrix Formulation by Means of Hermitian Polynomials.
56. R. D. COOK, D. S. MALKUS and M. E. PLESHA 1989 *John Wiley & Sons, New York, Third Edition*, 246-247. Concepts and Applications of Finite Element Analysis.
57. J. E. AKIN 1982, *Academic Press, London.* Application and Implementation of Finite Element Methods.
58. J. N. REDDY 1993 *McGraw-Hill. Inc. New York, Second Edition* 132. An Introduction to the Finite Element Method.
59. I. H. SHAMES and C. L. DYM 1985 *McGraw-Hill. Inc. New York* 526. Energy and Finite Element Methods in Structural Mechanics.
60. L. MEIROVITCH 1974 *AIAA Journal* **12** No. 10, 1337-1342. A New Method of Solution of the Eigenvalue Problem for Gyroscopic Systems.
61. J. S. ARCHER 1963 *Journal of the structural Division Proceedings of the ASME* **89**, ST4, 161. Consistent Mass Matrix for Distributed Mass Systems.
62. A. DIMAROGONAS 1938 *Second edition, Prentice Hall, New Jersey.* Vibration for Engineers.
63. W. T. THOMSON 1998 *Fifth Edition, Prentice Hall, New Jersey.* Theory of Vibration with Applications.
64. MICHEL LALANNE and GUY FERRARIS 1998 *John Wiley and Sons, Second*

Edition. Rotordynamics Prediction in Engineering.

65. J. N. REDDY 1986 *McGraw-Hill, Inc. New York. Applied Functional Analysis and Variational Methods in Engineering.*
66. L. MEIROVITCH 1967 *MacMillan Book Co., Analytical Methods in Vibration.*
67. R. NORDMANN, 1984 *Dynamics of Rotors: Stability and system Identification Springer-Verlag 3-27. Modal Analysis in Rotor Dynamics.*
68. C. W. LEE, R. KATZ, A. G. ULSOY and R. A. SCOTT 1988 *Journal. Sound and Vibration 122(1), 119. Modal Analysis of a Distributed Parameter Rotating Shaft.*
69. C. W. LEE and Y. G. JEI 1998 *Journal. Sound and Vibration 126(2), 345-361. Modal Analysis of Continuous Rotor-Bearing Systemes.*
70. Y. G. JEI and C. W. LEE 1989 *Twelfth Biennial ASME Conference on Mechanical Vibration and Noise, September. Vibrations of Anisotropic Rotor-Bearing Systems.*
71. C. W. LEE 1991 *Mech. Sys. And Signal Processing 5(2), 119-137. A Complex Modal Testing Theroy for Rotating Machinery*
72. C. W. LEE 1993 *Kluwer Academic Publishers. Vibration Analysis of Rotors.*
73. FREDRIC F. EHRICH 1992 *McGraw-Hill, Inc. Handbook of Rotordynamics.*
74. L. MEIROVITCH 1980 *Sijthoff and Noordhoff International Publishers. Computational Methods in Structural Dynamics.*
75. R. SUBBIAH 1985 *M.Sc Theses, Concordia University, Quebec, Canada. Dynamic Behavior of Rotor Systems with a Comprehensive Model for the Hydrodynamic Bearing Supports Using Modal Analysis and Testing.*
76. M. J. GOODWIN 1989 *Unwin Hyman, London, UK. Dynamics of Rotor-Bearing*

Systems.

77. E. KRAMER 1993 *Springer-Verlag, New York.* Dynamics of Rotors and Foundations.
78. R. K. LIVESLEY 1983 *Cambridge University Press Great Britain.* Finite Element: An Introduction for Engineers.

APPENDIX I

I.1 Deflection of beams-Sign Conventions:

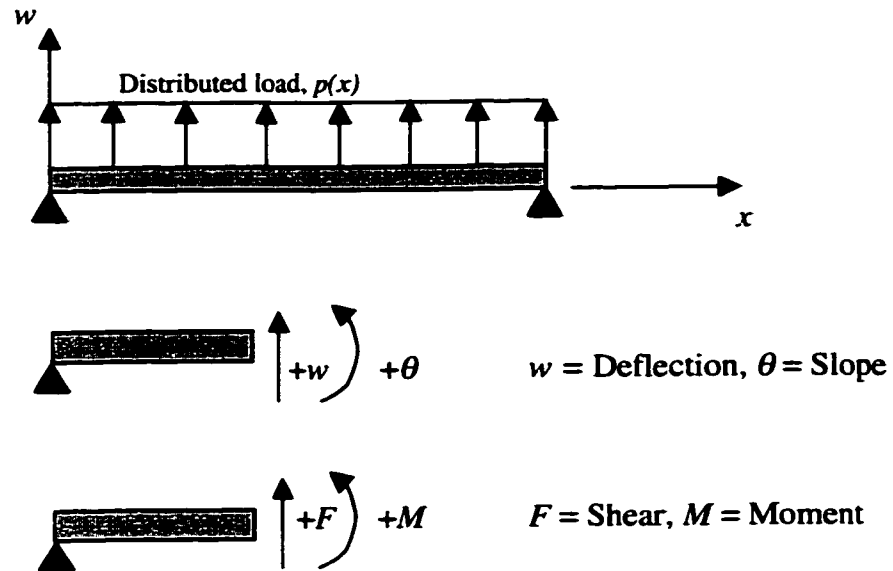


Figure (I.1) Deflection of beam-Sign conventions

In the figure, w = transverse deflection and

$$\frac{dw}{dx} = \theta = \text{Slope} \tag{I.1}$$

$$EI \frac{d^2w}{dx^2} = M = \text{bending moment}$$

We next consider the equilibrium of the moment of all the forces on the element shown in Fig (I.2).

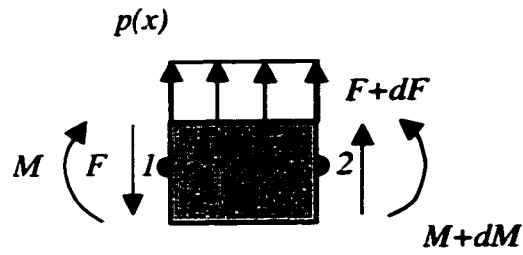


Figure (I.2)

Moment at point 2 will give us

$$M + p dx \frac{dx}{2} - F dx - M - dM = 0 \tag{I.2}$$

Ignoring the 2-nd term we would get

$$F = -\frac{dM}{dx} = -\frac{d}{dx} \left(EI \frac{d^2 w}{dx^2} \right) = \text{shear force} \tag{I.3}$$

I.2 Deflection of rotor beams-Sign conventions:

XY-plane

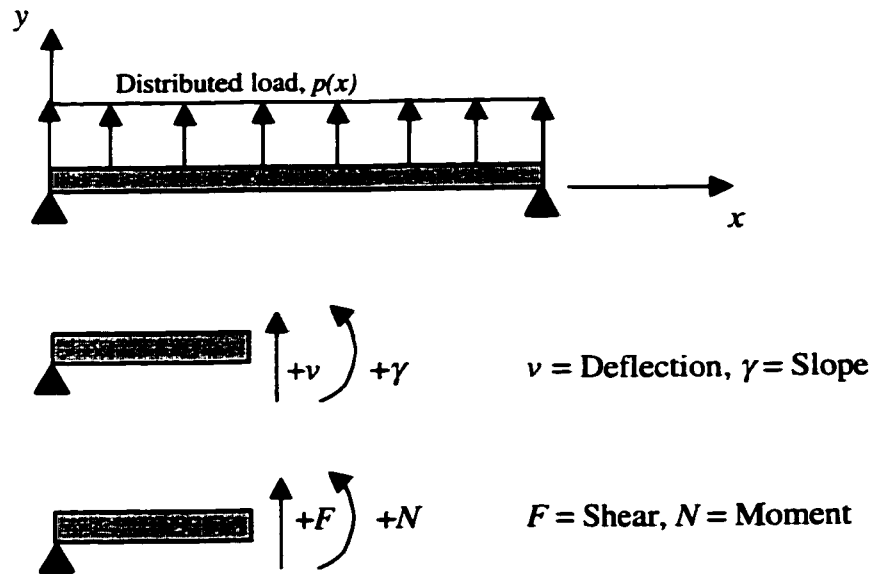


Figure (I.3) Deflection of rotor beam-Sign conventions

In the figure, $v =$ transverse deflection and

$$\frac{\partial v}{\partial x} = \gamma = \text{Slope} \tag{I.4}$$

$$EI \frac{\partial^2 v}{\partial x^2} = N = \text{bending moment}$$

We next consider the equilibrium of the moment of all the forces on the element shown in

Fig (11.2)

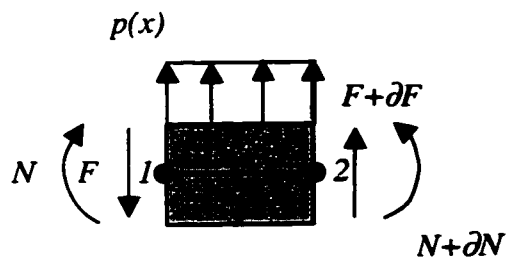


Figure (I.4)

Moment at point 2 will give us

$$N + p \frac{\partial x}{2} - F dx - N - dN = 0 \quad (I.5)$$

Ignoring the 2-nd term we would get

$$F = -\frac{\partial N}{\partial x} = -\frac{\partial}{\partial x} \left(EI \frac{\partial^2 v}{\partial x^2} \right) = \text{shear force} \quad (I.6)$$

XZ plane

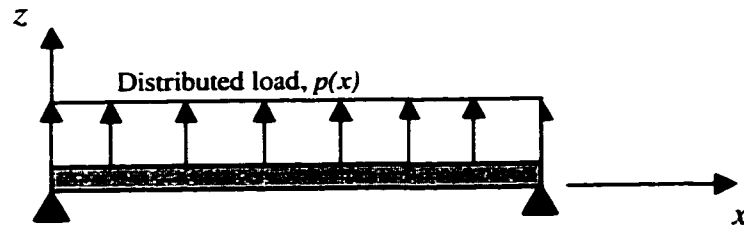


Figure (II.5) Deflection of rotor beam-Sign conventions

In the figure, w = transverse deflection and

$$-\frac{\partial w}{\partial x} = \beta = \text{slope} \tag{I.7}$$

$$EI \frac{\partial^2 w}{\partial x^2} = G = \text{bending moment}$$

We next consider the equilibrium of the moment of all the forces on the element shown in Fig. (II.4)

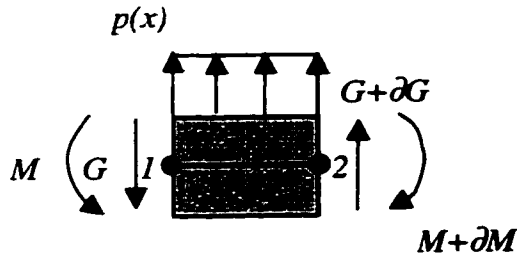


Figure (I.6)

Moment at point 2 will give us

$$-M + p dx \frac{\partial x}{2} - G dx + M + \partial M = 0 \tag{I.8}$$

Ignoring the 2-nd term we would get

$$G = \frac{\partial M}{\partial x} = \frac{\partial}{\partial x} \left(EI \frac{\partial^2 w}{\partial x^2} \right) = \text{shear force} \tag{I.9}$$

The displacement (v, w, β, γ) of a typical element

$$V = N_1 v_1 + N_2 \gamma_2 + N_3 v_2 + N_4 \gamma_2$$

$$W = N_1 w_1 + N_2 \beta_1 + N_3 w_2 + N_4 \beta_2 \tag{I.10}$$

can be written in matrix form as

$$\begin{Bmatrix} V \\ W \end{Bmatrix} = \begin{bmatrix} N_1 & 0 & 0 & N_2 & N_3 & 0 & 0 & N_4 \\ 0 & N_1 & -N_2 & 0 & 0 & N_3 & -N_4 & 0 \end{bmatrix} \begin{Bmatrix} v_1 \\ w_1 \\ \beta_1 \\ \gamma_1 \\ v_2 \\ w_2 \\ \beta_2 \\ \gamma_2 \end{Bmatrix} \quad (\text{I.11})$$

where

$$\begin{aligned} N_1 &= 1 - 3\left(\frac{x}{r}\right)^2 + 2\left(\frac{x}{r}\right)^3 \\ N_2 &= x\left[\left(\frac{x}{r}\right) - 1\right]^2 \\ N_3 &= \left(\frac{x}{r}\right)^2 \left[3 - 2\left(\frac{x}{r}\right)\right] \\ N_4 &= \frac{x^2}{r} \left[\left(\frac{x}{r}\right) - 1\right] \end{aligned} \quad (\text{I.12})$$

since

$$\beta = -\frac{\partial w}{\partial x}$$

N_2 and N_4 in XZ plane will take negative sign.

Similar concept has been adapted to the higher order polynomial for this structure.

APPENDIX II

Derivations involved in the formulation of finite element with efficient higher order basis functions:

General Case: The element deflection is assumed in the form

$$w(x) = c_0 + c_1 \cdot x + c_2 \cdot x^2 + c_3 \cdot x^3 + c_4 \cdot x^4 + c_5 \cdot x^5 + c_6 \cdot x^6 + c_7 \cdot x^7$$

The next step involves expressing $c(i)$ in terms of the primary nodal variables (i. e. generalized displacements). Further, since we have then eight coefficients we must, if we wish to be able to specify the state of the beam by means of values at the junctions or nodes of the elements, have four conditions at each node.

$$\theta(x) = \frac{d}{dx} w(x) \rightarrow c_1 + 2 \cdot c_2 \cdot x + 3 \cdot c_3 \cdot x^2 + 4 \cdot c_4 \cdot x^3 + 5 \cdot c_5 \cdot x^4 + 6 \cdot c_6 \cdot x^5 + 7 \cdot c_7 \cdot x^6$$

$$M(x) = b \cdot \frac{d^2}{dx^2} w(x) \rightarrow b \cdot (2 \cdot c_2 + 6 \cdot c_3 \cdot x + 12 \cdot c_4 \cdot x^2 + 20 \cdot c_5 \cdot x^3 + 30 \cdot c_6 \cdot x^4 + 42 \cdot c_7 \cdot x^5)$$

$$f(x) = -b \cdot \frac{d^3}{dx^3} w(x) \rightarrow -b \cdot (6 \cdot c_3 + 24 \cdot c_4 \cdot x + 60 \cdot c_5 \cdot x^2 + 120 \cdot c_6 \cdot x^3 + 210 \cdot c_7 \cdot x^4)$$

Where the function $b = EI$ is the product of the modulus of elasticity E and the moment of inertia I of the beam.

Using the boundary conditions

$$w_1 := w(0) \rightarrow c_0$$

$$\theta_1 := \theta(0) \rightarrow c_1$$

$$w_2 := w(r) \rightarrow c_0 + c_1 \cdot r + c_2 \cdot r^2 + c_3 \cdot r^3 + c_4 \cdot r^4 + c_5 \cdot r^5 + c_6 \cdot r^6 + c_7 \cdot r^7$$

$$\theta_2 := \theta(r) \rightarrow c_1 + 2 \cdot c_2 \cdot r + 3 \cdot c_3 \cdot r^2 + 4 \cdot c_4 \cdot r^3 + 5 \cdot c_5 \cdot r^4 + 6 \cdot c_6 \cdot r^5 + 7 \cdot c_7 \cdot r^6$$

$$f_1 := f(0) \rightarrow -6 \cdot b \cdot c_3$$

$$m_1 := M(0) \rightarrow 2 \cdot b \cdot c_2$$

$$f_2 := f(r) \rightarrow -b \cdot (6 \cdot c_3 + 24 \cdot c_4 \cdot r + 60 \cdot c_5 \cdot r^2 + 120 \cdot c_6 \cdot r^3 + 210 \cdot c_7 \cdot r^4)$$

$$m_2 := M(r) \rightarrow b \cdot (2 \cdot c_2 + 6 \cdot c_3 \cdot r + 12 \cdot c_4 \cdot r^2 + 20 \cdot c_5 \cdot r^3 + 30 \cdot c_6 \cdot r^4 + 42 \cdot c_7 \cdot r^5)$$

or we can express the above in a matrix form as

$$\begin{bmatrix} w1 \\ \theta1 \\ w2 \\ \theta2 \\ f1 \\ m1 \\ f2 \\ m2 \end{bmatrix} = \begin{bmatrix} 1 & 0 & 0 & 0 & 0 & 0 & 0 & 0 \\ 0 & 1 & 0 & 0 & 0 & 0 & 0 & 0 \\ 1 & r & r^2 & r^3 & r^4 & r^5 & r^6 & r^7 \\ 0 & 1 & 2\cdot r & 3\cdot r^2 & 4\cdot r^3 & 5\cdot r^4 & 6\cdot r^5 & 7\cdot r^6 \\ 0 & 0 & 0 & -6\cdot b & 0 & 0 & 0 & 0 \\ 0 & 0 & 2\cdot b & 0 & 0 & 0 & 0 & 0 \\ 0 & 0 & 0 & -6\cdot b & -24\cdot b\cdot r & -60\cdot b\cdot r^2 & -120\cdot b\cdot r^3 & -210\cdot b\cdot r^4 \\ 0 & 0 & 2\cdot b & 6\cdot b\cdot r & 12\cdot b\cdot r^2 & 20\cdot b\cdot r^3 & 30\cdot b\cdot r^4 & 42\cdot b\cdot r^5 \end{bmatrix} \begin{bmatrix} c0 \\ c1 \\ c2 \\ c3 \\ c4 \\ c5 \\ c6 \\ c7 \end{bmatrix}$$

Inverting this matrix equation to express "c(i)" in terms of w, Θ , f and M we obtain,

$$\begin{bmatrix} c0 \\ c1 \\ c2 \\ c3 \\ c4 \\ c5 \\ c6 \\ c7 \end{bmatrix} = \begin{bmatrix} 1 & 0 & 0 & 0 & 0 & 0 & 0 & 0 \\ 0 & 1 & 0 & 0 & 0 & 0 & 0 & 0 \\ 0 & 0 & 0 & 0 & 0 & \frac{1}{(2\cdot b)} & 0 & 0 \\ 0 & 0 & 0 & 0 & \frac{-1}{(6\cdot b)} & 0 & 0 & 0 \\ \frac{-35}{r^4} & \frac{-20}{r^3} & \frac{35}{r^4} & \frac{-15}{r^3} & \frac{2}{(3\cdot(b\cdot r))} & \frac{-5}{(b\cdot r^2)} & \frac{1}{(6\cdot(b\cdot r))} & \frac{5}{[2\cdot(b\cdot r^2)]} \\ \frac{84}{r^5} & \frac{45}{r^4} & \frac{-84}{r^5} & \frac{39}{r^4} & \frac{-1}{(b\cdot r^2)} & \frac{10}{(b\cdot r^3)} & \frac{-1}{[2\cdot(b\cdot r^2)]} & \frac{-7}{(b\cdot r^3)} \\ \frac{-70}{r^6} & \frac{-36}{r^5} & \frac{70}{r^6} & \frac{-34}{r^5} & \frac{2}{[3\cdot(b\cdot r^3)]} & \frac{-15}{[2\cdot(b\cdot r^4)]} & \frac{1}{[2\cdot(b\cdot r^3)]} & \frac{13}{[2\cdot(b\cdot r^4)]} \\ \frac{20}{r^7} & \frac{10}{r^6} & \frac{-20}{r^7} & \frac{10}{r^6} & \frac{-1}{[6\cdot(b\cdot r^4)]} & \frac{2}{(b\cdot r^5)} & \frac{-1}{[6\cdot(b\cdot r^4)]} & \frac{-2}{(b\cdot r^5)} \end{bmatrix} \begin{bmatrix} w1 \\ \theta1 \\ w2 \\ \theta2 \\ f1 \\ m1 \\ f2 \\ m2 \end{bmatrix}$$

Substituting the above result in the equation for $w(x)$, we obtain

$$w(x) = N1 \cdot w1 + N2 \cdot \theta1 + N3 \cdot w2 + N4 \cdot \theta2 + N5 \cdot f1 + N6 \cdot m1 + N7 \cdot f2 + N8 \cdot m2$$

where $N1, N2..N8$ are the shape functions or the interpolation functions and they can be expressed in terms of the local coordinate x

$$N1(x) := 1 - 35 \frac{x^4}{r^4} + 84 \frac{x^5}{r^5} - 70 \frac{x^6}{r^6} + 20 \frac{x^7}{r^7}$$

$$N2(x) := x - \frac{20 \cdot x^4}{r^3} + \frac{45 \cdot x^5}{r^4} - \frac{36 \cdot x^6}{r^5} + \frac{10 \cdot x^7}{r^6}$$

$$N3(x) := 35 \frac{x^4}{r^4} - 84 \frac{x^5}{r^5} + 70 \frac{x^6}{r^6} - 20 \frac{x^7}{r^7}$$

$$N4(x) := -15 \frac{x^4}{r^3} + 39 \frac{x^5}{r^4} - 34 \frac{x^6}{r^5} + 10 \frac{x^7}{r^6}$$

$$N5(x) := -\frac{x^3}{6 \cdot b} + 2 \frac{x^4}{3 \cdot b \cdot r} - \frac{x^5}{b \cdot r^2} + 2 \frac{x^6}{3 \cdot b \cdot r^3} - \frac{x^7}{6 \cdot b \cdot r^4}$$

$$N6(x) := \frac{x^2}{2 \cdot b} - 5 \frac{x^4}{b \cdot r^2} + 10 \frac{x^5}{b \cdot r^3} - 15 \frac{x^6}{2 \cdot b \cdot r^4} + 2 \frac{x^7}{b \cdot r^5}$$

$$N7(x) := \frac{x^4}{6 \cdot b \cdot r} - \frac{x^5}{2 \cdot b \cdot r^2} + \frac{x^6}{2 \cdot b \cdot r^3} - \frac{x^7}{6 \cdot b \cdot r^4}$$

$$N8(x) := 5 \frac{x^4}{2 \cdot b \cdot r^2} - 7 \frac{x^5}{b \cdot r^3} + 13 \frac{x^6}{2 \cdot b \cdot r^4} - 2 \frac{x^7}{b \cdot r^5}$$

The interpolation functions satisfy the following interpolation properties:

$$N1(0) \rightarrow 1 \quad N3(0) \rightarrow 0 \quad N5(0) \rightarrow 0 \quad N7(0) \rightarrow 0$$

$$N2(0) \rightarrow 0 \quad N4(0) \rightarrow 0 \quad N6(0) \rightarrow 0 \quad N8(0) \rightarrow 0$$

$$N1(r) \rightarrow 0 \quad N3(r) \rightarrow 1 \quad N5(r) \rightarrow 0 \quad N7(r) \rightarrow 0$$

$$N2(r) \rightarrow 0 \quad N4(r) \rightarrow 0 \quad N6(r) \rightarrow 0 \quad N8(r) \rightarrow 0$$

The first derivatives of $N(i)$ with respect to x are

$$N11(x) = \frac{d}{dx}N1(x) \rightarrow -140 \cdot \frac{x^3}{r^4} + 420 \cdot \frac{x^4}{r^5} - 420 \cdot \frac{x^5}{r^6} + 140 \cdot \frac{x^6}{r^7}$$

$$N22(x) = \frac{d}{dx}N2(x) \rightarrow 1 - 80 \cdot \frac{x^3}{r^3} + 225 \cdot \frac{x^4}{r^4} - 216 \cdot \frac{x^5}{r^5} + 70 \cdot \frac{x^6}{r^6}$$

$$N33(x) = \frac{d}{dx}N3(x) \rightarrow 140 \cdot \frac{x^3}{r^4} - 420 \cdot \frac{x^4}{r^5} + 420 \cdot \frac{x^5}{r^6} - 140 \cdot \frac{x^6}{r^7}$$

$$N44(x) = \frac{d}{dx}N4(x) \rightarrow -60 \cdot \frac{x^3}{r^3} + 195 \cdot \frac{x^4}{r^4} - 204 \cdot \frac{x^5}{r^5} + 70 \cdot \frac{x^6}{r^6}$$

$$N55(x) = \frac{d}{dx}N5(x) \rightarrow \frac{-1}{2} \cdot \frac{x^2}{b} + \frac{8}{3} \cdot \frac{x^3}{(b \cdot r)} - 5 \cdot \frac{x^4}{(b \cdot r^2)} + 4 \cdot \frac{x^5}{(b \cdot r^3)} - \frac{7}{6} \cdot \frac{x^6}{(b \cdot r^4)}$$

$$N66(x) = \frac{d}{dx}N6(x) \rightarrow \frac{x}{b} - 20 \cdot \frac{x^3}{(b \cdot r^2)} + 50 \cdot \frac{x^4}{(b \cdot r^3)} - 45 \cdot \frac{x^5}{(b \cdot r^4)} + 14 \cdot \frac{x^6}{(b \cdot r^5)}$$

$$N77(x) = \frac{d}{dx} N7(x) \rightarrow \frac{2}{3} \cdot \frac{x^3}{(b \cdot r)} - \frac{5}{2} \cdot \frac{x^4}{(b \cdot r^2)} + 3 \cdot \frac{x^5}{(b \cdot r^3)} - \frac{7}{6} \cdot \frac{x^6}{(b \cdot r^4)}$$

$$N88(x) = \frac{d}{dx} N8(x) \rightarrow 10 \cdot \frac{x^3}{(b \cdot r^2)} - 35 \cdot \frac{x^4}{(b \cdot r^3)} + 39 \cdot \frac{x^5}{(b \cdot r^4)} - 14 \cdot \frac{x^6}{(b \cdot r^5)}$$

$$N11(0) \rightarrow 0$$

$$N55(0) \rightarrow 0$$

$$N11(r) \rightarrow 0$$

$$N55(r) \rightarrow 0$$

$$N22(0) \rightarrow 1$$

$$N66(0) \rightarrow 0$$

$$N22(r) \rightarrow 0$$

$$N66(r) \rightarrow 0$$

$$N33(0) \rightarrow 0$$

$$N77(0) \rightarrow 0$$

$$N33(r) \rightarrow 0$$

$$N77(r) \rightarrow 0$$

$$N44(0) \rightarrow 0$$

$$N88(0) \rightarrow 0$$

$$N44(r) \rightarrow 1$$

$$N88(r) \rightarrow 0$$

The second derivatives of the interpolation functions:

$$n1(x) := \frac{d^2}{dx^2} N1(x) \rightarrow -420 \cdot \frac{x^2}{r^4} + 1680 \cdot \frac{x^3}{r^5} - 2100 \cdot \frac{x^4}{r^6} + 840 \cdot \frac{x^5}{r^7}$$

$$n2(x) = \frac{d^2}{dx^2} N2(x) \rightarrow -240 \cdot \frac{x^2}{r^3} + 900 \cdot \frac{x^3}{r^4} - 1080 \cdot \frac{x^4}{r^5} + 420 \cdot \frac{x^5}{r^6}$$

$$n3(x) := \frac{d^2}{dx^2} N3(x) \rightarrow 420 \cdot \frac{x^2}{r^4} - 1680 \cdot \frac{x^3}{r^5} + 2100 \cdot \frac{x^4}{r^6} - 840 \cdot \frac{x^5}{r^7}$$

$$n4(x) = \frac{d^2}{dx^2} N4(x) \rightarrow -180 \cdot \frac{x^2}{r^3} + 780 \cdot \frac{x^3}{r^4} - 1020 \cdot \frac{x^4}{r^5} + 420 \cdot \frac{x^5}{r^6}$$

$$n5(x) = \frac{d^2}{dx^2} N5(x) \rightarrow \frac{-x}{b} + 8 \cdot \frac{x^2}{(b \cdot r)} - 20 \cdot \frac{x^3}{(b \cdot r^2)} + 20 \cdot \frac{x^4}{(b \cdot r^3)} - 7 \cdot \frac{x^5}{(b \cdot r^4)}$$

$$n6(x) = \frac{d^2}{dx^2} N6(x) \rightarrow \frac{1}{b} - 60 \cdot \frac{x^2}{(b \cdot r^2)} + 200 \cdot \frac{x^3}{(b \cdot r^3)} - 225 \cdot \frac{x^4}{(b \cdot r^4)} + 84 \cdot \frac{x^5}{(b \cdot r^5)}$$

$$n7(x) = \frac{d^2}{dx^2} N7(x) \rightarrow 2 \cdot \frac{x^2}{(b \cdot r)} - 10 \cdot \frac{x^3}{(b \cdot r^2)} + 15 \cdot \frac{x^4}{(b \cdot r^3)} - 7 \cdot \frac{x^5}{(b \cdot r^4)}$$

$$n8(x) = \frac{d^2}{dx^2} N8(x) \rightarrow 30 \cdot \frac{x^2}{(b \cdot r^2)} - 140 \cdot \frac{x^3}{(b \cdot r^3)} + 195 \cdot \frac{x^4}{(b \cdot r^4)} - 84 \cdot \frac{x^5}{(b \cdot r^5)}$$

$$n1(0) \rightarrow 0 \quad n2(0) \rightarrow 0 \quad n3(0) \rightarrow 0 \quad n4(0) \rightarrow 0$$

$$n1(r) \rightarrow 0 \quad n2(r) \rightarrow 0 \quad n3(r) \rightarrow 0 \quad n4(r) \rightarrow 0$$

$$n5(0) \rightarrow 0 \quad n6(0) \rightarrow \frac{1}{b} \quad n7(0) \rightarrow 0 \quad n8(0) \rightarrow 0$$

$$n5(r) \rightarrow 0 \quad n6(r) \rightarrow 0 \quad n7(r) \rightarrow 0 \quad n8(r) \rightarrow \frac{1}{b}$$

The third derivatives of the interpolation functions:

$$n11(x) = \frac{d}{dx} b \cdot n1(x) \rightarrow b \cdot \left(-840 \cdot \frac{x}{r^4} + 5040 \cdot \frac{x^2}{r^5} - 8400 \cdot \frac{x^3}{r^6} + 4200 \cdot \frac{x^4}{r^7} \right)$$

$$n22(x) = \frac{d}{dx} b \cdot n2(x) \rightarrow b \cdot \left(-480 \cdot \frac{x}{r^3} + 2700 \cdot \frac{x^2}{r^4} - 4320 \cdot \frac{x^3}{r^5} + 2100 \cdot \frac{x^4}{r^6} \right)$$

$$n33(x) = \frac{d}{dx} b \cdot n3(x) \rightarrow b \cdot \left(840 \cdot \frac{x}{r^4} - 5040 \cdot \frac{x^2}{r^5} + 8400 \cdot \frac{x^3}{r^6} - 4200 \cdot \frac{x^4}{r^7} \right)$$

$$n44(x) = \frac{d}{dx} b \cdot n4(x) \rightarrow b \cdot \left(-360 \cdot \frac{x}{r^3} + 2340 \cdot \frac{x^2}{r^4} - 4080 \cdot \frac{x^3}{r^5} + 2100 \cdot \frac{x^4}{r^6} \right)$$

$$n55(x) = \frac{d}{dx} b \cdot n5(x) \rightarrow b \cdot \left[\frac{-1}{b} + 16 \cdot \frac{x}{(b \cdot r)} - 60 \cdot \frac{x^2}{(b \cdot r^2)} + 80 \cdot \frac{x^3}{(b \cdot r^3)} - 35 \cdot \frac{x^4}{(b \cdot r^4)} \right]$$

$$n66(x) = \frac{d}{dx} b \cdot n6(x) \rightarrow b \cdot \left[-120 \cdot \frac{x}{(b \cdot r^2)} + 600 \cdot \frac{x^2}{(b \cdot r^3)} - 900 \cdot \frac{x^3}{(b \cdot r^4)} + 420 \cdot \frac{x^4}{(b \cdot r^5)} \right]$$

$$n77(x) = \frac{d}{dx} b \cdot n7(x) \rightarrow b \cdot \left[4 \cdot \frac{x}{(b \cdot r)} - 30 \cdot \frac{x^2}{(b \cdot r^2)} + 60 \cdot \frac{x^3}{(b \cdot r^3)} - 35 \cdot \frac{x^4}{(b \cdot r^4)} \right]$$

$$n88(x) = \frac{d}{dx} b \cdot n8(x) \rightarrow b \cdot \left[60 \cdot \frac{x}{(b \cdot r^2)} - 420 \cdot \frac{x^2}{(b \cdot r^3)} + 780 \cdot \frac{x^3}{(b \cdot r^4)} - 420 \cdot \frac{x^4}{(b \cdot r^5)} \right]$$

$n11(0) \rightarrow 0$	$n11(r) \rightarrow 0$	$n55(0) \rightarrow -1$	$n55(r) \rightarrow 0$
$n22(0) \rightarrow 0$	$n22(r) \rightarrow 0$	$n66(0) \rightarrow 0$	$n66(r) \rightarrow 0$
$n33(0) \rightarrow 0$	$n33(r) \rightarrow 0$	$n77(0) \rightarrow 0$	$n77(r) \rightarrow -1$
$n44(0) \rightarrow 0$	$n44(r) \rightarrow 0$	$n88(0) \rightarrow 0$	$n88(r) \rightarrow 0$

Elements of stiffness matrix:

$$k_{11} := \int_0^r b \cdot n1(x) \cdot n1(x) dx \rightarrow \frac{280}{11} \cdot \frac{b}{r^3}$$

$$k_{22} := \int_0^r b \cdot n2(x) \cdot n2(x) dx \rightarrow \frac{600}{77} \cdot \frac{b}{r}$$

$$k_{33} := \int_0^r b \cdot n3(x) \cdot n3(x) dx \rightarrow \frac{280}{11} \cdot \frac{b}{r^3}$$

$$k_{12} := \int_0^r b \cdot n1(x) \cdot n2(x) dx \rightarrow \frac{140}{11} \cdot \frac{b}{r^2}$$

$$k_{23} := \int_0^r b \cdot n2(x) \cdot n3(x) dx \rightarrow \frac{-140}{11} \cdot \frac{b}{r^2}$$

$$k_{34} := \int_0^r b \cdot n3(x) \cdot n4(x) dx \rightarrow \frac{-140}{11} \cdot \frac{b}{r^2}$$

$$k_{13} := \int_0^r b \cdot n1(x) \cdot n3(x) dx \rightarrow \frac{-280}{11} \cdot \frac{b}{r^3}$$

$$k_{24} := \int_0^r b \cdot n2(x) \cdot n4(x) dx \rightarrow \frac{380}{77} \cdot \frac{b}{r}$$

$$k_{35} := \int_0^r b \cdot n3(x) \cdot n5(x) dx \rightarrow \frac{1}{22}$$

$$k_{14} := \int_0^r b \cdot n1(x) \cdot n4(x) dx \rightarrow \frac{140}{11} \cdot \frac{b}{r^2}$$

$$k_{43} := \int_0^r b \cdot n4(x) \cdot n3(x) dx \rightarrow \frac{-140}{11} \cdot \frac{b}{r^2}$$

$$k_{42} := \int_0^r b \cdot n4(x) \cdot n2(x) dx \rightarrow \frac{380}{77} \cdot \frac{b}{r}$$

$$k_{25} := \int_0^r b \cdot n2(x) \cdot n5(x) dx \rightarrow \frac{-8}{231} \cdot r$$

$$k_{36} := \int_0^r b \cdot n3(x) \cdot n6(x) dx \rightarrow \frac{-40}{(33 \cdot r)}$$

$$k_{15} := \int_0^r b \cdot n1(x) \cdot n5(x) dx \rightarrow \frac{-1}{22}$$

$$k_{26} := \int_0^r b \cdot n2(x) \cdot n6(x) dx \rightarrow \frac{379}{462}$$

$$k_{37} := \int_0^r b \cdot n3(x) \cdot n7(x) dx \rightarrow \frac{1}{22}$$

$$k_{16} := \int_0^r b \cdot n1(x) \cdot n6(x) dx \rightarrow \frac{40}{(33 \cdot r)}$$

$$k27 = \int_0^r b \cdot n2(x) \cdot n7(x) dx \rightarrow \frac{-5}{462} \cdot r$$

$$k38 = \int_0^r b \cdot n3(x) \cdot n8(x) dx \rightarrow \frac{40}{(33 \cdot r)}$$

$$k17 = \int_0^r b \cdot n1(x) \cdot n7(x) dx \rightarrow \frac{-1}{22}$$

$$k28 := \int_0^r b \cdot n2(x) \cdot n8(x) dx \rightarrow \frac{-181}{462}$$

$$k44 = \int_0^r b \cdot n4(x) \cdot n4(x) dx \rightarrow \frac{600}{77} \cdot \frac{b}{r}$$

$$k45 = \int_0^r b \cdot n4(x) \cdot n5(x) dx \rightarrow \frac{-5}{462} \cdot r$$

$$k46 = \int_0^r b \cdot n4(x) \cdot n6(x) dx \rightarrow \frac{181}{462}$$

$$k47 := \int_0^r b \cdot n4(x) \cdot n7(x) dx \rightarrow \frac{-8}{231} \cdot r$$

$$k48 = \int_0^r b \cdot n4(x) \cdot n8(x) dx \rightarrow \frac{-379}{462}$$

$$k18 = \int_0^r b \cdot n1(x) \cdot n8(x) dx \rightarrow \frac{-40}{(33 \cdot r)}$$

$$k55 = \int_0^r b \cdot n5(x) \cdot n5(x) dx \rightarrow \frac{2}{(3465 \cdot b)} \cdot r^3$$

$$k56 := \int_0^r b \cdot n5(x) \cdot n6(x) dx \rightarrow \frac{-1}{(99 \cdot b)} \cdot r^2$$

$$k77 := \int_0^r b \cdot n7(x) \cdot n7(x) dx \rightarrow \frac{2}{(3465 \cdot b)} \cdot r^3$$

$$k57 := \int_0^r b \cdot n5(x) \cdot n7(x) dx \rightarrow \frac{-1}{(4620 \cdot b)} \cdot r^3$$

$$k66 := \int_0^r b \cdot n6(x) \cdot n6(x) dx \rightarrow \frac{50}{(231 \cdot b)} \cdot r$$

$$k68 := \int_0^r b \cdot n6(x) \cdot n8(x) dx \rightarrow \frac{-1}{(462 \cdot b)} \cdot r$$

$$k67 := \int_0^r n6(x) \cdot n7(x) dx \rightarrow \frac{5}{2772} \cdot \frac{r^2}{b^2}$$

$$k58 := \int_0^r b \cdot n5(x) \cdot n8(x) dx \rightarrow \frac{-5}{(2772 \cdot b)} \cdot r^2$$

$$k78 := \int_0^r b \cdot n7(x) \cdot n8(x) dx \rightarrow \frac{1}{(99 \cdot b)} \cdot r^2$$

$$k88 := \int_0^r b \cdot n8(x) \cdot n8(x) dx \rightarrow \frac{50}{(231 \cdot b)} \cdot r$$

Calculating the coefficients m_{ij} of the mass matrix: note that the coefficients $m_{ij} = m_{ji}$.

$$m_{11} = \rho \cdot A \cdot \int_0^r N1(x) \cdot N1(x) dx \rightarrow \frac{521}{1287} \cdot \rho \cdot A \cdot r$$

$$m_{12} = \rho \cdot A \cdot \int_0^r N2(x) \cdot N1(x) dx \rightarrow \frac{151}{2002} \cdot \rho \cdot A \cdot r^2$$

$$m_{13} = \rho \cdot A \cdot \int_0^r N3(x) \cdot N1(x) dx \rightarrow \frac{245}{2574} \cdot \rho \cdot A \cdot r$$

$$m_{14} = \rho \cdot A \cdot \int_0^r N4(x) \cdot N1(x) dx \rightarrow \frac{-127}{4004} \cdot \rho \cdot A \cdot r^2$$

$$m_{15} = \rho \cdot A \cdot \int_0^r N5(x) \cdot N1(x) dx \rightarrow \frac{-383}{1081080} \cdot \rho \cdot A \cdot \frac{r^4}{b}$$

$$m_{16} = \rho \cdot A \cdot \int_0^r N6(x) \cdot N1(x) dx \rightarrow \frac{137}{18018} \cdot \rho \cdot \frac{A}{b} \cdot r^3$$

$$m_{17} = \rho \cdot A \cdot \int_0^r N7(x) \cdot N1(x) dx \rightarrow \frac{521}{2162160} \cdot \rho \cdot A \cdot \frac{r^4}{b}$$

$$m_{18} = \rho \cdot A \cdot \int_0^r N8(x) \cdot N1(x) dx \rightarrow \frac{155}{36036} \cdot \rho \cdot \frac{A}{b} \cdot r^3$$

$$m_{22} = \rho \cdot A \cdot \int_0^r N2(x) \cdot N2(x) dx \rightarrow \frac{5}{273} \cdot \rho \cdot A \cdot r^3$$

$$m_{23} = \rho \cdot A \cdot \int_0^r N3(x) \cdot N2(x) dx \rightarrow \frac{127}{4004} \cdot \rho \cdot A \cdot r^2$$

$$m_{24} = \rho \cdot A \cdot \int_0^r N2(x) \cdot N4(x) dx \rightarrow \frac{-373}{36036} \cdot \rho \cdot A \cdot r^3$$

$$m_{25} = \rho \cdot A \cdot \int_0^r N5(x) \cdot N2(x) dx \rightarrow \frac{-1}{10010} \cdot \rho \cdot A \cdot \frac{r^5}{b}$$

$$m_{26} = \rho \cdot A \cdot \int_0^r N6(x) \cdot N2(x) dx \rightarrow \frac{7}{3432} \cdot \rho \cdot A \cdot \frac{r^4}{b}$$

$$m_{27} = \rho \cdot A \cdot \int_0^r N7(x) \cdot N2(x) dx \rightarrow \frac{1}{13104} \cdot \rho \cdot A \cdot \frac{r^5}{b}$$

$$m_{28} = \rho \cdot A \cdot \int_0^r N8(x) \cdot N2(x) dx \rightarrow \frac{199}{144144} \cdot \rho \cdot A \cdot \frac{r^4}{b}$$

$$m_{33} = \rho \cdot A \cdot \int_0^r N3(x) \cdot N3(x) dx \rightarrow \frac{521}{1287} \cdot \rho \cdot A \cdot r$$

$$m_{34} = \rho \cdot A \cdot \int_0^r N3(x) \cdot N4(x) dx \rightarrow \frac{-151}{2002} \cdot \rho \cdot A \cdot r^2$$

$$m_{35} = \rho \cdot A \cdot \int_0^r N3(x) \cdot N5(x) dx \rightarrow \frac{-521}{2162160} \cdot \rho \cdot A \cdot \frac{r^4}{b}$$

$$m_{36} = \rho \cdot A \cdot \int_0^r N3(x) \cdot N6(x) dx \rightarrow \frac{155}{36036} \cdot \rho \cdot \frac{A}{b} \cdot r^3$$

$$m37 := \rho \cdot A \cdot \int_0^r N3(x) \cdot N7(x) dx \rightarrow \frac{383}{1081080} \cdot \rho \cdot A \cdot \frac{r^4}{b}$$

$$m38 := \rho \cdot A \cdot \int_0^r N3(x) \cdot N8(x) dx \rightarrow \frac{137}{18018} \cdot \rho \cdot A \cdot \frac{r^3}{b}$$

$$m44 := \rho \cdot A \cdot \int_0^r N4(x) \cdot N4(x) dx \rightarrow \frac{5}{273} \cdot \rho \cdot A \cdot r^3$$

$$m45 := \rho \cdot A \cdot \int_0^r N4(x) \cdot N5(x) dx \rightarrow \frac{1}{13104} \cdot \rho \cdot A \cdot \frac{r^5}{b}$$

$$m46 := \rho \cdot A \cdot \int_0^r N4(x) \cdot N6(x) dx \rightarrow \frac{-199}{144144} \cdot \rho \cdot A \cdot \frac{r^4}{b}$$

$$m47 := \rho \cdot A \cdot \int_0^r N4(x) \cdot N7(x) dx \rightarrow \frac{-1}{10010} \cdot \rho \cdot A \cdot \frac{r^5}{b}$$

$$m48 := \rho \cdot A \cdot \int_0^r N4(x) \cdot N8(x) dx \rightarrow \frac{-7}{3432} \cdot \rho \cdot A \cdot \frac{r^4}{b}$$

$$m55 := \rho \cdot A \cdot \int_0^r N5(x) \cdot N5(x) dx \rightarrow \frac{1}{1621620} \cdot \rho \cdot A \cdot \frac{r^7}{b^2}$$

$$m56 := \rho \cdot A \cdot \int_0^r N5(x) \cdot N6(x) dx \rightarrow \frac{-1}{83160} \cdot \rho \cdot A \cdot \frac{r^6}{b^2}$$

$$m57 := \rho \cdot A \cdot \int_0^r N5(x) \cdot N7(x) dx \rightarrow \frac{-1}{1853280} \cdot \rho \cdot A \cdot \frac{r^7}{b^2}$$

$$m_{58} = \rho \cdot A \cdot \int_0^r N5(x) \cdot N8(x) dx \rightarrow \frac{-43}{4324320} \cdot \rho \cdot A \cdot \frac{r^6}{b^2}$$

$$m_{66} = \rho \cdot A \cdot \int_0^r N6(x) \cdot N6(x) dx \rightarrow \frac{43}{180180} \cdot \rho \cdot A \cdot \frac{r^5}{b^2}$$

$$m_{67} = \rho \cdot A \cdot \int_0^r N6(x) \cdot N7(x) dx \rightarrow \frac{43}{4324320} \cdot \rho \cdot A \cdot \frac{r^6}{b^2}$$

$$m_{68} = \rho \cdot A \cdot \int_0^r N6(x) \cdot N8(x) dx \rightarrow \frac{131}{720720} \cdot \rho \cdot A \cdot \frac{r^5}{b^2}$$

$$m_{77} = \rho \cdot A \cdot \int_0^r N7(x) \cdot N7(x) dx \rightarrow \frac{1}{1621620} \cdot \rho \cdot A \cdot \frac{r^7}{b^2}$$

$$m_{78} = \rho \cdot A \cdot \int_0^r N7(x) \cdot N8(x) dx \rightarrow \frac{1}{83160} \cdot \rho \cdot A \cdot \frac{r^6}{b^2}$$

$$m_{88} = \rho \cdot A \cdot \int_0^r N8(x) \cdot N8(x) dx \rightarrow \frac{43}{180180} \cdot \rho \cdot A \cdot \frac{r^5}{b^2}$$

For the case in which $b (= ED)$ is a constant over an element, the element characteristic stiffness matrix $[K]$ will be

$$K := \begin{bmatrix} k_{11} & k_{12} & k_{13} & k_{14} & k_{15} & k_{16} & k_{17} & k_{18} \\ k_{12} & k_{22} & k_{23} & k_{24} & k_{25} & k_{26} & k_{27} & k_{28} \\ k_{13} & k_{23} & k_{33} & k_{34} & k_{35} & k_{36} & k_{37} & k_{38} \\ k_{14} & k_{24} & k_{34} & k_{44} & k_{45} & k_{46} & k_{47} & k_{48} \\ k_{15} & k_{25} & k_{35} & k_{45} & k_{55} & k_{56} & k_{57} & k_{58} \\ k_{16} & k_{26} & k_{36} & k_{46} & k_{56} & k_{66} & k_{67} & k_{68} \\ k_{17} & k_{27} & k_{37} & k_{47} & k_{57} & k_{67} & k_{77} & k_{78} \\ k_{18} & k_{28} & k_{38} & k_{48} & k_{58} & k_{68} & k_{78} & k_{88} \end{bmatrix}$$

For the case in which $A = \text{constant}$, The characteristic mass matrix of the element is given by

$$M := \begin{bmatrix} m_{11} & m_{12} & m_{13} & m_{14} & m_{15} & m_{16} & m_{17} & m_{18} \\ m_{12} & m_{22} & m_{23} & m_{24} & m_{25} & m_{26} & m_{27} & m_{28} \\ m_{13} & m_{23} & m_{33} & m_{34} & m_{35} & m_{36} & m_{37} & m_{38} \\ m_{14} & m_{24} & m_{34} & m_{44} & m_{45} & m_{46} & m_{47} & m_{48} \\ m_{15} & m_{25} & m_{35} & m_{45} & m_{55} & m_{56} & m_{57} & m_{58} \\ m_{16} & m_{26} & m_{36} & m_{46} & m_{56} & m_{66} & m_{67} & m_{68} \\ m_{17} & m_{27} & m_{37} & m_{47} & m_{57} & m_{67} & m_{77} & m_{78} \\ m_{18} & m_{28} & m_{38} & m_{48} & m_{58} & m_{68} & m_{78} & m_{88} \end{bmatrix}$$